REGISTERED No. M. 3121

PROCEEDINGS
OF
THE INDIAN ACADEMY OF SCIENCES

Vol. III] FEBRUARY, 1936 [No. 2

CONTENTS

SECTION A

	PAGE
Unitary Theory of Field and Matter. II. Classical Treatment. Charged Particle with Electric and Magnetic Moment. By MAX BORN ..	85
The Measurement of the Transmission of Heat by Convection from Insolated Ground to the Atmosphere. By P. K. RAMAN	98
Studies in Thorium Phosphate Gels. By M. U. PARMAR, S. M. MEHTA and MATA PRASAD	107
The Diffraction of Light by High Frequency Sound Waves: Part IV. Generalised Theory. By C. V. RAMAN and N. S. NAGENDRA NATH	119
Molecular Clustering in Liquid Fatty Acids. By R. S. KRISHNAN ..	126
Deformation Frequencies in the Raman Spectra of Linear Molecules: Acetylene. By S. BHAGAVANTAM and A. VEERABHADRA RAO ..	135
Intensities in the Bands of the Violet Cyanogen System. By DR. N. R. TAWDE, B.A., M.SC. (BOM.), PH.D. (LOND.), A.INST.P. (LOND.) ..	140
The Absorption Spectra of Some Aromatic Compounds. Part I.—Hydrocarbons. By P. K. SESHAN	148
The Absorption Spectra of Some Aromatic Compounds. Part II.—Quinones and Hydroquinones. By P. K. SESHAN	172
Diamagnetic Susceptibility of Sulphuric Acid-Water Mixture. By B. NAGESHA RAO	188

Price Rs. 2 or 3 Sh. *Annual Subscription Rs. 18*

UNITARY THEORY OF FIELD AND MATTER.

II. Classical Treatment. Charged Particle with Electric and Magnetic Moment.

By Max Born.

(From the Department of Physics, Indian Institute of Science, Bangalore.)

Received December 30, 1935.

(Communicated by Sir C. V. Raman, Kt., F.R.S., N.L.)

Introduction.

In the preceding paper we have derived Kramers's " classical " equations of motion of a spinning electron from the unitary field theory. This seems very satisfactory, but we have already mentioned in the conclusion of that paper that a closer examination of the problem leads to serious difficulties. We shall explain these here and proceed then to avoid them by more general assumptions.

1. Kramers's " classical " equations of motion of the spinning electron.

Following Kramers's reasoning, we write the equations of motion I, (5, 42), (5, 43), (5, 44) for the rest system.

$$(1,\ 1)\qquad \begin{cases} \dfrac{d\vec{G}}{dt} = e\vec{E}, & \dfrac{dE}{dt} = 0, \\ \dfrac{d\vec{M}}{dt} = \vec{B} \times \vec{m}, & \dfrac{d\vec{P}}{dt} = \vec{E} \times \vec{m} \end{cases}$$

They hold also in any system for a slow moving particle where $\vec{v}$ and

$$(1,\ 2)\qquad \vec{p} = \vec{m} \times \vec{v}$$

are small quantities.

Now $(\vec{m}, \vec{p})$ and $(\vec{M}, \vec{P})$ are two 6-vectors. Kramers assumes that they are proportional, writing

$$(1,\ 3)\qquad \vec{m} = a\vec{M}, \quad \vec{p} = a\vec{P}.$$

Now from (1, 1) it follows that

$$(1,\ 4)\qquad E = E_0 = \mu$$

is a constant, the rest-mass, and

$$(1,\ 5) \qquad \frac{d\vec{G}}{dt} = \mu \frac{d\vec{v}}{dt} = e\vec{E},$$

therefore

$$(1,\ 6) \qquad \frac{d\vec{p}}{dt} = \alpha \frac{d\vec{P}}{dt} = \alpha(\vec{E} \times \vec{m}) = \frac{\alpha\mu}{e}\left(\frac{d\vec{v}}{dt} \times \vec{m}\right).$$

But from (1, 2) one has, for small $\vec{v}$,

$$(1,\ 7) \qquad \frac{d\vec{p}}{dt} = \vec{m} \times \frac{d\vec{v}}{dt}$$

(1, 6) and (1, 7) are compatible only if

$$(1,\ 8) \qquad \alpha = -\frac{e}{\mu}.$$

Since α is the ratio of magnetic moment and angular momentum, we have derived the fundamental formula of Uhlenbeck and Goudsmit's theory of the spinning electron (usually expressed in common units as the assumption that the ratio $\frac{m}{M}$ is $\frac{e}{\mu c}$ — not $\frac{e}{2\mu c}$ as for the orbital motion).

2. Critical considerations.

From Kramers's standpoint this seems to be extremely welcome ; it indicates that the main property of the spin can be described by classical mechanics.

But from the standpoint of the unitary field theory the situation is not at all satisfactory.

For in this theory, one should expect the problem of determining the motion of a singularity in a constant external field must have a definite solution whatever the Lagrangian L may be (if it satisfies only the conditions of relativity invariance). But the condition (1, 8) which can be written

$$(2,\ 1) \qquad \frac{\vec{M}_0}{\vec{E}_0} = \frac{\vec{m}}{e}$$

is a condition restricting L ; for the left-hand term is the ratio of integrals depending on the solution of the field equations, *i.e.*, on L. We shall explain this for the case of quasi-stationary motion, where the acceleration of the singularity is so small that the inner field in the rest system can be considered as static :

$$(2,\ 2) \qquad \begin{cases} \text{rot } E^0 = 0, & \text{div } D^0 = 0: \text{ Electro-static field} \\ \text{rot } H^0 = 0, & \text{div } B^0 = 0: \text{ Magneto-static field} \end{cases}$$

We have to solve these equations under the boundary conditions

$$(2,\ 3)\quad \left\{\begin{array}{l} \int_0 (\vec{n}\cdot\vec{D}^0)\,d\sigma = e, \\ \int_0 (\vec{a}\ \vec{r})\cdot(\vec{n}\times\vec{E}^0)\,d\sigma = 0 \end{array}\right\} \text{electric boundary conditions,}$$

$$(2,\ 4)\quad \left\{\begin{array}{l} \int_0 (\vec{n}\cdot\vec{B}^0)\,d\sigma = 0, \\ \int_0 (\vec{a}\ \vec{r})\cdot(\vec{n}\times\vec{H}^0)\,d\sigma = \vec{a}\times\vec{m} \end{array}\right\} \text{magnetic boundary conditions,}$$

(where $\vec{a}$ is an arbitrary vector), and

$$(2,\ 5)\quad \left\{\begin{array}{l} \int_0 (\vec{X}\ \vec{n})\,d\sigma = 0, \cdots\cdots \\ \int_0 (\vec{S}\ \vec{n})\,d\sigma = 0,\ \int_0 \vec{r}\,(\vec{S}\ \vec{n})\,d\sigma = 0 \end{array}\right\} \text{dynamical conditions.}$$

The distribution of the field depends linearly on e and $\vec{m}$, which can be arbitrarily given, but also essentially on the Lagrangian L, which determines the functions representing D^0, H^0 in terms of E^0, B^0. Therefore

$$(2,\ 6)\quad E_0 = \int (L + E^0D^0)\,dv,\quad \vec{M}_0 = \int [\vec{r}\times(D^0\times B^0)]\,dv$$

depend also on the choice of L, and there seems to be no general theorem which guarantees the fulfilment of the relation (2, 1).

If Kramers's arguments are considered as right they would imply a sharp condition for the choice of the Lagrangian L, the analytical meaning of which is rather obscure.

But I do not believe that Kramers's considerations are convincing, since the spin $\frac{1}{2}$ of the electron has no classical analogy. It is well known that the spin is closely connected with the two valued representation of the Lorentz-group which cannot be interpreted in terms of classical theory. The classical analogy of a particle with the spin $\frac{1}{2}$ is the non-rotating system; the value $\frac{1}{2}$ means a kind of zero-point rotation—just as the zero-point energy of the linear oscillator $\frac{1}{2}h\nu$ corresponds classically to the non-oscillating state.

My collaborator Pryce has recently put forward the idea that the state of one-quantum rotation represents the proton, and I have confirmed this

by an estimate of the mass-ratio, proton : electron.[1] If this idea is sound Kramers's considerations leading to (2, 1) should not be considered as stringent. Then the problem arises how to modify the theory to avoid these conclusions.

It is clear that they spring from the assumption of a pure magnetic moment in the rest-system, expressed by (1, 2). This assumption leads also to other difficulties, if one combines it with the simplest Lagrangian which in the rest-system has the expression

$$(2,\ 7)\quad L = \sqrt{1 + B_0^2 - E_0^2} - 1.$$

For there exists no statical solution for an uncharged particle with a magnetic moment. In this case one has

$$(2,\ 8)\quad \vec{B}_0 = \frac{\vec{H}_0}{\sqrt{1 - H_0^2}},$$

and $\vec{H}_0$ has a singularity of the character of a classical dipole. Then (2, 8) shows that B_0 becomes infinite at a finite distance from the singularity of $\vec{H}_0$.[2]

This difficulty may disappear if besides the magnetic moment the particle has a charge, or an electric moment or both. We shall therefore modify the theory given in Part I so as to represent the motion of a charged particle having in the rest-system an electric and a magnetic moment $\vec{p}_0$ and $\vec{m}_0$. We do this chiefly because the generalised theory, owing to its higher symmetry, is mathematically more perfect. The question whether such a system is likely to represent a real particle will be touched at the end of this communication.

3. *Charged particle with electric and magnetic moment.*

We use the notations of Part I with a few modifications which shall be given here.

The orbit of the singularity is given by the vector $\vec{r}_0\ (t)$, its velocity by $\vec{v}\ (t) = \frac{d\vec{r}_0}{dt}$. We introduce the 4-vector

$$(3,\ 1)\quad (v^1, v^2, v^3, v^4) = \left(\frac{\vec{v}}{a}, \frac{1}{a}\right), \qquad a = \sqrt{1 - v^2}.$$

---

[1] M. Born, *Nature*, 1935, **136**, 952.

[2] The reason for the difference of the electrostatic and magnetostatic cases is the difference of the signs of B_0^2 and E_0^2 in (2, 7). In the electric case the corresponding formula to (2, 8) is $\vec{E}_0 = \vec{D}_0/\sqrt{1 + D_0^2}$; there $\vec{D}_0$ has an infinity, but $\vec{E}_0$ remains finite.

$\delta_0(\vec{r} - \vec{r}_0)$ is a 3-dimensional δ-function in the rest-system, and

$$(3,\ 2)\quad \delta(\vec{r} - \vec{r}_0, t) = \frac{\delta_0}{\sqrt{1 - v^2}} = \frac{\delta_0}{a}$$

the corresponding δ-function in any system. One has

$$(3,\ 3)\quad \int f\delta_0 dv_0 = \int f\delta dv = f(\vec{r}_0).$$

The electric rest-density is

$$(3,\ 4)\qquad \rho_0 = e\delta_0$$

where e is the electric charge.

The 4-vector current-density is given by

$$(3,\ 5)\quad (\rho^1, \rho^2, \rho^3, \rho^4) = \rho_0(v^1, v^2, v^3, v^4) = \left(\frac{\rho_0 \vec{v}}{a}, \frac{\rho_0}{a}\right),$$

or, if we introduce the density

$$(3,\ 6)\quad \rho = \frac{\rho_0}{a} = \frac{e\delta_0}{a} = e\delta,$$

we have

$$(3,\ 7)\quad (\rho^1, \rho^2, \rho^3, \rho^4) = (\rho \vec{v}, \rho) = (e \vec{v}\,\delta, e\delta).$$

The continuity equation is

$$(3,\ 8)\quad \frac{\partial e v^k \delta}{\partial x^k} = 0, \quad \text{or} \quad e \vec{v}\ \text{grad}\ \delta + \frac{\partial e \delta}{\partial t} = 0.$$

Integrating this over space, one gets

$$(3,\ 9)\qquad \frac{de}{dt} = 0, \quad e = \text{const.}$$

Multiplying (3, 8) by x and then integrating, one has

$$\int x \left(v_x \frac{\partial \delta}{\partial x} + v_y \frac{\partial \delta}{\partial y} + v_z \frac{\partial \delta}{\partial z}\right) dv + \frac{d}{dt}\int x\delta dv = 0,$$

or

$$-v_x + \frac{dx_0}{dt} = 0, \cdots\cdots$$

in agreement with the definition of $\vec{v}$.

The electric moment is assumed to be a space vector in the rest-system, $\vec{p}_0$; it corresponds to a 4-vector

$$(3,\ 10)\quad (p^1, p^2, p^3, p^4) = [\vec{p}_0, (\vec{v}\,\vec{p}_0)],$$

satisfying the condition

$$(3,\ 11)\qquad v^k p_k = 0.$$

In the same way one has for the magnetic moment

$$(3, 12)\quad (m^1, m^2, m^3, m^4) = [\vec{m}_0, (\vec{v}\ \vec{m}_0)],$$

$$(3, 13)\quad v^k m_k = 0.$$

The corresponding part of the Lagrangian must be a simultaneous invariant of the three 4-vectors v^k, p^k, m^k and the field 6-vector f_{kl} which reduces to

$$\vec{m}_0 \vec{\mathrm{B}} - \vec{p}_0 \vec{\mathrm{E}}$$

in the rest-system. To construct this invariant, we form first the 6-vector[3]

$$(3, 14)\quad m^{kl} = (v^k p^l - v^l p^k) + (v^k m^l - v^l m^k)^*$$

and write

$$(3, 15)\quad (m_{23}, m_{31}, m_{12}) = \frac{1}{a}\vec{m}, \qquad (m_{14}, m_{24}, m_{34}) = \frac{1}{a}\vec{p},$$

where

$$(3, 16)\quad \begin{cases} \vec{p} = \vec{p}_0 - \vec{v}\,(\vec{p}_0 \vec{v}) - (\vec{v} \times \vec{m}_0), \\ \vec{m} = \vec{m}_0 - \vec{v}\,(\vec{m}_0 \vec{v}) + (\vec{v} \times \vec{p}_0). \end{cases}$$

Then the invariant in question is evidently

$$(3, 17)\quad \tfrac{1}{2} m^{kl} f_{kl} = \tfrac{1}{2}\{(v^k p^l - v^l p^k) + (v^k m^l - v^l m^k)^*\} f_{kl} = \vec{m}\vec{\mathrm{B}} - \vec{p}\vec{\mathrm{E}}.$$

Since for any two tensors f_{kl}, g_{kl} there is $f_{kl} g^{*kl} = f^*_{kl} g^{kl}$ we write (3, 17) as

$$(3, 18)\quad \tfrac{1}{2} m^{kl} f_{kl} = f_{kl} v^k p^l + f^*_{kl} v^k m^l = (f_{kl} p^l + f^*_{kl} m^l) v^k.$$

The first of these expressions may be interpreted as the negative work done by the electric and magnetic forces:

$$(3, 19)\quad \begin{cases} f_{kl} v^l = \dfrac{1}{a}[\vec{\mathrm{E}} + (\vec{v} \times \vec{\mathrm{B}})], \\ f^*_{kl} v^l = \dfrac{1}{a}[\vec{\mathrm{B}} - (\vec{v} \times \vec{\mathrm{E}})] \end{cases}$$

on the electric and magnetic rest-momenta $\vec{p}_0$, $\vec{m}_0$.

The Lagrangian of the singularity is

$$(3, 20)\quad \begin{cases} l\delta = \delta_0(e v^k \phi_k + \tfrac{1}{2} m^{kl} f_{kl}) \\ \quad = \delta(e\phi - e\,\vec{v}\vec{\mathrm{A}} + \vec{m}\vec{\mathrm{B}} - \vec{p}\vec{\mathrm{E}}) \end{cases}$$

in complete agreement with I, (3, 1).

---

[3] a^*_{kl} is the dual tensor of a_{kl}; one has $a^{*23} = a_{14}$, ····, $a^{*14} = a_{23}$, ····, but $a^*_{23} = -a^{14}$, ···· $a^*_{14} = -a^{23}$, ····; or $a^{*23} = -a^{14}$, ···· $a^{*14} = a^{23}$, ····, and $a^*_{23} = a_{14}$, ····, $a^*_{14} = -a_{23}$, ·····

4. *Field equations and boundary conditions.*

The field equations are exactly the same as those given in I, (1, 5), (1, 6). We write only the essential set

$$(4,\ 1)\qquad \frac{\partial p^{kl}}{\partial x^l} = \rho_0 v^k - \frac{\partial m^{kl}\delta}{\partial x^l},$$

or

$$(4,\ 2)\qquad \begin{cases} \operatorname{rot} \vec{H} - \dot{\vec{D}} = \delta(e\vec{v} + \dot{\vec{p}}) - \operatorname{rot}(\vec{m}\,\delta), \\ \operatorname{div} \vec{D} = \delta e - \operatorname{div}(\vec{p}\,\delta). \end{cases}$$

As explained in I, one can replace the right-hand terms by o, adding the boundary conditions

$$(4,\ 3)\qquad \begin{cases} \int_0 (\vec{n} \times \vec{H})\, d\sigma = e\vec{v} + \dot{\vec{p}}, & \int_0 \vec{n}\,\vec{D}\, d\sigma = e, \\ \int_0 (\vec{n} \times \vec{E})\, d\sigma = 0, & \int_0 \vec{n}\,\vec{B}\, d\sigma = 0, \end{cases}$$

$$(4,\ 4)\qquad \begin{cases} \int_0 (\vec{a}\,\vec{r})(\vec{n} \times \vec{H})\, d\sigma = \vec{a} \times \vec{m}, & \int_0 \vec{r}\,(\vec{u}\,\vec{D})\, d\sigma = e\vec{r}_0 + \vec{p}, \\ \int_0 (\vec{a}\,\vec{r})(\vec{n} \times \vec{E})\, d\sigma = 0, & \int_0 \vec{r}\,(\vec{n}\,\vec{B})\, d\sigma = 0, \end{cases}$$

where $\vec{a}$ is an arbitrary vector.

5. *Dynamical boundary conditions.*

For the variation of the world line of the singularity we use the second expression (3, 18) ; then we have the variation problem :

$$(5,\ 1)\qquad \int \delta_0(e\phi_k + f_{kl}p^l + f^*_{kl}m^l)\,\dot{x}^k\, dv_0\, d\tau = \text{Extremum},$$

with the conditions

$$(5,\ 2)\qquad \dot{x}^k\dot{x}_k = 1, \qquad \dot{x}^k p_k = 0, \qquad \dot{x}^k m_k = 0\,;$$

the first of these expresses that τ is the proper time, the others are a repetition of (3, 11), (3, 13).

We vary first p^l and m^l ; with the help of two Lagrangian multipliers λ_1, λ_2, we get

$$(5,\ 3)\qquad \begin{cases} f_{kl}\dot{x}^k + \lambda_1 \dot{x}_l = 0, \\ f^*_{kl}\dot{x}^k + \lambda_2 \dot{x}_l = 0. \end{cases}$$

Multiplication with $\dot{x}^l$ and summation gives

$$(5,\ 4)\qquad \begin{cases} \lambda_1 = -f_{kl}\dot{x}^k\dot{x}^l = 0, \\ \lambda_2 = -f^*_{kl}\dot{x}^k\dot{x}^l = 0, \end{cases}$$

since f_{kl} is antisymmetric. Therefore (5, 3) reduces to

$$(5,\ 5)\quad f_{kl}\dot{x}^k = 0, \qquad f^*_{kl}\dot{x}^k = 0,$$

or

$$(5,\ 6)\quad [\vec{E} + (\vec{v} \times \vec{B})]_0 = 0, \quad [\vec{B} - (\vec{v} \times \vec{E})]_0 = 0.$$

The electric and magnetic "Lorentz-force" vanishes at the singularity.[4]

Since λ_1, λ_2 vanish, the second and third condition (5, 2) can be omitted. The first condition (5, 2) corresponds to a Lagrangian multiplier μ. Varying x^n, we get

$$(5,\ 7)\quad \iiint \delta_0 \left\{ \frac{d\mu \dot{x}_n}{dt} - K_n \right\} dv_0 = 0,$$

or symbolically

$$(5,\ 8)\qquad \left[\frac{d\mu \dot{x}_n}{dt} - K_n \right]_0 = 0,$$

where

$$K_n = \frac{\partial}{\partial x^n}(e\phi_k + f_{kl}p^l + f^*_{kl}m^l)\ \dot{x}^n - \frac{d}{d\tau}(e\phi_n + f_{nl}p^l + f^*_{nl}m^l)$$

or

$$(5,\ 9)\quad K_n = \left\{ ef_{kn} + \left(\frac{\partial f_{kl}}{\partial x^n} - \frac{\partial f_{kl}}{\partial x^k} \right) p^l + \left(\frac{\partial f^*_{kl}}{\partial x^n} - \frac{\partial f^*_{nl}}{\partial x^k} \right) m^l \right\} \dot{x}^k.$$

The bracket is antisymmetric in k, n; therefore

$$(5,\ 10)\qquad K_n \dot{x}^n = 0.$$

Multiplying (5, 8) by $\dot{x}^n$ we have

$$\dot{x}^n \frac{d\mu \dot{x}_n}{dt} = \mu \dot{x}^n \ddot{x}_n + \dot{\mu}\dot{x}^n \dot{x}_n = 0,$$

or, since $\dot{x}^n \dot{x}_n = 1$, $\dot{x}^n \ddot{x}_n = 0$:

$$(5,\ 11)\qquad \dot{\mu} = 0, \quad \mu = \text{const.}$$

---

[4] We remind the reader that the vanishing of a quantity at the singularity, written symbolically $f_0 = 0$ means really $\int_0 \delta_0 f dv_0 = 0$. For instance, for the Lagrangian $L = \sqrt{1 - E^2} - 1$ the field of a point charge is $\vec{E} = \frac{e}{\sqrt{e^2 + r^4}} \cdot \frac{\vec{r}}{r}$, it has a "harmless" singularity at $\vec{r} = 0$, *i.e.*, E_x jumps from -1 to $+1$ if one passes the singular point along the X-axis. But one has

$$\int_0 \delta_0 E_x\, dv_0 = \int_0 \delta_0 \frac{x}{r}\, dv_0 = 0,$$

or symbolically $(E_x)_0 = 0$. The expressions (5, 6), etc., have to be interpreted in the same way.

μ represents therefore (as in Part I) a constant rest-mass attached to the singularity. According to the fundamental idea of the unitary theory, we put

$$\mu = 0 \tag{5, 12}$$

and have

$$[\mathrm{K}_n]_0 = 0. \tag{5, 13}$$

Taking account of (5, 5), this means

$$[\mathrm{K}_n]_0 = \left[\left\{\left(\frac{\partial f_{kl}}{\partial x^n} - \frac{\partial f_{nl}}{\partial x^k}\right) p^l + \left(\frac{\partial f^*_{kl}}{\partial x^n} - \frac{\partial f^*_{nl}}{\partial x^k}\right) m^l\right\} \dot{x}^k\right]_0 = 0. \tag{5, 14}$$

In the rest-system the dynamical conditions (5. 6), (5, 14) reduce to

$$\begin{cases} \vec{\mathrm{E}}_0 = 0, \quad \vec{\mathrm{B}}_0 = 0, \\ \vec{\mathrm{K}}_0 = -\,[\mathrm{grad}\,(\vec{\mathrm{B}}\,\vec{m}_0 - \vec{\mathrm{E}}\,\vec{p}_0)]_0 = 0. \end{cases} \tag{5, 15}$$

6. *Conservation Laws.*

The conservation laws can be taken over unchanged from Part I, (4, 5):

$$\frac{\partial \mathrm{T}_k{}^l}{\partial x^l} = \delta_0 f_{kn}\rho^n + \tfrac{1}{2} f_{nl}\frac{\partial (m^{nl}\delta)}{\partial x^k} - \frac{\partial (t_k{}^l \delta)}{\partial x^l}, \tag{6, 1}$$

where

$$t_k{}^l = \lambda \delta_k{}^l - m^{ln} f_{kn}, \tag{6, 2}$$

$$\lambda = \tfrac{1}{2} m^{nl} f_{nl}\,; \tag{6, 3}$$

or, in space-vector notation [I, (4, 14)] for the rest-system:

$$\begin{cases} \dfrac{\partial \rho_x}{\partial t} + \mathrm{div}\,\vec{\mathrm{X}} = \delta_0 e \mathrm{E}_x + \vec{\mathrm{B}}\dfrac{\partial (\vec{m}_0 \delta_0)}{\partial x} - \vec{\mathrm{E}}\dfrac{\partial (\vec{p}\,\delta_0)}{\partial x} - \delta_0 \dot{\vec{s}}_x - \mathrm{div}\,(\vec{x}\,\delta_0), \\ - - - - \\ - - - - \\ \dfrac{\partial \mathrm{U}}{\partial t} + \mathrm{div}\,\vec{\mathrm{S}} = \delta_0 (\vec{\mathrm{B}}\,\dot{\vec{m}}_0 - \vec{\mathrm{E}}\,\dot{\vec{p}}_0) - \delta_0 u - \mathrm{div}\,(\vec{s}\,\delta_0). \end{cases} \tag{6, 4}$$

Integrating over a small sphere surrounding $\vec{r}_0$, and using (5, 15), one gets

$$\begin{cases} \int_0 (\vec{\mathrm{X}}\,\vec{n})\, d\sigma = -\left[\vec{m}_0 \dfrac{\partial \vec{\mathrm{B}}}{\partial x} - \vec{p}_0 \dfrac{\partial \vec{\mathrm{E}}}{\partial x}\right]_0 = -\,[\mathrm{K}_x]_0 = 0, \\ \int_0 (\vec{\mathrm{S}}\,\vec{n})\, d\sigma = \left[\dot{\vec{m}}_0 \vec{\mathrm{B}} - \dot{\vec{p}}_0 \vec{\mathrm{E}}\right]_0 = 0. \end{cases} \tag{6, 5}$$

In the same way one finds

$$\int_0 (\vec{\mathrm{N}}_x \vec{n})\, d\sigma = 0, \tag{6, 6}$$

where $\vec{N}_x$ is defined in Part I, (4, 17), and

$$(6,\ 7)\qquad \int_0 \vec{r}\ (\vec{S}\,\vec{n})\ d\sigma = 0.$$

For all fields satisfying the boundary conditions (6, 5), (6, 6), (6, 7) one has the conservative in laws

$$(6,\ 8)\qquad \begin{cases} \dfrac{\partial \vec{S}_x}{\partial t} + \operatorname{div} \vec{X} = 0, \cdots\cdots \\ \dfrac{\partial U}{\partial t} + \operatorname{div} \vec{S} = 0. \end{cases}$$

7. *Equations of motion in a constant field.*

The considerations of I, section 5, can be transferred without change to our more general case. We have [I (5, 4), (5, 5)] :

$$(7,\ 1)\qquad \begin{cases} \dfrac{dG_x}{dt} + \int_\infty (\vec{X}\,\vec{n})\ d\sigma = 0, \cdots\cdots \\ \dfrac{dE}{dt} + \int_\infty (\vec{S}\,\vec{n})\ d\sigma = 0, \end{cases}$$

$$(7,\ 2)\qquad \begin{cases} \dfrac{dM_x}{dt} + \int_\infty (\vec{N}_x\,\vec{n})\ d\sigma = 0, \cdots\cdots \\ \dfrac{dE\vec{q}}{dt} - \vec{G} + \int_\infty \vec{r}\ (\vec{S}\,\vec{n})\ d\sigma = 0. \end{cases}$$

Splitting the field into an external and an internal field we get [I (5, 11), (5, 12)] :

$$(7,\ 3)\qquad \begin{cases} \vec{G} = \vec{G}^i + \left(\vec{D}^e \times \int \vec{B}^i\, dv\right) - \left(\vec{B}^e \times \int \vec{D}^i\, dv\right), \\ M_x = M_x{}^i + D_x{}^e \int (\vec{r}\,\vec{B}^i)\, dv - \vec{D}^e \cdot \int \vec{r}\, B_x{}^i\, dv \\ \qquad\qquad - B_x{}^e \int (\vec{r}\,\vec{D}^i)\, dv + \vec{B}^e \cdot \int \vec{r}\, D_x{}^i\, dv\,; \end{cases}$$

and [I (5, 33), (5, 3)] :

$$(7,\ 4)\qquad \begin{cases} \dfrac{dE}{dt} = \dfrac{dE^i}{dt} + \vec{H}^e \cdot \int \dot{\vec{B}}^i\, dv + \vec{E}^e \cdot \int \dot{\vec{D}}^i\, dv, \\ \dfrac{dEq_x}{dt} = \dfrac{dE^i q_x{}^i}{dt} + \vec{H}^e \cdot \int x\, \dot{\vec{B}}^i\, dv + \vec{E}^e \cdot \int x\, \dot{\vec{D}}^i\, dv, \\ \vec{G} = \vec{G}^i + (\vec{E}^e \times \int \vec{H}^i\, dv) - (\vec{H}^e \times \int \vec{E}^i\, dv). \end{cases}$$

On the other hand the scalar products in the surface integrals (7, 1) have the values I, (5, 15), (5, 16), (5, 17):

$$(7,\ 5)\quad \begin{cases} (\vec{X}\,\vec{n}) = (\vec{X}^e\,\vec{n}) + H_x{}^e\,(\vec{B}^i\,\vec{n}) + E_x{}^e\,(\vec{D}^i\,\vec{n}) \\ \qquad - [\vec{B}^e \times (\vec{n} \times \vec{H}^i)]_x - [\vec{D}^e \times (\vec{n} \times \vec{E}^i)]_x \\ (\vec{S}\,\vec{n}) = (\vec{S}^e\,\vec{n}) - \vec{E}^e \cdot (\vec{n} \times \vec{H}^i) + \vec{H}^e \cdot (\vec{n} \times \vec{E}^i), \\ (\vec{N}_x\,\vec{n}) = (\vec{N}_x{}^e\,\vec{n}) + (\vec{B}^e\,\vec{r})\,(\vec{n} \times \vec{H}^i)_x - B_x{}^e\,\vec{r} \cdot (\vec{n} \times \vec{H}^i) \\ \qquad\qquad + (\vec{D}^e\,\vec{r})\,(\vec{n} \times \vec{E}^i)_x - D_x{}^e\,\vec{r} \cdot (\vec{n} \times \vec{E}^i) \\ \qquad\qquad - (\vec{H}^e \times \vec{r})_x\,(\vec{n}\,\vec{B}^i) - (\vec{E}^e \times \vec{r})_x\,(\vec{n}\,\vec{D}^i). \end{cases}$$

We shall now proceed (deviating from I) without specialising the co-ordinate system. Integrating the field equations (4, 2) and taking account of the boundary conditions (4, 3), (4, 4) we get

$$(7,\ 6)\quad \begin{cases} \int_\infty (\vec{n} \times \vec{H}^i)\,d\sigma = \int \dot{\vec{D}}^i\,dv - e\,\dot{\vec{v}} - \dot{\vec{p}}, & \int_\infty \vec{n}\,\vec{D}^i\,d\sigma = -e, \\ \int_\infty (\vec{n} \times \vec{E}^i)\,d\sigma = -\int \dot{\vec{B}}_i\,dv, & \int_\infty \vec{n} \cdot \vec{B}^i\,d\sigma = 0; \end{cases}$$

$$(7,\ 7)\quad \begin{cases} \int_\infty (\vec{a}\,\vec{r})\,(\vec{n} \times \vec{H}^i)\,d\sigma = \int \left\{ (\vec{a}\,\vec{r})\,\dot{\vec{D}}^i + (\vec{a} \times \vec{H}^i) \right\} dv - (\vec{a} \times \vec{m}), \\ \int_\infty \vec{r}\,(\vec{n}\,\vec{D}^i)\,d\sigma = \int \vec{D}^i\,dv - e\,\vec{r}_0 - \vec{p}; \end{cases}$$

$$(7,\ 8)\quad \begin{cases} \int_\infty (\vec{a}\,\vec{r})\,(\vec{n} \times \vec{E}^i)\,d\sigma = -\int \left\{ (\vec{a}\,\vec{r})\,\dot{\vec{B}}^i - (\vec{a} \times \vec{E}^i) \right\} dv, \\ \int_\infty \vec{r}\,(\vec{n}\,\vec{B}^i)\,d\sigma = \int \vec{B}^i\,dv. \end{cases}$$

Introducing this into (7, 1), (7, 2) one finds (omitting the indices e, i):

$$(7,\ 9)\quad \begin{cases} \dfrac{d\vec{G}}{dt} = e[\vec{E} + (\vec{v} \times \vec{B})] + (\dot{\vec{p}} \times \vec{B}), \\ \dfrac{dE}{dt} = e(\vec{v}\,\vec{E}) + (\dot{\vec{p}}\,\vec{E}); \end{cases}$$

$$(7,\ 10)\quad \begin{cases} \dfrac{d\vec{M}}{dt} = (\vec{B} \times \vec{m}) - (\vec{E} \times \vec{p}) - e(\vec{E} \times \vec{r}_0), \\ \dfrac{dE\,\vec{q}}{dt} - \vec{G} = (\vec{E} \times \vec{m}) + (B \times \vec{p}) + e(\vec{B} \times \vec{r}_0). \end{cases}$$

Here $\vec{G}$, $\vec{E}$, $\vec{M}$, $\vec{q}$ refer to the inner field; $\vec{E}$, $\vec{B}$ represent the constant external field.

$\vec{M}$ and $\vec{q}$ are angular momentum and position of the centre of energy relative to the arbitrary origin. We introduce instead the corresponding quantities relative to the particle

$$(7, 11) \quad \begin{cases} \vec{M'} = \vec{M} - (\vec{r_0} \times \vec{G}), \\ \vec{q'} = \vec{q} - \vec{r_0}. \end{cases}$$

If we restrict ourselves to the quasi-stationary case where $\vec{G}$, $\vec{E}$ depend on $\vec{v}$ in the same way as for free motion ($\vec{E} = 0$, $\vec{B} = 0$), then

$$(7, 12) \quad \vec{G} = \vec{E}\vec{v}, \qquad \dot{\vec{r}}_0 \times \vec{G} = \vec{v} \times \vec{G} = 0,$$

therefore

$$(7, 13) \quad \frac{d\vec{M'}}{dt} = \frac{d\vec{M}}{dt} - \left(\vec{r}_0 \times \frac{d\vec{G}}{dt}\right).$$

(7, 10) can be written

$$(7, 14) \quad \begin{cases} \dfrac{d\vec{M'}}{dt} = (\vec{B} \times \vec{m}) - (\vec{E} \times \vec{p}) + [\vec{r}_0 \times \{\vec{B} \times (e\vec{v} + \dot{\vec{p}})\}]. \\ \dfrac{d\vec{E}\vec{q'}}{dt} = (\vec{E} \times \vec{m}) + (\vec{B} \times \vec{p}) + e(\vec{B} \times \vec{r_0}) - \vec{r_0}\,[\vec{E} \cdot (e\vec{v} + \dot{\vec{p}})]. \end{cases}$$

The additional terms which are proportional to $\vec{r_0}$ have been omitted in Part I, just as the terms with $\dot{\vec{p}}$ in (7, 9). They have the following meaning: The " displacement current " $\dot{\vec{p}}$ is attacked by the magnetic field just as the convection current $e\vec{v}$, and modifies the orbit; conversely the orbit acts with a kind of centrifugal force on the angular momentum and the energy-centre. These effects can be neglected for slow motions (as done in I) if $\vec{p}$ is supposed to vanish for $\vec{v} = 0$ (Kramers's assumption $\vec{p} = \vec{m} \times \vec{v}$); but here, in the general case, this is not allowed.

8. *Conclusion.*

The equations (7, 9), (7, 14) are a generalisation of Kramers's equations, derived in I, to which they reduce for $\vec{p_0} = 0$. The new equations are self-consistent without imposing a restriction on the Lagrangian. This seems

satisfactory from the purely formal standpoint. But on the other hand the elementary particles occurring in nature (electrons, protons) have no electric rest-moment, as far as we know. If the classical treatment of the unitary theory has a meaning at all, it leads to the conclusion that point singularities are not the correct representation of the particles. The question whether there exist other possibilities will be considered later.

THE MEASUREMENT OF THE TRANSMISSION OF HEAT BY CONVECTION FROM INSOLATED GROUND TO THE ATMOSPHERE.

By P. K. Raman.

Received December 12, 1935.
(Communicated by Dr. K. R. Ramanathan, D.Sc.)

Introduction.

For more than six hours on a clear day in tropical and subtropical continental areas, the ground is often more than 15° C. warmer than the air at a level of 4 ft. above ground, and at the time of maximum ground-temperature, the excess may be as much as 25–35° C. This implies the transfer of a considerable amount of heat every day from the heated ground to the atmosphere and this process of convective heating plays a large part in determining the thermal properties of the air over these regions. A few attempts have been made by European workers[1,2,3] to estimate the quantities of heat transferred to the atmosphere by convection in temperate regions. But quantitative measurements are few and the methods are often indirect. Dines[2] estimates the average daily addition of heat throughout the earth by convective processes to be 200 calories/cm.^{2} This includes the heat (150 cal./cm.^{2}) contributed by condensation of moisture. In the present paper is described a simple apparatus for determining the rate at which heat is transferred from dry ground to the atmosphere; the instrument was used to determine the quantity of heat transferred to the atmosphere by convection on a number of days in clear weather at Poona during the period, January-May 1935. The results of the open-air measurements are compared with those from laboratory experiments obtained by other workers and it is shown that a simple formula can be used for estimating the rate at which heat is transferred to the atmosphere from heated ground in terms of the surface temperature of the ground and the meteorologically measured quantities, temperature of air and wind-velocity at 4 ft.

As a problem of general ærodynamics, the subject of heat transfer from a hot body by convection to the surrounding fluid has been investigated by a number of workers, both experimentally and theoretically. When the fluid has no general movement, but has only internal movements arising from the differences of density caused by the contact of portions of the fluid

with the hot solid, the convection is called 'free' or 'natural'; when a general movement of the fluid is super-posed, the convection is called 'forced'. In the atmosphere natural convection is of comparatively less importance, as absolute calm is very rare, especially in the hot hours of the day. For theoretical calculations, the surface of the earth may be considered as a rough horizontal plane of infinite extent and the stream of fluid roughly parallel to the surface.

Apparatus and Method of Measurement.

The apparatus used for measuring the rate of transfer of heat is similar in principle to that of the Angstrom's Pyrgeometer. A thin polished silver-plated constantan strip AB (Fig. 1) is mounted between the ends of a pair

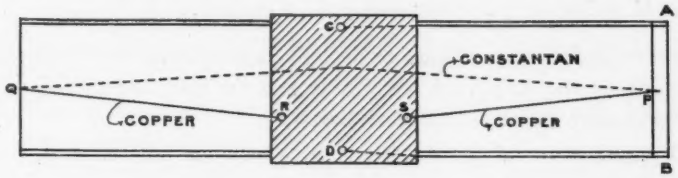

FIG. 1.

of parallel copper rods (nickel-plated and polished) carried on a base of ebonite. The copper rods are connected to two terminals C and D. One junction P of a copper-constantan thermo-couple is placed in thermal contact with the centre of the surface of the strip AB; the other junction at Q being suitably mounted on silk fibres so that it can be placed in contact with the surface under investigation. The under-side of the constantan strip is lined with a layer of cork so that when placed on the ground it is thermally insulated from it. R and S are the terminals for connecting the thermo-couple to a suspended coil galvanometer. The strip can be heated electrically as required and the current measured on a calibrated ammeter. The convection apparatus was exposed in the open while the battery, electrical instruments, etc., were housed in an adjoining hut.

The measurements were made on clear days during the winter of 1935 at the Agricultural Meteorological Observatory at Poona which is situated in an open place well removed from buildings. On a selected plot of level ground the apparatus was placed with the under-surface of the strip thermally insulated from the ground and the junction Q in thermal contact with the soil surface. The upper surface of the strip was placed flush with the surface of the ground (but not actually touching it) so as to reduce the boundary effects to a minimum. The current required to be passed through the strip when it was at the same temperature as the soil surface was measured.

Because of turbulent wind movements a perfectly steady null position could not be obtained. The reading of the current was taken when the galvanometer oscillated symmetrically about its zero position.

When the strip is in thermal equilibrium with the surface of the ground it gains heat energy from the electric current passing through it, and from the radiation of the sun and the sky; it loses heat by long wave radiation and by convection. The convective loss which is equal to that of the surrounding ground can be evaluated if the gain and loss of heat due to the remaining factors can be determined.

The energy consumed for heating the strip can be calculated from the current i, the resistance R and the area A of the strip. Thus

$$H = Ki^2 = \frac{60\,R}{AJ} i^2 \text{ gm. cal./cm.}^2 \text{ min.} \quad .. \quad .. \quad .. \quad (1)$$

To estimate the loss or gain of heat by radiation we require the effective absorptivity of the strip both for visible and for infra-red radiation. These were determined experimentally as below.

A Pyrheliometer of the Angstrom type was constructed with two strips of constantan cut from the same strip as was used for the convection instrument. One strip was kept with the original polish on and the other was given a thin uniform coating of lamp black. A series of measurements were taken with this Pyrheliometer with both the strips or the black strip alone successively exposed to direct solar radiation. From these the percentage of the incoming energy absorbed by the bright strip can be calculated. The average of a series of measurements showed that the bright strip absorbed 0·25 of the incident solar radiation. This same Pyrheliometer was used as a Pyrgeometer for measurements of nocturnal radiation and comparative observations taken with a standard Angstrom Pyrgeometer showed that the effective absorptivity of the bright strip was not appreciably different from 0·25 for thermal radiation also.

The heat transferred to the air from unit area of the strip in a unit of time by convection can be calculated as follows :—

$$H = \frac{Ri^2}{AJ} + a\Sigma + a_1 (s - \sigma T^4) \quad .. \quad .. \quad .. \quad (2)$$

where

H is the heat transferred by convection in gm.cal./cm.^{2} min.,

i is the heating current in amperes,

R and A are the resistance and area of the strip respectively,

Σ solar and visible sky radiation on a horizontal surface in gm.cal./cm.^{2} min.,

s atmospheric radiation (gm.cal./cm.^{2} min.) obtained from the mean of observations with Angstrom's Pyrgeometer on the previous night,

σT^4 the black body radiation (gm.cal./cm.^{2} min.) at the temperature T° Absolute of the ground at the time of observation ; σ being the Stefan-Boltzmann constant,

a and a_1 are the effective absorptivities of the strip for solar radiation and for long wave radiation respectively.

Measurements were also taken of the following elements before and after each reading with the convection apparatus :—

(1) The temperature of the surface of the ground with a surface thermometer.

(2) The temperature of the air above ground by an Assmann thermometer at about 1 cm. above surface.

(3) The temperature of the air at 4 ft. (from thermometer in Stevenson screen).

(4) The wind-velocity at the two levels $1\frac{1}{2}$ ft. and 6 ft. by Robinson cup anemometers.

(5) The radiation from the sun and the sky received on a horizontal surface at the time of each observation as read off from the Kipp and Zonen Solarigraph installed at the Observatory.

Results and Discussion.

Measurements of heat loss from ground due to convection show considerable fluctuations especially when the excess temperature of the ground is more than 10° C. Ordinarily, in winter and early hot season, the fluctuations are found to be greatest between the hours 10 and 14. Analysing the observations according to wind-velocity of 4 ft. above ground, the mean rates of loss of heat measured on different occasions are given in Tables I and II expressed as the ratio of the rate of loss of heat to the temperature difference between ground and air at 4 ft. For purposes of general application, it is necessary to find a formula that would fit the observations with a reasonable degree of accuracy. In the analysis of the results of laboratory experiments made by different investigators M. Fishenden and O. A. Saunders[4] have given the following formula for the rate of heat transmission under conditions of natural convection from a horizontal surface with colder air above :—

$$H = 0{\cdot}38\ \theta^{5/4}\ \frac{\text{British Thermal Units}}{\text{ft.}^2\ \text{hr.}}$$ where θ is expressed in °F or

$$H/\theta = 0{\cdot}0036\ \theta^{\frac{1}{4}}\ \frac{\text{Cal.}}{\text{cm.}^2\text{min. °C.}} \quad \ldots \quad \ldots \quad \ldots \quad \ldots \quad \ldots \quad (3)$$

In (3), θ is the difference of temperature between the surface and the air outside the 'boundary' layer. The thickness of this layer is very variable when the wind-velocity approaches zero; under laboratory conditions with surfaces of limited area, it is 0·5 to 2 cm. In the open air, temperature continues to decrease for much greater heights, although the largest falls take place within the first 1 cm. In calculating H/θ according to (3) in Table I, the difference between the temperature of the ground (T_s) and the temperature of the air at 4 ft. (T_4) has been used. Very near the ground, the fluctuations of temperature are very large and the difficulty of defining the height also is great when the reference surface is as rough as the ground. It was found that in calm weather during the hot hours of the day, the temperature difference at about 1 cm. above ground was 1·5–1·6 times that at 4 ft. If in evaluating H/θ in column 3 of Table I, the difference of temperature between ground and air at 1 cm. had been used, the calculated values would have been still smaller. For purposes of calculation it appears that we can take the temperature of the air at 4 ft. level as the effective temperature of the air.

TABLE I.

θ °C.	H (observed)	H (calculated)
8·0	·066	·048
11·2	·086	·074
16·9	·184	·123
18·3	·148	·136

For forced convection, Jurges' laboratory experiments gave the following relation for the heat loss from a rough surface. The surfaces were copper plates 50 cm. square placed in alignment with the walls of a duct through which air was blown by means of a fan. Jurges' relation for rough surfaces was taken as representing the best approach to natural conditions.

For velocities $v < 5$ metres per sec., $H/\theta = ·0088 + ·0059\,v$ .. (4)
where H is expressed in cal./cm.^{2} min., θ in degree Centigrade and v in metres/sec. The temperature and velocity of the air were presumably measured well outside the skin layer.

In Table II are grouped the mean values of H/θ for different values of v, measured in the open air at Poona and the values calculated according to

equation (4). The values of θ and v used in the calculation refer to air at 4 ft. above ground.

TABLE II.

v m/s	Mean H/θ observed	H/θ calculated according to (4)
0	·009	·0088
0·6	·016	·0123
0·9	·013	·0141
1·2	·018	·0159
1·5	·022	·0177
1·8	·020	·0194
2·4	·028	·0230
2·7	·027	·0247
3·0	·026	·0265
3·6	·031	·0300
3·9	·035	·0318
4·2	·033	·0336
4·8	·037	·0371

Velocities greater than 5 m./sec. were rarely experienced at 4 ft., but Jurges' relation for rough surfaces for these velocities takes the form

$$H/\theta = 0{\cdot}011\, v^{0{\cdot}78} \qquad .. \qquad .. \qquad .. \qquad (5)$$

K. Buttner, working in Tripolian Sahara, obtained the values 0·016 and 0·021 for H/θ for values of wind-velocity 0·8 to 1·5 m./sec. and 2 to 2·5 m./sec. at ½ metre height above ground.

In Fig. 2 are plotted the curve of equation (4) and the individual observational values. It appears that on the whole, the equation gives an under-estimate for the actual amount of heat transferred by convection. We have, however, to remember the difference between the definitions of v and θ in the laboratory and open-air experiments. It is not easy to make a theoretically unexceptionable choice regarding the level at which v and θ

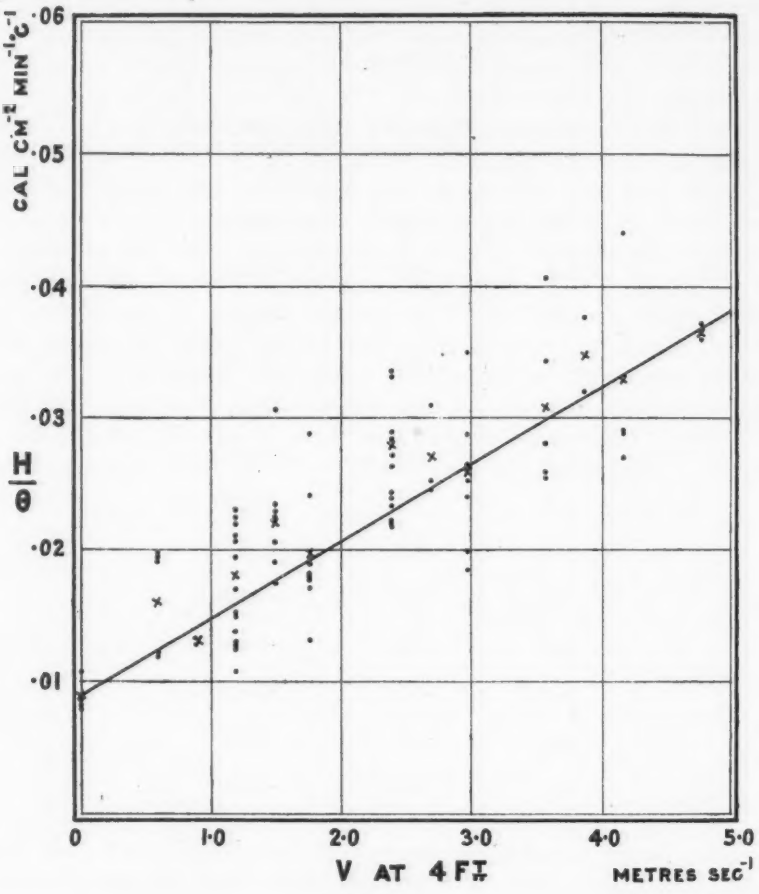

FIG. 2.

should be measured for open-air experiments. Both these quantities vary rapidly with height immediately above the ground. The four-foot level* was chosen partly because it is well outside the region of largest fluctuations and partly because this is the level at which meteorological observations are usually taken, so that the results can later be extended to other places and conditions. To obtain a general estimate of the quantities involved, it appears that Jurges' formula can be employed, if θ and v are taken to refer

* Actually, the wind-velocity was measured at 1½ feet above ground by means of a cup anemometer and converted to that at 4 feet by means of the relation $v_{1\cdot5}/v_4 = 0\cdot75$.

to 4 ft. level. Further measurements with an improved apparatus are projected for a more rigorous test of the applicability of the formula.

In Fig. 3 is shown a curve showing the variation of heat transmission by convection at different times on 2. 2. 35. The curve represents the values calculated by (4) and the marked points the measured values. The integrated loss of heat by convection on this day comes to be 175 calories. The

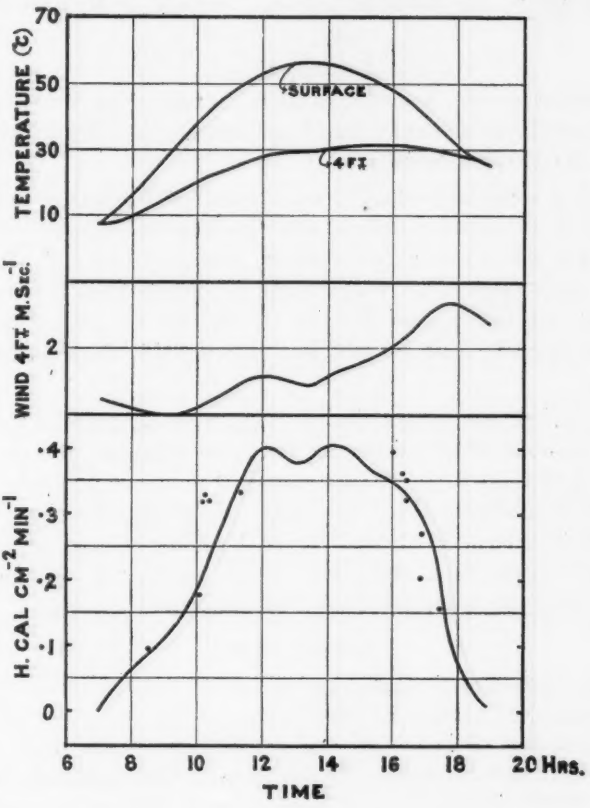

FIG. 3.

integrated heat loss on a number of days in the period February to May ranged from 175 to 340 cal. per day. In the region of sub-tropical highs in which Poona is situated in this season, we may take the average daily quantity of heat transferred by convection to the atmosphere on clear days to be about 250 calories. When the ground is dry, this will appear directly in the form of increase of temperature. When we are considering moist

ground or sea areas, the energy will go into the atmosphere partly in the form of latent energy of water-vapour. In dry land areas, the effect of this daily transference of heat to the lower atmosphere would be to raise the temperatures of the lower layers and set up a large lapse-rate in the first few kilometres of the atmosphere. Assuming that all the heat added by convection in one day goes to increase the temperature of the first 3 km. of the atmosphere, the resulting average increase of temperature will be

$$\frac{250}{0{\cdot}241\times1{\cdot}0\times10^{-3}\times10^{5}\times3} \text{ or } 3^{0}{\cdot}4\,\text{C.}$$

Rise of temperature will, however, cause an increase of radiation of heat from the atmospheric layer and this, operating both day and night, would reduce the actual rise of temperature.

Cold air is sometimes brought down into lower latitudes during winter in the wake of western depressions, and this often spreads over the Deccan. The cold spells which follow are, however, brought to an end within two or three days when there is no fresh advent of cold air from the north. It is evident that the heat gained by the atmosphere by convection from the insolated ground will itself be sufficient to bring this about in two or three days.

In conclusion, the author desires to express his grateful thanks to the Director-General of Observatories for the facilities given and to Dr. K. R. Ramanathan and Dr. I,. A. Ramdas for their guidance and help during the progress of this investigation. His best thanks are also due to Mr. G. Chatterji, Meteorologist-in-Charge, Upper Air Observatory, Agra, for kindly sending a reel of thin constantan strip which was used in this investigation. The experiments are being continued with improved apparatus.

REFERENCES.

1. F. Albrecht, *Gerl. Beitr. z. Geoph.*, 1930, **25**, 1–35.
2. W. H. Dines, *Q. J. Roy. Met. Soc.*, 1917, **43**, 151.
3. K. Buttner, *Veroff. des Preuss. Met. Inst.*, Abhandlungen 10, 1934, No. 5.
4. M. Fishenden and O. A. Saunders, *The Calculation of Heat Transmission*, London, H.M. Stationery Office, 1932.

STUDIES IN THORIUM PHOSPHATE GELS.

By M. U. Parmar, S. M. Mehta
and
Mata Prasad.
(From the Department of Inorganic and Physical Chemistry, Royal Institute of Science, Bombay.)

Received November 25, 1935.

Thorium phosphate gels were first prepared by Satya Prakash[1] by directly mixing solutions of thorium nitrate and potassium phosphate. A precipitate which is first obtained disappears on shaking and gives rise to a more or less opaque solution. This when kept for some time becomes clear and sets to a firm transparent gel. According to him the precipitated thorium phosphate is peptised by the hydrogen and thorium ions present in the gel-forming mixtures and this process is greatly accelerated by shaking. Later on, the colloidal solution of thorium phosphate coagulates and the particles get hydrated and in course of time the whole mixture sets to a solid looking mass imbibing within itself all the liquid present in the mixture, provided suitable concentrations of solutions of thorium nitrate and potassium phosphate are employed.

It has been found by the authors that thorium phosphate gels can be easily prepared if a solution of phosphoric acid instead of that of potassium phosphate is used. Only a slight precipitate is obtained when solutions of thorium nitrate and phosphoric acid are mixed and it quickly disappears on shaking. The resulting solution is quite transparent and sets to a firm transparent gel.

In the following an attempt has been made to investigate systematically the factors that affect the time of setting of these gels. Consequently the behaviour of thorium and hydrogen ions and the effect of temperature and of the addition of extra amounts of electrolytes and non-electrolytes to the gel-forming mixtures has been investigated.

Experimental

Kahlbaum's purest thorium nitrate and phosphoric acid whose purity was tested, were used. A number of trials indicated that 6 per cent. solution of thorium nitrate and 2N solution of phosphoric acid gave very good

[1] *J. Indian Chem. Soc.*, 1929, **6**, 587.

gels when different volumes of these solutions were mixed. Hence these solutions were used throughout the investigation.

A known amount of thorium nitrate solution was taken in one test tube and in another a known amount of the solution of phosphoric acid together with some distilled water so that when the two solutions were mixed the total volume of the mixture was 10 c.c. The mixture was then slightly shaken for about 15 seconds and was then poured into a tube which was gently inverted twice and set aside. This method of mixing was followed throughout the investigation.

The time required by the gel-forming mixture to reach a state when it did not flow out of the tube and showed a firm meniscus on inverting it was taken to be the time of setting of the gel. The accuracy of these measurements was increased by repeating the observations several times and each time disturbing the mixture as few times as possible during setting. This enabled the determination of the time of setting fairly accurately. The results obtained are given in Tables I and II in which

Q = grams of thorium nitrate in 10 c.c. of mixture ;
X = equivalent of phosphoric acid in the mixture ; and
T = time of setting in minutes.

TABLE I.

Q	0·48	0·42	0·36	0·39
X	T	T	T	T
0·24 N	8	ppt. settles down ; no gel.	ppt.	ppt.
0·22 N	15	7·5	ppt.	ppt.
0·20 N	32	20	6	ppt.
0·18 N	105	49	23	2
0·16 N	233	162	88	18
0·14 N	about 24 hrs.	about 12 hrs.	185	42·5
0·12 N	does not set : a clear sol.	a clear viscous sol : does not set.	about 14 hrs.	91

TABLE II.

X	0·18	0·16	0·14	0·12
Q	T	T	T	T
0·48	105	233	about 24 hrs.	Clear viscous sol: no gel.
0·42	49	162	about 12 hrs.	,,
0·36	23	88	185	about 14 hrs.
0·30	2	18	42·5	91
0·24	no gel: ppt.	no gel: ppt.	6·5	22·5
0·18	,,	,,	ppt.	2
0·12	,,	,,	,,	ppt.
0·06	,,	,,	,,	,,

All the gels mentioned in the tables were absolutely transparent throughout the entire process of gelation and the gel-forming mixtures were acidic.

It will be seen that for the same thorium nitrate content of the mixture the time of setting decreases as the concentration of phosphoric acid in the mixture is increased while for the same concentrations of phosphoric acid it increases with an increase in the amount of thorium nitrate in the mixture.

It may be pointed out that gels can be obtained only within the range of concentrations of thorium nitrate and phosphoric acid given in the above tables. If the amount of phosphoric acid in the mixture is increased or decreased beyond these limits a curd (or a gelatinous precipitate) or a perfectly transparent solution which never sets to a stiff gel, is obtained. The reverse happens in the case of thorium nitrate. A more or less viscous and transparent loose mass is obtained when the amount of thorium nitrate in the mixture is more and a curd when it is less than the amounts given in the above tables.

Effect of Temperature

Prakash[2] has found that the time of setting of thorium phosphate gels decreases as the setting takes place at a higher temperature. Table III gives

[2] *J. Indian Chem. Soc.*, 1932, **9**, 192.

the results obtained with gels prepared in the manner mentioned above. These results are in agreement with the conclusions of Prakash.

TABLE III.

X = 0·16 N

Temp.	Q	0·30	0·36	0·42	0·48
50°C.	T	6	17	61	170
40°C.	T	10	38	130	192
28°C.	T	18	88	182	233

It was noticed that gels prepared at higher temperatures were cloudy and the cloudiness disappeared gradually after some time. They were also stiffer than those prepared at lower temperatures. These observations indicate that the gels prepared at higher temperature consist of bigger aggregates which are not highly hydrated.

Effect of Electrolytes

Electrolytes are known to cause the coagulation of a sol. In a gel-forming mixture this is brought about by the electrolytes formed due to the metathetical reaction. If extra amounts of electrolytes are added to this mixture, the coagulation process may be hastened. Thus Prasad and Hattiangadi[3] found that the time of setting of the silicic acid gel-forming mixtures is decreased as a larger quantity of electrolytes is added to them. In the following the effect of the addition of some salts, acids and sodium hydroxide on the setting of thorium phosphate gels has been described. For this purpose different quantities of the solutions of the electrolytes were added to fixed amounts of phosphoric acid solutions and the requisite amount of distilled water was added to make up the total volume of the gel-forming mixture to 10 c.c. In the following tables A represents the normality of the electrolytes in the gel-forming mixtures.

(*a*) *Effect of salts.*—The salts used were chlorides of sodium and barium and sodium sulphate.

[3] *J. Indian Chem. Soc.*, 1930, 7, 341.

TABLE IV.

NaCl

Q = 0·36

X	A	0	0·2 N	0·4 N	0·6 N	0·8 N	1·0 N
0·12 N	T (hrs.)	14	10	6·5	5	3·5	1·5
0·14 N	T (min.)	200	155	117	84	58	36
0·16 N	T (min.)	88	57	37	32	28	17

TABLE V.

Q = 0·36. X = 0·16 N

$BaCl_2$			Na_2SO_4		
A	T	Remarks	A	T	Remarks
0	88	transparent gel	0	88	transparent gel
0·005 N	63	translucent gel	0·02 N	60	,,
0·010 N	56	,,	0·04 N	16	translucent gel
0·015 N	50	,,	0·06 N	4	opaque
0·020 N	41	completely opaque gel	0·08 N	—	disjointed hydrates

It is clear that the time of set decreases as the amount of salts in the gel-forming mixtures is increased.

The gels obtained in the presence of sodium chloride were quite transparent from the beginning of gelation till they set, but slight turbidity developed when the amount of sodium chloride was fairly large. No transparent gels were obtained in the presence of $BaCl_2$ and Na_2SO_4 when concentrations equivalent to NaCl were used but only a gelatinous precipitate separated out. However, with very small amounts of these electrolytes translucent and opaque gels were obtained.

(*b*) *Effect of sodium hydroxide.*—1 N sodium hydroxide solution was used.

TABLE VI.

Q = 0·36

X	0·16 N		0·18 N		0·20 N	
A	T	Remarks	T	Remarks	T	Remarks
0	88	transparent gel	20	transparent gel	6	transparent gel
0·02 N	102	,,	26	turbid mixture	7	turbid mixture
0·05 N	108	gel-forming mixture turbid	35	,,	—	—
0·10 N	360		105	,,	14	translucent gel ; ppt. separates and settles down
0·20 N	—	no gel ; ppt. slowly settles down	—	no gel ; ppt. separates and settles down	—	—

TABLE VII.

X = 0·18 N

Q	0·30		0·36		0·42	
A	T	Remarks	T	Remarks	T	Remarks
0	1	transparent gel	20	transparent gel	72	transparent gel.
0·02 N	3	gel-forming mixture turbid	26	turbid mixture	90	,,
0·05 N	5	,,	35	,,	120	,,
0·10 N	7	,,	105	,,	about 6 hrs.	,,
0·15 N	15	translucent gel	140	,,	—	——
0·20 N	—	ppt. separates and settles down	—	No gel ; ppt. separates and settles down	—	transparent viscous mass ; ppt. separates and settles down

While preparing the gels it was noticed that they were turbid and the turbidity persisted in some gels till the setting point and disappeared in others just when they were about to set. Also the opacity of these mixtures increased with an increase in the concentration of NaOH. Thus in the presence of limited amounts of NaOH both transparent and opaque gels were obtained. Some of the set opaque gels became clear on keeping for some time while others did not undergo any change in their opacity. The

gels obtained by Satya Prakash[4] by using potassium phosphate were similar to those obtained by us in the presence of NaOH. These gels, however, do not look quite homogeneous.

It will be seen that the time of set increases as the amount of NaOH in the gel is increased. On testing the various gel-forming mixtures by various indicators it was found that they were fairly acidic. The pH of the mixture with no amount of NaOH was nearly 1·2 and this increased to nearly 2·5 as different amounts of NaOH were added to them. If larger amounts of NaOH were added, no gel but an amorphous precipitate was formed.

(*c*) *Effect of acids.*—4 N nitric and hydrochloric acids and 0·5 N sulphuric acid were used for the purpose. As the behaviour of nitric acid was found to be similar to that of hydrochloric acid, only the results with the latter acids are given.

TABLE VIII.

Effect of Hydrochloric Acid

X = 0·14 N

A	Q = 0·30		A	Q = 0·36	
	T	Remarks		T	Remarks
0	42·5	transparent gel	0	185	transparent gel
0·2 N	29	,,	0·08 N	70	,,
0·4 N	40	,,	0·20 N	30	,,
0·6 N	about 12 hrs.	,,	0·40 N	22	,,
0·8 N	20	opaque	0·60 N	50	,,
1·0 N	17	,,	0·72 N	21	slightly opalescent
1·2 N	12	transparent	1·0 N	7	opaque gel
			1·2 N	—	hydrated flakes

It is clear that with increasing amounts of hydrochloric acid the time of setting at first diminishes, reaches a minimum, then suddenly increases and again diminishes till a second minimum is reached. With the addition of sulphuric acid, however, the time of setting at first increases and then begins to decrease and the first minimum found with hydrochloric acid is

[4] *Loc. cit.*

TABLE IX.

Effect of Sulphuric Acid.

Q = 0·36

A	X = 0·14 N		X = 0·16 N	
	T	Remarks	T	Remarks
0	185	transparent gel	88	transparent gel
0·01 N	255	loose and translucent gel	110	loose and translucent gel
0·02 N	310	,,	90	,,
0·03 N	220	,,	58	,,
0·04 N	71	,,	18	,,
0·05 N	35	,,	8	,,
0·06 N	14	,,	4	,,
0·07 N	6	,,	1·5	,,
0·08 N	3	,,	< 1	,,
0·09 N	1	,,	—	no gel; the ppt. separates and settles down slowly
0·10 N	< 1	,,	—	—

not observed. It may correspond to some concentration of the acid lower than 0·01 N which has not been used in the investigation. With further increase in the amount of the acid, *i.e.*, more than that corresponding to the minimum, at first hydrated flakes are formed and then a clear solution is obtained which shows no turbidity nor any increase in viscosity on keeping.

Effect of Non-electrolytes

The rôle of non-electrolytes in their action towards colloidal solutions is not yet clearly understood. Several examples are known in which they act either as coagulating or inhibiting agents. Billitzer[5] found that a

[5] *Zeit. Phys. Chem.*, 1903, **45**, 312.

negatively charged platinum sol could be sensitized, discharged or even changed into a positive sol by the addition of suitable amounts of alcohol. Prasad and Hattiangadi[6] found that the addition of alcohols decreases the time of setting of the alkaline silicic acid gels and increases that of the acidic ones. In the following the effect of the addition of methyl, ethyl and propyl alcohols and glycerine on the time of setting of thorium phosphate gels has been described. The addition of the non-electrolytes was done in the same manner as that of electrolytes.

TABLE X.

$Q = 0{\cdot}36$. $X = 0{\cdot}16$ N

Amount of non-electrolyte.	Methyl alcohol	Ethyl alcohol	Propyl alcohol	Glycerine
	T	T	T	T
0	88	88	88	88
1·0 c.c.	104	115	97	4·5 hrs.
2·0 c.c.	125	175	178	7 ,,
3·0 c.c.	230	213	about 5 hrs.	about 24 hrs.

It will be seen that the setting of gels is retarded by the presence of the non-electrolytes and this effect is enhanced as the amount of the non-electrolytes is increased.

Gels prepared with larger amounts of alcohols were turbid in the beginning, but after some time the turbidity slowly disappeared and transparent gels were obtained. Glycerine seems to have a considerable retarding influence. All gels obtained in the presence of glycerine were perfectly transparent from the beginning to the end of gelation but the structure of these gels was extremely loose.

Discussion of Results

The observations described above can be used to define the conditions which govern the formation of thorium phosphate gels. When solutions of thorium nitrate and phosphoric acid are mixed, they react and thorium phosphate and nitric acid are formed ; all the gel-forming mixtures, therefore, show an acid reaction. A slight precipitate is obtained because thorium phosphate dissolves only in concentrated solution of acids and is insoluble

[6] *J. Indian Chem. Soc.*, 1929, **6**, 991.

in dilute ones. The insolubility and the appearance of the precipitate are necessary, for when this precipitate goes over to the colloidal state on shaking, it supersaturates the solution with the gelling substance and in accordance with the views of von Weimarn creates circumstances favourable for the formation of a gel. The gel formation is, of course, determined by the hydration tendency of thorium phosphate and the agglomeration tendency of the micelles.

An increase in temperature (i) decreases the hydration tendency and increases the agglomeration tendency of the micelles and (ii) may also decrease the peptising capacity of the peptising ions. Both these effects cause the gel to set early with larger aggregates at a higher temperature. If the temperature is, however, further increased, no gel but only a precipitate should be obtained. This is probable as it was observed that in mixture, containing 0·30 g. of thorium nitrate and 0·18 N phosphoric acid, the precipitate obtained remained suspended for a long time before a homogeneous mass was formed.

The addition of extra amounts of salts also increases the agglomeration tendency of the gelling substance and decreases the hydration tendency since such an addition hastens the coagulation of the micelles more so if ions of higher valency are employed. Thus the gels set early and are turbid.

$H^{\cdot}$-ions seem to be very effective in peptising thorium phosphate. The first decrease in the time of setting observed in Table VIII is an evidence of this effect since with an increase in the $H^{\cdot}$-ion concentration in the mixture the rate of peptisation of the precipitate is also increased. Reverse happens when the $H^{\cdot}$-ion concentration is decreased by the addition of sodium hydroxide (*cf.* Tables VI and VII). This effect of the $H^{\cdot}$-ions is supported by the observation that the precipitate in mixtures containing the amount of the acid corresponding to the first minimum gets peptised without shaking.

With an increase in the concentration of the acid beyond that corresponding to the first minimum the increased peptising action of the $H^{\cdot}$-ions increases the degree of dispersity of the micelles and delays the setting. After a certain concentration of the acid which imparts the maximum charge to the micelles any further addition increases the concentration of the coagulating ion and decreases the time of set ; at some concentration the coagulation becomes very rapid and a precipitate is formed. The gels corresponding to the range between the maximum and the second minimum are opalescent and this supports the view that further addition of acids increases the agglomeration tendency. The coagulating effect of the anions is also apparent from the fact that gels of greater opalescence are obtained as the concentration of sulphuric acid beyond that corresponding to the maximum is

increased. Further, due to the increased coagulating effect of the divalent sulphate ion the concentrations of sulphuric acid employed are ten times smaller than those of hydrochloric acid.

Prasad and Hattiangadi[7] have also observed that with concentrated acids a second minimum time of set is obtained in the gelation of silicic acid. Holmes[8] has also made a similar observation in the gelation of silicic acid by sulphuric and hydrochloric acids. He has pointed out that the second minimum is caused by the dehydrating influence of the concentrated acids, but Prasad and Hattiangadi have shown that it is the coagulating effect of the anion which comes more into play after the density of charge on the colloidal particles of the gelling substance has attained its maximum value.

Thorium phosphate is peptised to a fairly large extent by thorium ions as well. This is seen from the fact that all mixtures in Tables I and II contain thorium nitrate in excess of that required for the complete precipitation of thorium phosphate. Consequently if the amount of thorium nitrate in mixtures containing the same concentration of phosphoric acid is increased, the degree of dispersity of the colloidal particles increases and they take longer time to form bigger aggregates in order to set to a stiff gel. If the amount of thorium nitrate in the mixtures is increased or decreased beyond the limits indicated in the tables, the amount of the peptising ion in the mixture is either too great or too small and hence, as observed, either a viscous mass or a curd, respectively, is obtained.

If the concentration of phosphoric acid is increased beyond the limit given in the tables, the amount of thorium phosphate formed is increased and the concentration of thorium ions falls. Thus the gelling substance does not reach a sufficiently high degree of dispersity and supersaturation and a curd are obtained. If the concentration of phosphoric acid is lower than that indicated in the tables no gel but a viscous mass is formed for (i) the dispersity of the precipitate is very high as there are a large number of thorium ions to peptise a small amount of the precipitate and (ii) the amount of the precipitate (number of micelles) is insufficient to enmesh the whole of the liquid.

These observations, therefore, support the suggestion of Fernau and Pauli[9] that for the formation of a gel it is necessary that the concentration of the micelles must be high. Their second suggestion that the micelles

[7] *Loc. cit.*

[8] *J. Phys. Chem.*, 1918, **22**, 510.

[9] *Biochem. Zeit.*, 1915, **70**, 426; *Kolloid Zeit.*, 1917, **20**, 20.

should be hydrophillic in nature and should remain so upon coagulation is satisfied by the chemical nature of thorium phosphate which has a great tendency for hydration.

The action of alcohols and glycerine is similar to that observed by Prasad and Hattiangadi[10] for the acidic silicic acid gel-forming mixtures as these gels also take a longer time to set in the presence of alcohols. These authors concluded from their observation that alcohols exert a protective influence on the positively charged sols by causing an increase in the density of charge on the particles. In the present case an increase in the density of charge and thereby in the degree of dispersity of thorium phosphate is caused by alcohols probably by effecting an increase in the adsorption of H^+-ions by the micelles. The first appearance of the turbidity in the presence of alcohols caused by the insolubility of thorium phosphate in alcohol-water mixtures and its disappearance after a certain time leads one to believe that the above assumption is justifiable. In the presence of glycerine thorium phosphate gets dispersed to such a high degree that aggregates big enough to give a rigid structure are not formed.

[10] *Loc. cit.*

THE DIFFRACTION OF LIGHT BY HIGH FREQUENCY SOUND WAVES: PART IV.

Generalised Theory.

By C. V. Raman
and
N. S. Nagendra Nath.
(From the Department of Physics, Indian Institute of Science, Bangalore.)

Received February 7, 1936.

1. *Introduction.*

In Part III[1] of this series of papers, we considered the Doppler effects and coherence phenomena among the diffracted components of light emerging from a rectangular cell of a medium traversed by supersonic waves perpendicular to the direction of the propagation of the incident plane wave of light. We showed, in the case of a progressive supersonic wave, that the nth order diffraction component which is inclined at an angle $\sin^{-1}(-n\lambda/\lambda^*)$ to the direction of propagation of the incident light has the frequency $\nu - n\nu^*$, where ν and λ denote the frequency and the wave-length of the incident light while ν^* and λ^* correspond to those of the sound wave. In the case of the diffraction of light by a standing sound wave, we got the interesting result that in any even order, radiations with frequencies $\nu \pm 2r\nu^*$, $(r = 0, 1, 2, \ldots)$, would be present while in any odd order, radiations with frequencies $\nu \pm \overline{2r+1}\,\nu^*$, $(r = 0, 1, 2, \ldots)$, would be present. These results give a satisfactory interpretation of the coherence phenomena among the diffraction components observed by Bär.[2] In the following, we show that our previous results remain valid even if we consider a *general* periodic supersonic wave and that they can be derived in a simple and direct fashion. We have also presented in the following, some general considerations of the problem on hand.

2. *Doppler effect and coherence phenomena.*

The partial differential equation governing the propagation of light in a medium with time-variation and space-variation in its refractive index is

$$\frac{\partial^2\psi}{\partial x^2} + \frac{\partial^2\psi}{\partial y^2} + \frac{\partial^2\psi}{\partial z^2} = \left[\frac{\mu(x, y, z, t)}{c}\right]^2 \frac{\partial^2\psi}{\partial t^2}$$

[1] C. V. Raman and N. S. Nagendra Nath, *Proc. Ind. Acad. Sci. (A)*, 1936, **3**, 75.
[2] R. Bär, *Helv. Phy. Acta*, 1935, **8**, 591.

if the frequency of the time-variation of $\mu\,(x, y, z, t)$ is very slow compared to the time-variation of the wave-function of light. This would be so in the case of the propagation of light in a medium filled with sound waves for the frequency of the variation of $\mu\,(x, y, z, t)$ corresponds to the frequency of the sound waves present in the medium, which is negligible compared to the frequency of light.

If we choose our axes of reference such that the X-axis points to the direction of the propagation of the plane sound waves and the Z-axis points to the direction of the propagation of the incident plane wave of light, we could ignore the dependence of ψ on y and write the differential equation as

$$\frac{\partial^2\psi}{\partial x^2}+\frac{\partial^2\psi}{\partial z^2}=\left[\frac{\mu\,(x,\,t)}{c}\right]^2\frac{\partial^2\psi}{\partial t^2}$$

If $\mu\,(x, t)$ did not depend on time, ψ would have had the only time factor $\exp\,(2\pi i\nu t)$ where ν is the frequency of the incident light. If we consider the time variation of $\mu\,(x, t)$, we can write ψ as given by

$$\psi = \exp\,[2\pi i\nu t]\;\phi\,(x, z, t)$$

where $\phi\,(x, z, t)$ varies slowly in time compared to $\exp\,[2\pi i\nu t]$. On the consideration that $\nu^* << \nu$, we can show that

$$\left|\,4\pi\nu\frac{\partial\phi}{\partial t}\,\right| << \left|\,4\pi^2\nu^2\phi\,\right| \quad\text{and}\quad \left|\,\frac{\partial^2\phi}{\partial t^2}\,\right| << \left|\,4\pi^2\nu^2\phi\,\right|.$$

With these considerations, we can consider the differential equation

$$\frac{\partial^2\phi}{\partial x^2}+\frac{\partial^2\phi}{\partial z^2}=-\frac{4\pi^2}{\lambda^2}\{\mu\,(x,\,t)\}^2\phi$$

and obtain ψ by the equation

$$\psi = \exp\,[2\pi i\nu t]\;\phi\,(x, z, t).$$

As the sound waves which travel along the X-axis are periodic in space and time, we can regard $\mu\,(x, t)$ to be also periodic in x and t with the same periods in space and time. It should be noticed that we do not restrict $\mu\,(x, t)$ to be simply periodic in x and t but it may be a general periodic function of x and t, amenable to Fourier Analysis. Thus

$$\mu\,(x+p\lambda^*,\;t) = \mu\,(x,\,t)$$

and

$$\mu\,(x, t+p/\nu^*) = \mu\,(x,\,t)$$

where p is any integer.

If we consider the differential equation in which $\mu\,(x, t)$ has the above properties, we see that $\phi\,(x, z, t)$ should also be periodic in x and t with the same periods in the case we are considering. That is,

$$\phi\,(x+p\lambda^*,\,z,\,t) = \phi\,(x,\,z,\,t)$$

and

$$\phi\,(x,\,z,\,t+p/\nu^*) = \phi\,(x,\,z,\,t)$$

Hence we can write the double-Fourier expansion of $\phi(x, z, t)$ as

$$\sum_{-\infty}^{\infty}\sum_{-\infty}^{\infty} f_{rs}(z)\, e^{2\pi i r x/\lambda^*}\, e^{2\pi i s \nu^* t}$$

Progressive Sound Waves.—In the case of the progressive waves travelling along the positive direction of the X-axis, we have the property that

$$\mu(x+\rho\lambda^*, t) = \mu(x, t-\rho/\nu^*)$$

where ρ is any number. Thus

$$\phi(x+\rho\lambda^*, z, t) = \phi(x, z, t-\rho/\nu^*) \quad .. \quad .. \quad .. \quad (1)$$

Using the double-Fourier expansion, we can write (1) as

$$\Sigma\Sigma f_{rs}(z)\, e^{2\pi i r x/\lambda^*}\, e^{2\pi i s \nu^* t} e^{2\pi i r \rho}$$
$$= \Sigma\Sigma f_{rs}(z)\, e^{2\pi i r x/\lambda^*}\, e^{2\pi i s \nu^* t}\, e^{-2\pi i s \rho} \quad .. \quad .. \quad .. \quad (2)$$

Comparing the Fourier coefficients on each side of (2), we get

$$f_{rs}(z)\, e^{2\pi i r \rho} = f_{rs}(z)\, e^{-2\pi i s \rho}$$

This could be true only if

$$f_{rs}(z) = 0 \quad \text{when } r \neq -s \quad .. \quad .. \quad .. \quad (3)$$

The condition (3) restricts the number of terms in the Fourier expansion of ϕ, so that

$$\phi(x, z, t) = \sum_{-\infty}^{\infty} f_r(z)\, e^{2\pi i r x/\lambda^*}\, e^{-2\pi i r \nu^* t}$$

Thus

$$\psi(x, z, t) = \sum_{-\infty}^{\infty} f_r(z)\, e^{2\pi i r x/\lambda^*}\, e^{2\pi i (\nu - r\nu^*) t} \quad .. \quad .. \quad (4)$$

If one considers the diffraction effects of $\psi(x, z, t)$ given by (4), it is fairly obvious that the nth order diffraction component will be inclined at an angle $\sin^{-1}(-n\lambda/\lambda^*)$ with the incident beam of light and will have the frequency $\nu - n\nu^*$ and the relative intensity expression $|f_n(z)|^2$.

Standing Sound Waves.—In the case of standing waves, we have the property that

$$\mu\left(x + \frac{p\lambda^*}{2}, t\right) = \mu\left(x, t \pm \frac{p}{2\nu^*}\right), \quad p \text{ an integer,}$$

so that

$$\phi\left(x + \frac{p\lambda^*}{2}, z, t\right) = \phi\left(x, z, t \pm \frac{p}{2\nu^*}\right) \quad .. \quad .. \quad .. \quad (5)$$

If we use (5) in the double Fourier expansion of ϕ we get

$$\Sigma\Sigma f_{rs}(z)\, e^{2\pi i r x/\lambda^*}\, e^{2\pi i s \nu^* t}\, e^{\pi i r p}$$
$$= \Sigma\Sigma f_{rs}(z)\, e^{2\pi i r x/\lambda^*}\, e^{2\pi i s \nu^* t}\, e^{\pi i s p} \quad .. \quad .. \quad .. \quad (6)$$

Comparing the Fourier coefficients in (6), we get

$$f_{rs}(z)\, e^{\pi i r p} = f_{rs}(z)\, e^{\pi i s p}$$

This means that $f_{rs}(z)$ is zero unless r and s are both even integers or odd integers.

Returning now to the Fourier expansion of ϕ, we could write it as

$$\phi(x, z, t) = \sum_{-\infty}^{\infty}\sum_{-\infty}^{\infty} f_{2r,\,2s}(z)\, e^{2\pi i 2rx/\lambda^*}\, e^{2\pi i 2s\nu^* t}$$

$$+ \sum_{-\infty}^{\infty}\sum_{-\infty}^{\infty} f_{2r+1,\,2s+1}(z)\, e^{2\pi i \overline{2r+1}x/\lambda^*}\, e^{2\pi i \overline{2s+1}\nu^* t}$$

Thus

$$\psi(x, z, t) = \sum_{-\infty}^{\infty}\sum_{-\infty}^{\infty} f_{2r,\,2s}(z)\, e^{2\pi i 2rx/\lambda^*}\, e^{2\pi i(\nu+2s\nu^*)t}$$

$$+ \sum_{-\infty}^{\infty}\sum_{-\infty}^{\infty} f_{2r+1,\,2s+1}(z)\, e^{2\pi i \overline{2r+1}x/\lambda^*}\, e^{2\pi i(\nu+\overline{2s+1}\nu^*)t} \quad .. \quad (7)$$

If one considers the diffraction effects of $\psi(x, z, t)$ given by (7), it will be quite easy to see that the diffraction orders could be classed into two groups, one containing the even ones and the other odd ones; any even order contains radiations with frequencies, $\nu, \nu \pm 2\nu^*, \ldots, \nu \pm 2r\nu^*, \ldots$, and any odd order contains radiations with frequencies, $\nu \pm \nu^*, \nu \pm 3\nu^*, \ldots, \nu \pm \overline{2r+1}\nu^*, \ldots$

3. The case when the disturbance in the medium is simple harmonic.

If we suppose that the variation in the refractive index of the medium is simple harmonic along the X-axis, it can be represented as

$$\mu(x, t) = \mu_0 + \mu \sin 2\pi(\nu^* t - x/\lambda^*)$$

in the case of a progressive wave, while it will be of the form

$$\mu(x, t) = \mu_0 - \mu \sin(2\pi x/\lambda^*) \sin(2\pi\nu^* t)$$

in the case of a standing wave, where $\mu(x, t)$ is the refractive index of the medium at height x and at time t, μ_0 is the constant refractive index of the medium when there is no sound wave and μ is the *maximum variation* of the refractive index from μ_0.

Progressive Wave.—To obtain the wave function for the emerging wave-front of light, we have to solve the differential equation

$$\frac{\partial^2\phi}{\partial x^2} + \frac{\partial^2\phi}{\partial z^2} = -\frac{4\pi^2}{\lambda^2}\{\mu(x, t)\}^2\phi$$

$$= \left[A + \frac{B}{2i}\{e^{i(bx-\epsilon)} - e^{-i(bx-\epsilon)}\}\right]\phi \quad .. \quad .. \quad (8)$$

where $b = 2\pi/\lambda^*$, $\epsilon = 2\pi\nu^* t$, $A = -4\pi^2\mu_0^2/\lambda^2$ and $B = 8\pi^2\mu_0\mu/\lambda^2$ omitting the second order term with coefficient μ^2.

We have shown in the previous section that ϕ can be developed as a Fourier series in x and t as

$$\sum_{-\infty}^{\infty} f_r(z)\, e^{2\pi i r x/\lambda^*}\, e^{-2\pi i r \nu^* t}$$

or
$$\sum_{-\infty}^{\infty} f_r(z)\, e^{irbx}\, e^{-ir\epsilon} \quad .. \quad .. \quad .. \quad .. \quad (9)$$

Substituting the Fourier series (9) in the differential equation (8) and comparing the Fourier coefficients we obtain the equation

$$\frac{d^2 f_n}{dz^2} - (A + b^2 n^2)\, f_n = \frac{B}{2i}\,(f_{n-1} - f_{n+1})$$

Putting $f_n(z) = \exp(-iu\mu_0 z)\ \phi_n(z)$ where $u = 2\pi/\lambda$
we obtain

$$\frac{d^2\phi_n}{dz^2} - 2iu\mu_0 \frac{d\phi_n}{dz} - b^2 n^2 \phi_n = -\frac{Bi}{2}(\phi_{n-1} - \phi_{n+1})$$

Putting $z = (2\pi\mu)^{-1}\lambda\xi$, we obtain

$$\mu^2 \frac{d^2\phi_n}{d\xi^2} - 2i\mu_0\mu \frac{d\phi_n}{d\xi} - \frac{n^2\lambda^2}{\lambda^{*2}}\phi_n = -\mu_0\mu i\,(\phi_{n-1} - \phi_{n+1})$$

As μ_0, being the refractive index of the medium, is in the neighbourhood of unity and μ is in the neighbourhood of 10^{-5}, we can omit the first term on the left hand side and consider the differential equation

$$2\frac{d\phi_n}{d\xi} - (\phi_{n-1} - \phi_{n+1}) = \frac{in^2\lambda^2}{\mu_0\mu\lambda^{*2}}\,\phi_n.$$

If there were no term on the right hand side, ϕ_n, would be the Bessel Function $J_n(\xi)$ or $J_n(2\pi\mu z/\lambda)$ satisfying the required boundary conditions. This follows as a consequence of Sonine's[3] theorem which gives that if

$$2\frac{d\phi_n}{d\xi} - (\phi_{n-1} - \phi_{n+1}) = 0,$$

then ϕ_n could be developed as a series in Bessel Functions as

$$\phi_n(\xi) = \phi_n(0)\, J_0(\xi) + \sum_1^{\infty} [\phi_{n-s}(0) + (-)^s \phi_{n+s}(0)]\, J_s(\xi)$$

Setting the boundary conditions that

$$\phi_0(0) = 1 \text{ and } \phi_s(0) = 0, \qquad s \neq 0$$

we get

$$\phi_n(\xi) = J_n(\xi).$$

If n is not too great and $\lambda^2/\lambda^{*2}\mu$ is small, we can approximate

$$\phi_n(\xi) \simeq J_n(\xi) = J_n\left(\frac{2\pi\mu z}{\lambda}\right)$$

---

[3] N. Nielsen, *Handbuch der theorie der Cylinderfunktionen*, p. 286 (1904 edition).

If the cell is bound by $z = L$ at the emerging face, it will be easy to see that the relative intensity of the nth order diffraction component would be $J_n^2\ (2\pi\mu L/\lambda)$.

The case of the standing wave.—In this case we have to write $\phi\ (x, z, t)$ as given by

$$\phi\ (x, z, t) = \sum_{-\infty}^{\infty}\sum_{-\infty}^{\infty} f_{2r,\,2s}\ e^{2\pi i 2rx/\lambda^*}\ e^{2\pi i 2s\nu^* t}$$

$$+ \sum_{-\infty}^{\infty}\sum_{-\infty}^{\infty} f_{2r+1,\,2s+1}\ e^{2\pi i\overline{2r+1}x/\lambda^*}\ e^{2\pi i\overline{s2+1}\nu^* t}$$

$$= \sum_{-\infty}^{\infty} g_r\ (z, t)\ e^{2\pi i r x/\lambda^*} \qquad \ldots \qquad \ldots \qquad \ldots \qquad (10)$$

Substituting (10) the differential equation for ϕ and comparing the coefficients, we obtain

$$\frac{\partial^2 g_n}{\partial z^2} - \frac{4\pi i\mu_0}{\lambda}\frac{\partial g_n}{\partial z} - \frac{4\pi^2 n^2}{\lambda^{*2}}\,g_n = \frac{4\pi^2\mu_0\mu\,\sin\epsilon}{\lambda^2 i}\,(g_{n-1} - g_{n+1})$$

Putting $z = (2\pi\mu)^{-1}\lambda\xi$ we obtain

$$\mu^2\frac{\partial^2 g_n}{\partial\xi^2} - 2i\mu_0\,\mu\,\frac{\partial g_n}{\partial\xi} - \frac{n^2\lambda^2}{\lambda^{*2}}\,g_n = -\,\mu_0\,\mu i\,\sin\epsilon\,(g_{n-1} - g_{n+1}).$$

Under the same considerations as in the previous paragraph, we will have to solve the equation

$$2\,\frac{\partial g_n}{\partial\xi} - \sin\epsilon\,(g_{n-1} - g_{n+1}) = \frac{in^2\lambda^2}{\mu_0\mu\lambda^{*2}}\,g_n.$$

If n is not too great and $\lambda^2/\lambda^{*2}\mu$ is small we can approximate

$$g_n\ (\xi, \epsilon) \simeq J_n\ (\xi\,\sin\epsilon) = J_n\left(\frac{2\pi\mu z}{\lambda}\,\sin\,\overline{2\pi\nu^* t}\right).$$

But we have shown in Part III,[1] that

$$J_{2n}\ (v\,\sin\epsilon) = \sum_{-\infty}^{\infty}(-)^r\,J_{n-r}\ (v/2)\ J_{n+r}\ (v/2)\ e^{i2r\epsilon}$$

$$J_{2n+1}\ (v\,\sin\epsilon) = -\,i\sum_{-\infty}^{\infty}(-)^r\,J_{n-r}\ (v/2)\ J_{n+r+1}\ (v/2)\ e^{i\overline{2r+1}\epsilon}.$$

Hence,

$$\psi\ (x, z, t) \simeq \sum_{-\infty}^{\infty}\sum_{-\infty}^{\infty}(-)^r\,J_{r-s}\ (v/2)\ J_{r+s}\ (v/2)\ e^{2\pi i 2rx/\lambda^*}\ e^{2\pi i(\nu+2s\nu^*)t}$$

$$- i\sum_{-\infty}^{\infty}\sum_{-\infty}^{\infty}(-)^r\,J_{r-s}\ (v/2)\ J_{r+s+1}\ (v/2)\ e^{2\pi i\overline{2r+1}x/\lambda^*}\ e^{2\pi i(\nu+\overline{2s+1}\nu^*)t}$$

If one considers now the diffraction effects due to this emerging wave-front at $z = L$, it can be seen that an even order, say $2n$, contains radiations with frequencies $\nu \pm 2r\nu^*$, $(r = 0, 1, 2, \ldots)$, the relative intensity of the $\nu \pm 2r\nu^*$

sub-component being $J^2_{n-r}(\pi\mu L_1/\lambda)\ J^2_{n+r}(\pi\mu L_1/\lambda)$ and an odd order, say $2n+1$, contains radiations with frequencies $\nu \pm \overline{2r+1}\nu^*$, $(r = 0, 1, 2, \ldots)$, the relative intensity of the $\nu \pm \overline{2r+1}\nu^*$ sub-component being $J^2_{n-r}(\pi\mu L_1/\lambda)\ J^2_{n+r+1}(\pi\mu L_1/\lambda)$.

4. Summary.

The essential idea that the phenomenen of the diffraction of light by high frequency sound waves depends on the corrugated nature of the transmitted wave-front of light, pointed out by the authors in their first paper, has been developed on general considerations in this paper. The results in this paper can be summarised as follows :—

(1) If progressive sound-waves travel in a rectangular medium normal to two faces and the direction of propagation of a plane beam of incident light, the incident light will be diffracted at the angles given by $\sin^{-1}(-n\lambda/\lambda^*)$ and the light belonging to the nth order will have the frequency $\nu - n\nu^*$.

(2) If the sound waves are stationary, the incident light will be diffracted at the angles given by $\sin^{-1}(-n\lambda/\lambda^*)$, an even order would contain radiations with frequencies, ν, $\nu \pm 2\nu^*$, $\nu \pm 4\nu^*, \ldots$, $\nu \pm 2r\nu^*, \ldots$, and an odd order would contain radiations with frequencies $\nu \pm \nu^*$, $\nu \pm 3\nu^*$, $\nu \pm 5\nu^*, \ldots$, $\nu \pm \overline{2r+1}\ \nu^*, \ldots$.

(3) A differential-difference equation has been obtained for the amplitude function of the diffracted orders whose approximate solution is satisfied by the Bessel Functions already obtained by the authors in their previous papers.

MOLECULAR CLUSTERING IN LIQUID FATTY ACIDS.

By R. S. Krishnan.

(*From the Department of Physics, Indian Institute of Science, Bangalore.*)

Received January 29, 1936.

(Communicated by Sir C. V. Raman, Kt., F.R.S., N.L.)

1. *Introduction.*

It is well known that the light scattered transversely by a liquid is not in general perfectly polarised, but shows a defect of polarisation which is characteristic of each liquid. This partial depolarisation arises from the fact that in general, we are dealing with two types of scattering in an ordinary liquid, one type called the density scattering arising from the molecular disarray in the medium and consequent local fluctuations in its optical density, and the other type called the orientation scattering arising from the varying orientations of the molecules which are anisotropic. The density scattering is completely polarised, while the orientation scattering is depolarised to the extent of 6/7. Due to the combined effect, the light scattered transversely is depolarised to some extent depending upon the proportion in which the two types of scattering exist. The above idea is based on the supposition that the scattering in a liquid is completely molecular in origin, *i.e.*, the ultimate scattering particles are the molecules of size small compared with the wave-length of light. Using incident unpolarised light, as also light polarised with electric vector respectively vertical and horizontal, different measures of the state of polarisation of the transversely scattered light are obtained, namely, ρ_u, ρ_v and ρ_h corresponding to the three cases. For any liquid where the scattering is really molecular in origin

$$\rho_h = 1 \text{ and } \rho_u = 2\rho_v/(1 + \rho_v) \quad .. \quad .. \quad .. \quad (1)$$

and consequently it is not necessary to measure all the three quantities separately. But once the above condition is not fulfilled, *i.e.*, when the particles in the medium can no longer be identified with the individual molecules but only with molecular clusters or aggregates, ρ_h does not have its limiting value unity, but is definitely less than 1 and the simple relation (1) between ρ_u and ρ_v given above will no longer be satisfied. Consequently it will be quite insufficient to measure ρ_u alone. In such a case it has already been shown by the author[1] that there is a simple general relation connecting

[1] R. S. Krishnan, *Proc. Ind. Acad. Sci.*, (A), 1935, **1**, 782.

the three quantities ρ_u, ρ_v and ρ_h, namely,

$$\rho_u = (1 + 1/\rho_h)/(1 + 1/\rho_v) \quad .. \quad .. \quad .. \quad (2)$$

Relation (1) is a special case of this very general relation. In any scattering experiment, therefore, it is highly necessary to make comparative studies of the intensity and state of polarisation of the scattered light with the incident light in the three different states of polarisation, in order to get a correct idea of the state of dispersion of the scattering particles in the medium. Any departure of the value of ρ_h from unity will at once indicate an appreciable size of the scattering particles.

The above method has been successfully employed by the author in the case of liquid mixtures in the neighbourhood of the critical solution temperature.[2] The observations furnished for the first time positive evidence for the existence of large clusters in liquid mixtures not only at the critical solution temperature but also at temperatures considerably above that temperature. It was, therefore, considered desirable to extend this sensitive method to the case of highly associated liquids in order to know more about the state of dispersion of the molecules in them. In the present investigation, a detailed study of the scattering of light in the first four members of the fatty acids, namely, formic acid, acetic acid, propionic acid and normal butyric acid, at different temperatures with the incident light in the three different states of polarisation. The experimental results have obviously an important bearing on some of the anomalies observed in these acids by the earlier investigators on light scattering.

2. *Experimental Details.*

Merck's extra pure sample of formic acid was further purified by redistillation over pure anhydrous boric oxide (free from silicon) in an all-glass distillation apparatus. Extra pure glacial acetic acid (Merck's) was used as such without further chemical purification, whereas propionic acid and butyric acid were also purified by distillation over phosphorus pentoxide. The pure liquids were contained in small sealed bulbs about 2″ in diameter of clear and homogeneous glass. They were rendered dust-free by repeated slow distillation *in vacuo* in the usual way before they were sealed off. Particular care was taken to see that the liquids were absolutely free from dust. The bulb containing the liquid to be examined was kept immersed in distilled water contained in a rectangular brass vessel provided with three glass windows for the incident and the scattered beams. The bath was heated electrically. The source of light and the optical arrangement were

[2] R. S. Krishnan, *Proc. Ind. Acad. Sci.*, (A), 1935, **1**, 915; 1935, **2**, 221.

the same as those employed in the earlier investigations of the author. Extraneous light, if any, coming out in the direction of observation was cut off by suitably blackening the bulb and the vessel and making observations at a distance of about 10″ from the cell.

On inserting a double-image prism in the track of the incident beam and one in the track of the scattered beam (both of them oriented in such a way that the upper image as seen through them corresponded to vertical vibrations), it was found that in the case of acetic and formic acids the lowest image out of the four images observed was distinctly brighter than either of the middle two. The depolarisation factors ρ_u, ρ_v and ρ_h of the transversely scattered light were measured as usual with a double-image prism and a nicol using respectively incident unpolarised light, incident light polarised with vibrations vertical and horizontal. The value of ρ_h was found to be unusually less than its limiting value of 100%. The observations were repeated with the four fatty acids at various temperatures. The relative intensity of scattering in these liquids at different temperatures was determined by using a photo cell in conjunction with a valve bridge amplifier, in the manner described in the author's earlier paper.[3] The results are tabulated below.

The value of ρ_h is found to be less than 100% in the case of the first two members at lower temperatures. This raises the question whether the observed value of ρ_h is genuine or is due to some errors in the experiment. Dust particles, if any, in the liquid would vitiate the results very much. But in the present experiment this question does not arise at all since the liquids used were completely free from dust. Another source of error is fluorescence. It was found that none of the liquids studied was sensibly fluorescent.

TABLE I.

Liquid	Nature of the container	ρ_h %	ρ_v %	ρ_u %
Acetic acid	Pyrex cross temp. = 25° C.	90	30·5	49·5
	Spherical bulb temp. = 25° C.	91	30	50
Formic acid	Pyrex cross temp. = 25° C.	88	31	51
	Spherical bulb temp. = 25° C.	87	30·5	49

[3] R. S. Krishnan, *Proc. Ind. Acad. Sci.*, (A), 1935, **2**, 221.

TABLE II.

(*a*) *Formic acid* (*Bulb as container*).

Temperature $t°$ C.	ρ_k (Observed) %	ρ_v (Observed) %	ρ_u (Observed) %	ρ_u Calculated from eqn. (1) %	ρ_u Calculated from eqn. (2) %	Relative intensity of scattering
25	87	30·5	49	47	50	1·2
41	90	27	47	43	45	1·1
55	91	24	40	39	40·5	1·05
70	93	21·5	36	35	37	1·0 (assumed)
90	100	18·5	30	32	32	1·2

TABLE III.

(*b*) *Acetic acid* (*M.P.* = 15° *C.*) (*Bulb as container*).

Temperature $t°$ C.	ρ_k (Observed) %	ρ_v (Observed) %	ρ_u (Observed) %	ρ_u Calculated from eqn. (1) %	ρ_u Calculated from eqn. (2) %	Relative intensity of scattering
20	91	33	52·5	50	52	1·3
25	91	31	50	47	50	1·3
45	93	23·5	40·5	38	40	1·25
60	95	22	38	36	37·5	1·2
80	96·5	19·5	33	32·5	33·5	1·0 (assumed)
93	100	18	29	30	30	1·0

TABLE IV. (*c*) *Propionic acid* (*Bulb as container*).

Temperature $t°$ C.	ρ_h (Observed) %	ρ_v (Observed) %	ρ_u (Observed) %	ρ_u Calculated from eqn. (2) %	Relative intensity of scattering
25	100	27	42·0	42·5	1·00 (assumed)
42	100	23·5	37	38	1·05
60	100	19·5	33	33	1·11
75	100	17	28·5	29	1·25
85	100	16	27	27	1·33

TABLE V. (*d*) *Normal Butyric acid* (*Bulb as container*).

Temperature $t°$ C.	ρ_h (Observed) %	ρ_v (Observed) %	ρ_u (Observed) %	ρ_u Calculated from eqn. (2) %	Relative intensity of scattering
25	100	20	34·5	33	1·08
45	100	19	32·5	32	1·00 (assumed)
60	100	16	27·5	27·5	1·00
74	100	13·5	24	24	1·08
88	100	11	18	20·5	1·19

where ρ_u and ρ_v are defined as the ratio of the intensity of the horizontal component to that of the vertical component of the scattered light and ρ_h is defined as the ratio of the intensity of the vertical component to that of the horizontal component. Column 5 in Tables II and III gives the values of ρ_u calculated from the observed values of ρ_v using the simplified relation (1). The column 6 in these tables gives the values of ρ_u calculated from the observed values of ρ_v and ρ_h using relation (2). It is seen that these calculated values of ρ_u are decidedly in better agreement with the observed values showing thereby that equation (1) is no longer true for these two acids.

Moreover, fluorescence, if any, would never have the effect of lowering the value of ρ_h. Another possible source of error in the measurement of depolarisation is the convergence of the incident beam. In the present case the diameter of the long focus lens employed for focussing the light emerging out of the square aperture was 4 cms. The light was brought to a focus at a distance of about 52 cms. from the lens. Consequently the angle of convergence is equal to 1/13th of a radian. This angle was further reduced to 3/52 radian inside the medium by the liquid in the rectangular cell. According to Gans[4] and Ananthakrishnan[5] the convergence correction for ρ_u is $\omega^2/8$, where ω is the angle of convergence, and for a convergence angle of 3/52 radian, the correction would be 0·0004. This is negligibly small compared with the high depolarisation of the fatty acids and consequently it can be neglected. The corrections for ρ_v and ρ_h are also likewise negligibly small.

In order to be sure that the observed values of the depolarisation were not vitiated by any irregularity in the walls of the container, a pyrex cross was made. Each of its arms was 3″ long and 1½″ in diameter. Strain free pyrex plates were fused on to the ends. This cross was connected to a flask. Acetic and formic acids were distilled dust-free into the cross from the flask, one after the other. The measurements of depolarisation were repeated at the room temperature with the cross as container. The readings taken with the bulb and the cross as containers are given in Table I. The two corresponding readings are quite in agreement within the limits of experimental error.

3. *Discussion of Results.*

The most striking characteristic of acetic and formic acids is that ρ_h is only about 90% at 25° C., showing thereby that the scattering in these liquids is no longer purely molecular in origin, but should be attributed to the presence of molecular clusters. The average size of these aggregates is not small compared with the wave-length of light. This fact is also evidenced from the accuracy with which the data satisfy the theoretical relation (2). As the temperature is increased, the value of ρ_h increases steadily and finally attains its limiting value of 100%. From this it naturally follows that the degree of association and the size of the molecular aggregates formed depend very much on temperature. The lower the temperature, the greater is the association and larger is the size of the clusters. In the case of propionic and butyric acids ρ_h is found to be always equal to 100%.

---

[4] R. Gans, *Phys. Zeits.*, 1927, **28**, 661.

[5] R. Ananthakrishnan, *Proc. Ind. Acad. Sci.*, (A), 1935, **2**, 133.

These two acids may also be associated to some extent; but the degree of association is not so great as to be detected by the present experimental technique. In spite of the high value of ρ_u for formic acid, the value of ρ_k is least for this. From this it directly follows that of all the fatty acids, formic acid is the most highly associated one and the degree of association diminishes as the number of carbon atoms increases.

The intensity of scattering in acetic and formic acids shows some anomalies. On the basis of molecular theory, the orientation scattering in a liquid which depends on the number of molecules per unit volume, does not vary appreciably with rise of temperature; whereas, the density scattering which is directly proportional to the absolute temperature T and the compressibility β increases with rise in temperature. Therefore, the total intensity of scattering in a liquid where the scattering is truly molecular, should rise with temperature. This fact is well illustrated in the case of propionic and butyric acids. On the other hand in the case of the first two members of the fatty acid series, the intensity of scattering diminishes at first with rise in temperature up to about 80° C. and above this temperature it begins to increase. This also shows that at the ordinary temperatures the scattering in these two liquids is not in accordance with the molecular theory, but is influenced by the presence of large molecular aggregates.

In this connection it would be interesting to mention the anomalies observed by the earlier investigators on light scattering in these fatty acids. I. Ramakrishna Rao[6] has determined the depolarisation of the transversely scattered light and the optical anisotropy of a large number of organic vapours, and in almost all the cases he finds that the molecular anisotropy in the liquid state is definitely less than that in the vapour state. The significant exceptions are formic acid and acetic acid where the anisotropy in the liquid state is greater than that in the vapour state. He has calculated the anisotropy from the observed value of the depolarisation using the modified formula of Ramanathan.[7] The values of the anisotropy δ for these four fatty acids are given in the accompanying Table VI.

S. Ramachandra Rao[8] has studied the variations of intensity and depolarisation factor of the transversely scattered light in the case of a large number of liquids. He finds that in almost all liquids the optical anisotropy as calculated from the depolarisation values using Ramanathan's modified formula, increases with rise in temperature. But in the case of acetic acid

---

[6] I. Ramakrishna Rao, *Ind. Journ. Phys.*, 1927, **2**, 61.

[7] K. R. Ramanathan, *Ind. Journ. Phys.*, 1926-7, **1**, 401.

[8] S. Ramachandra Rao, *Ind. Journ. Phys.*, 1928, **3**, 1.

TABLE VI.

No.	Liquid	δ in the vapour state	δ in the liquid state
1	Formic acid ..	$33{\cdot}3 \times 10^{-3}$	47×10^{-3}
2	Acetic acid ..	$25{\cdot}9 \times 10^{-3}$	$36{\cdot}2 \times 10^{-3}$
3	Propionic acid..	$23{\cdot}5 \times 10^{-3}$	$20{\cdot}1 \times 10^{-3}$
4	Butyric acid ..	15×10^{-3}	$16{\cdot}5 \times 10^{-3}$

it is found that the optical anisotropy decreases from a value of 34×10^{-3} at 30° C. to 19×10^{-3} at 120° C. and above that temperature it increases steadily in the normal way. Formic acid was not included in his investigation as the values of its compressibility at different temperatures were not available. On the basis of molecular association this anomalous behaviour could be easily accounted for. The depolarisation factor arises not only from the actual anisotropy of the individual scattering particles, but also from their finite size. Consequently the anisotropy as calculated from the observed values of ρ_u without applying correction for the finite size of the molecular aggregates, is bound to give a higher value. Besides, the aggregates formed may also possess a higher effective anisotropy than the individual molecules themselves and consequently the anisotropy in the liquid state at the ordinary temperatures which is an aggregate of molecular clusters may be higher than that in the vapour state. This increase in the effective anisotropy will itself give rise to a higher value for the depolarisation factor ρ_u and also for the total intensity of scattering. As the liquid is heated up, the degree of association diminishes and the anisotropy decreases tending to attain its normal in the state of no association.

The present investigation furnishes for the first time definite experimental evidence for the existence of molecular clusters, of size not small compared with the wave-length of light in highly associated fatty acids. Further experimental work with other highly associated liquids and also with supercooled liquids is in progress.

In conclusion the author takes this opportunity to express his grateful thanks to Prof. Sir C. V. Raman, KT., F.R.S., N.L., for his continued interest and guidance during the progress of this investigation.

5. *Summary.*

The variations in intensity and depolarisation factor of the transversely scattered light have been studied in detail in the case of the first four fatty

acids, namely, formic acid, acetic acid, propionic acid and normal butyric acid, with the incident light in the three different states of polarisation, namely, unpolarised, horizontally polarised and vertically polarised. In the case of formic and acetic acids at the room temperature the depolarisation factor ρ_h was found to be about 90% when the incident light is polarised with vibrations horizontal. This observation furnishes for the first time definite experimental evidence for the existence of large molecular aggregates in these highly associated liquids, of size not small compared with the wave-length of light.

ρ_h increases with rise in temperature and at about 90° C. it attains its limiting value of 100% in these two acids. The intensity of scattering also at first diminishes with rise in temperature in these two cases, contrary to the molecular theory of light scattering. It is shown that molecular association is distinctly the cause for the extraordinary behaviour of formic and acetic acids in the initial stages. Propionic and normal butyric acids do not show such anomalies.

DEFORMATION FREQUENCIES IN THE RAMAN SPECTRA OF LINEAR MOLECULES: ACETYLENE.

By S. Bhagavantam
and
A. Veerabhadra Rao.
(From the Department of Physics, Andhra University, Waltair.)

Received February 8, 1936.

1. *Introduction.*

The fundamental vibrations of a linear molecule may be divided into two different types, *viz.*, the valency vibrations and the deformation vibrations. If the molecule possesses a centre of symmetry a further sub-division may be effected under the headings (i) totally symmetrical and (ii) antisymmetrical vibrations (Mecke, 1931). Of these various types, we may expect the total symmetric ones of both the valency and deformation vibrations to be 'Raman-active'. It must, however, be mentioned that the selection rules regarding the rotational structure differ very considerably in the two cases (Placzek, 1934). For valency vibrations we should expect a strong Q branch accompanied by O and S branches ($\Delta J = \pm 2$) and numerous examples of this type have already been found in the Raman spectra of gases like CO_2, N_2O, etc. On the other hand, a deformation vibration should consist of only an extremely feeble Q branch accompanied by both O and S branches ($\Delta J = \pm 2$) and P and R branches ($\Delta J = \pm 1$) of normal intensity. No examples of this type have yet been experimentally observed in Raman spectra. Acetylene gas constitutes a very favourable case from this point of view. In this paper, is obtained and described a particularly intense Raman spectrum of this substance showing a pair of Raman bands at $\Delta \nu$ 600 arising from a deformation vibration. The structure of this band agrees satisfactorily with the theoretical predictions.

2. *The Normal Vibrations of the Acetylene Molecule.*

The normal vibrations of the acetylene molecule have been discussed in detail by Mecke (*loc. cit.*) and by Sutherland (1935) and are represented diagrammatically in Fig. 1.

In the description of the diagram π stands for 'parallel' or valency oscillations and δ for 'perpendicular' or deformation oscillations. *s* and *a* stand for symmetric and anti-symmetric types respectively. It will be noticed

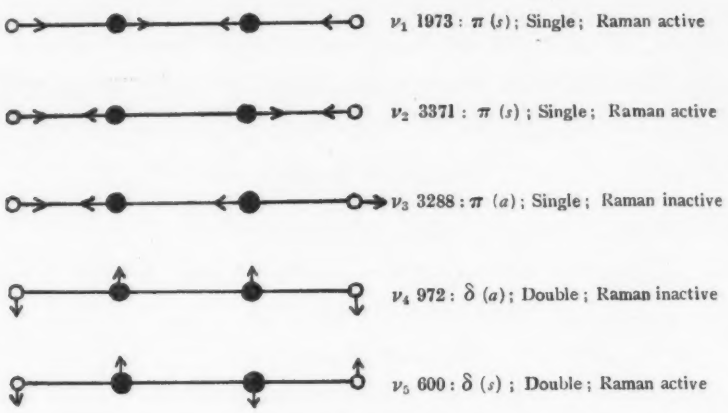
ν_1 1973 : π (s) ; Single ; Raman active
ν_2 3371 : π (s) ; Single ; Raman active
ν_3 3288 : π (a) ; Single ; Raman inactive
ν_4 972 : δ (a) ; Double ; Raman inactive
ν_5 600 : δ (s) ; Double ; Raman active

FIG. 1.

that of the three 'Raman-active' oscillations two are of the valency type and have already been observed in the Raman spectrum of acetylene gas (Bhagavantam, 1931). The third one is a deformation oscillation and has not yet been recorded in the Raman spectrum. From a detailed study of the combination bands appearing in the infra-red absorption spectrum of acetylene, Mecke and Sutherland have however deduced that its value should be about 600.

3. Raman Spectrum of Acetylene.

Using a 2-prism glass spectrograph, the Raman spectrum of acetylene gas is obtained at a pressure of 18 atmospheres by giving an exposure of about 28 days. The picture is reproduced in the plate accompanying this paper. The pair of bands at about $\Delta\nu$ 600 excited both by λ 4046 and λ 4358 and recorded here for the first time are marked with arrows. It is proposed to interpret these as the unresolved O P and R S branches of the total symmetric deformation oscillation for which the Q branch is of negligible intensity. Measurements of the individual lines are contained in Table I (see next page).

The values given below the Table for ν_1 and ν_2 are the mean figures and are in good agreement with those reported earlier (Bhagavantam, 1931). It may also be noted that the mean of the two bands excited by 4358 is 617 whereas the mean of the corresponding bands excited by λ 4046 is 613. In view of the breadth of the bands the discrepancy is not very much and an average figure of 615 is assigned for ν_5. The very faint line with a shift of 1941 wave numbers is to be attributed to the isotopic molecule $C_{12}C_{13}H_2$. This aspect is being investigated in greater detail by extending it to similar

TABLE I.

Raman Spectrum of Acetylene.

Wave-length	Intensity	Exciting line	Frequency
4768·4	10	4358	1972
4686·3	3	4046	3372
4606·0	0	4358 (?)	1233
4484·8	1 *b*	4358	646
4473·3	1 *b*	,,	589
4435·0	1	4077	1974
4397·8	10	4046	1973
4391·7	0	,,	1941
4179·2	1	3663	3372
4168·0	1	3654	3368
4162·2	2	3650	3370
4154·0	0 *b*	4046	639
4145·2	0 *b*	,,	587
3948·7	3	3663	1975
3938·7	3	3654	1972
3933·4	5	3650	1973

$\nu_1 = 1973$ (10); $\nu_2 = 3371$ (3); $\nu_5 = 615$ (0)
1941 (0).

molecules such as ethylene and will be dealt with by one of us in a later communication. There is, however, another very weak but a definite line at λ 4605·λ 0 which, if attributed to λ 4358, gives a frequency shift of 1233. The origin of this is not clear.

4. Discussion of Results.

The most outstanding feature of the present investigation is the pair of bands at about $\Delta\nu$ 600. It is suggested that they represent the maximum

of the unresolved rotational wings accompanying the total symmetric deformation oscillation of acetylene. The following points constitute the evidence in favour of such a suggestion.

The mean position of the bands corresponds to a frequency shift of 615 cm.$^{-1}$ which is in agreement with the figure derived indirectly from infra-red absorption.

In a deformation vibration, we should expect the Q branch to be of negligible intensity in comparison with the O, P, R and S branches and this is confirmed.

The separation of the maxima is 57 cm.$^{-1}$ for the pair of bands excited by λ 4358 and 52 cm.$^{-1}$ for those excited by λ 4046. The former figure, which is more reliable, is in excellent agreement with the theory. In Fig. 2, the

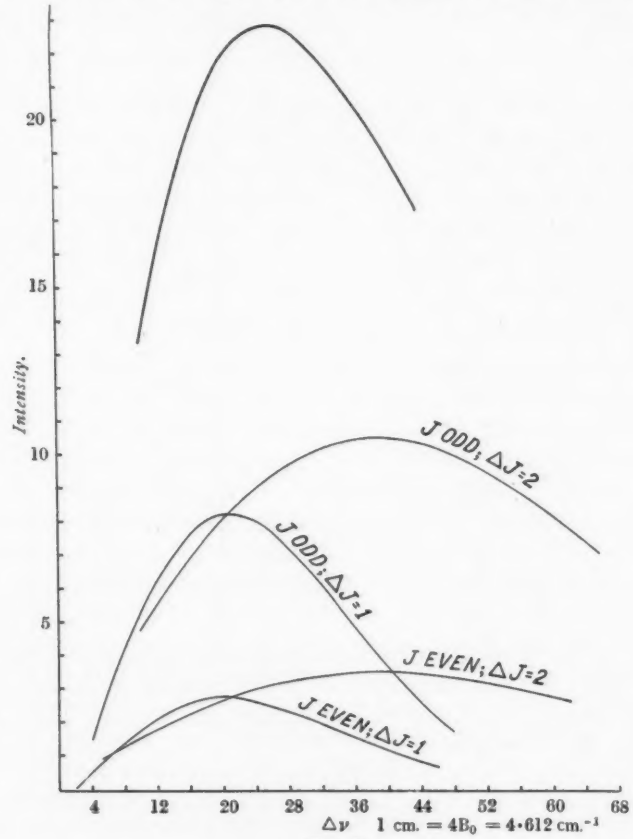

FIG. 2.

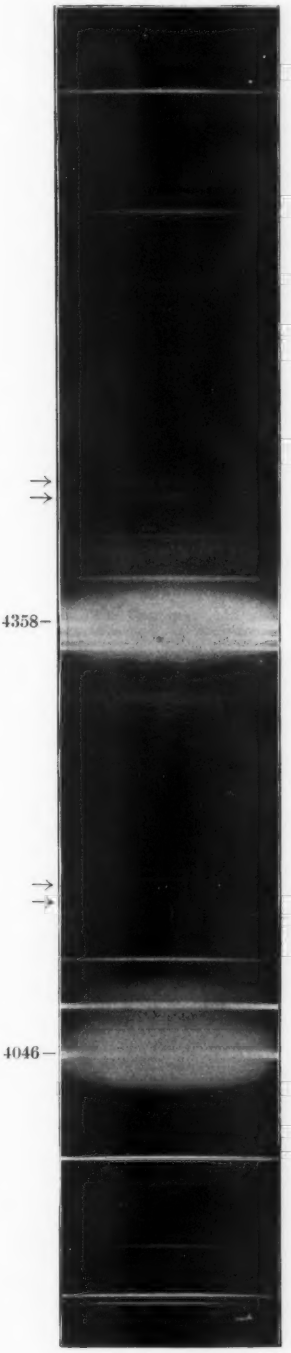

Raman Spectrum of Acetylene gas.

thin curves represent various branches that are to be expected on the Stokes side which in the unresolved state add up to give the aggregate band denoted by the thick line. The maxima of this aggregate band is fairly sharp and occurs at a distance of about 29 wave numbers from the centre or the missing Q branch so that the distance between the maxima should be 58 cm.$^{-1}$ which is in good agreement with the observation. In drawing the curves of Fig. 2, it is assumed that the moment of inertia of the acetylene molecule is 24×10^{-40} gm. cms.^{2} and the odd rotational states are given a statistical weight 3 times as large as that given to the even rotational states. Calculations are carried out for a temperature of 30°C. on the basis of expressions given by Placzek.

5. Summary.

Two new bands at $\Delta\nu$ 589 and 646 have been recorded in the Raman spectrum of acetylene gas by giving a long exposure. These are interpreted as the maxima of the unresolved O, P, R and S branches of the total symmetric deformation vibration of the acetylene molecule. The negligible intensity of the Q branch and the observed separation of about 57 wave numbers between the bands are in accordance with such an interpretation. The frequency shift of about 615 corresponding to the mean position of the bands is in good agreement with the value deduced from the infra-red absorption for the frequency of this oscillation.

REFERENCES.

R. Mecke, *Leipziger Vortrage*, 1931, 23.
G. Placzek, *Handbuch Der Radiologie*, 1934, **6**, Part **2**, 205.
G. B. B. M. Sutherland, *Infra-Red and Raman Spectra*, 1935, 93.
S. Bhagavantam, *Ind. Jour. Phys.*, 1931, **6**, 319.

INTENSITIES IN THE BANDS OF THE VIOLET CYANOGEN SYSTEM.

By Dr. N. R. Tawde, B.A., M.Sc. (Bom.), Ph.D.(Lond.), A.Inst.P. (Lond.),
Royal Institute of Science, Bombay.

Received January 6, 1936.

Introduction.

The application of Maxwell-Boltzmann distribution to vibrational levels in a band system has yielded very interesting results in many cases. The Franck-Condon theory of maximum transitions examined in relation to different functions expressing the nuclear potential energy of a diatomic molecule in a given electronic state gives different results which require to be verified by experiment. For this reason the subject of vibrational intensities in band spectra has assumed a great importance.

The violet bands of cyanogen form a system which is associated with violet glow when a carbon arc is struck in air. Other methods of exciting these bands are (*a*) active nitrogen, (*b*) electric furnace and (*c*) cyanogen gas burning in flame. The method of carbon arc in air has been chosen here on account of the easy occurrence of the bands and its nearer approach to conditions of thermal equilibrium.

In a paper by Ornstein and Brinkman,[1] one of the aspects, namely, of temperature by intensity measurements in this system, has been studied by the authors. In order to tackle the problem in all aspects and in view of the recent systematic work on gross intensities in some band systems, a thorough investigation of these bands was undertaken and the results are presented in this paper.

For the purposes of this paper, only the peak intensities near the heads of unresolved bands will be taken. Sufficient justification for taking the unresolved bands has been provided by Johnson and Tawde[2] and by Johnson and Dunston[3] in recent papers. This is further supported by the work of Ornstein and Brinkman[1] who have proved by measurements that peak intensities near the heads are in the ratio of the sum of intensities of all the lines into which the band is resolved.

Experimental.

The technique of intensity measurements is the same as that indicated in previous papers[2,3,4] in which further references relevant to the subject

can be found. The carbon arc was run at 3 amps. on 100 volts, the arc length being on an average 8 mm. The band system was photographed on Hilger E_1 spectrograph having quartz system, along with the intensity marks taken with a step-slit having 8 elements. For this, a standard lamp of known energy distribution was used. The calibration of the lamp was done on Hilger quartz double monochromator of the Government Chemical Laboratory, London. The plates used were the Ilford Rapid Process Panchromatic and sufficient number of photographs were taken so as to enable a set of bands to come with measurable density. All observations were taken from microphotometer records. The measured intensities were duly corrected for energy distribution ($E\lambda$: λ curve) of the lamp and the varying sensitivity of the photographic plate in different regions of the spectrum.

Results.

(1) *Intensities.*

The results of intensity measurements are entered in the following v'-v'' (Table I) with 0—0 band as 100. The 0—0 band being very strong in

TABLE I

Intensities and I/ν^4 Values.

v' \ v''	0	1	2	3	4	5	6	7	$\Sigma I/\nu^4$
0	100 22·57	11·27 3·54	1·26 ·74						26·85
1	10·26 1·68	50·23 11·19	12·08 3·72	2·09 0·91					17·50
2		12·45 2·04	28·64 6·32	10·75 3·26	1·37 0·58				12·20
3			5·22 0·85	16·44 3·60	10·15 3·04	1·04 0·43			7·92
4					10·82 2·35	8·15 2·42	1·01 0·41		5·18
5							7·26 2·13	0·87 0·35	2·48

comparison to 0, 1 or 0, 2, a number of intermediate exposures had to be made to express it on the relative scale.

The intensity of a band connected with a given pair of vibrational levels v'–v'' is proportional to ν^4, to the number of molecules in the initial level and to the probability of the transition from the initial to the final level. If the distribution in the initial level corresponds to thermal equilibrium

at an absolute temperature T, the number of molecules with the vibrational energy $E_{v'}$ is proportional to the Boltzmann factor $e^{-\frac{E_{v'}}{kT}}$ and the intensity of a band can be written down as $I = C.\ \nu^4\ p_{v'v''}.\ e^{-\frac{E_{v'}}{kT}}$ where p = transition probability, C=constant, the other symbols having their usual significance. Consequently I/ν^4 values are calculated separately for each band and these are put below the intensity values in the above table. The sum $\Sigma\ I/\nu^4$ for each initial level is put in the last column of the table and these numbers represent values proportional to the statistical weight of the level.

(2) *Effective Temperature of the Arc.*

The data $\Sigma\ I/\nu^4$ from Table I have been utilized to calculate 'effective' temperature of the source. In the case of CN $^2\Sigma \rightarrow {}^2\Sigma$ system, the following equation holds for the vibrational energy in the upper state:

$$2164 \cdot 15\ (v'+\tfrac{1}{2}) - 20 \cdot 25\ (v'+\tfrac{1}{2})^2 = 1 \cdot 6083\ T\ log_{10} \frac{N_0}{N_{v'+\frac{1}{2}}}$$

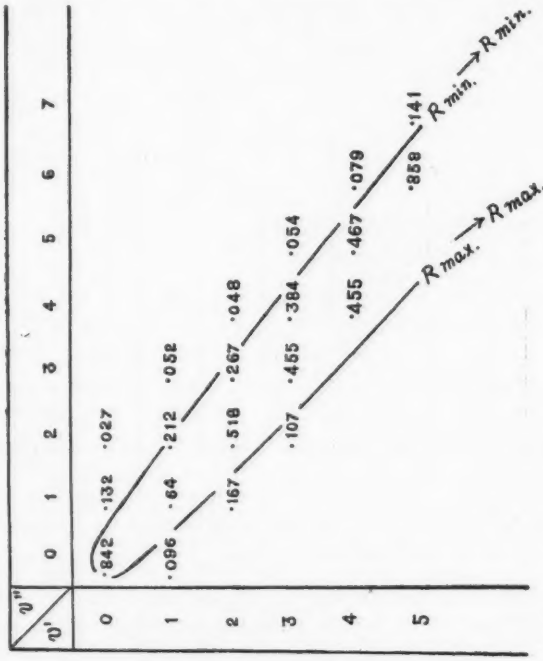

FIG. 1. Transition Probabilities.

The values of N, the number of molecules are taken proportional to $\Sigma I/\nu^4$ in each initial level. By plotting $log_{10}\frac{N_0}{N_{v'+\frac{1}{2}}}$ against the vibrational energy it is possible to get the value of T the absolute temperature from the slope of the linear relation and this has been found in our case to be 7210±500K.

(3) *Transition Probabilities.*

Fig. 1 above has been constructed giving numbers proportional to vibrational transition probabilities. They have been calculated according to procedure adopted in a previous paper from I/ν^4 values of Table I. They represent only relative values. The Condon parabola of maximum transitions has been shown as a curve passing through preferred vibrational levels. Its agreement with theory can be judged from the following Table II which gives comparative values.

TABLE II.

Transition Probabilities.

Comparative Values.

Experimental	Morse	Rydberg
	$r_{max} \rightarrow r_{max}$	
4,4	4, 3 and 4, 4	4, 4
3, 2 and 3, 3	3, 2	3, 2 and 3, 3
2, 2 and 2, 1	2, 1	2, 2 and 2, 1
1, 1	1, 0 and 1, 1	1, 0 and 1, 1
0, 0	—	0, 0
	$r_{min} \rightarrow r_{min}$	
5, 6 and 5, 7	5, 7	5, 7
4, 5	4, 6	4, 6
3, 4	3, 5	3, 5
2, 3	2, 4	2, 4
1, 2	1, 2	1, 2
0, 1	0, 1	0, 1 and 0, 0

Column 1 of the Table gives experimental transitions, while columns 2 and 3 give the transitions as derived theoretically by graphical method from Morse and Rydberg functions. The potential energy curves drawn to scale according to these are shown in Figs. 2 and 3.

(4) *Behaviour in Sequences.*

It has been shown by Ornstein and Brinkman[1] that in the sequences of this system, there is a linear relation between *log* I/ν^4 of a band and the vibrational energy $E_{v'}$. This means that the vibrational transition probabilities in each sequence are proportional to $e^{-\alpha E_{v'}}$ after a certain value of v', α being a constant. The linearity of this relation in some sequences has been verified by the author in a previous paper.[6] Calculation of the value of α gives in the case of v'-$v''=0$ sequence $\alpha = +1{\cdot}15 \times 10^{-4}$ and that

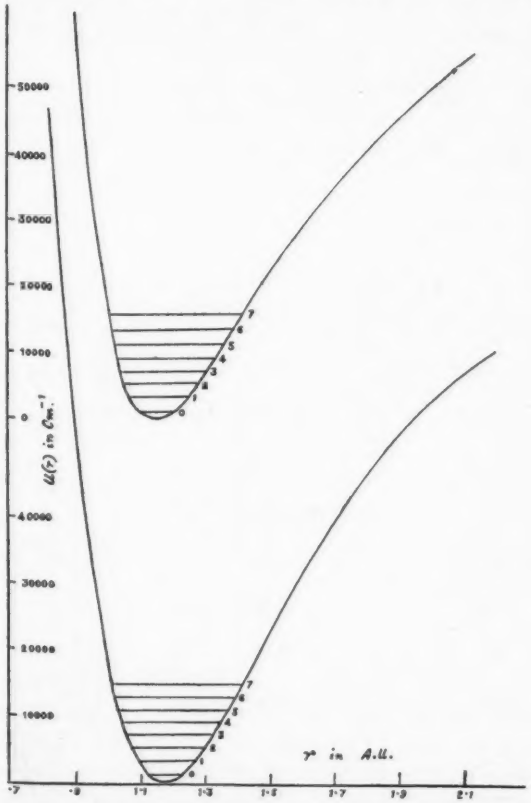

FIG. 2. Morse Potential Energy Curves for Violet CN System.

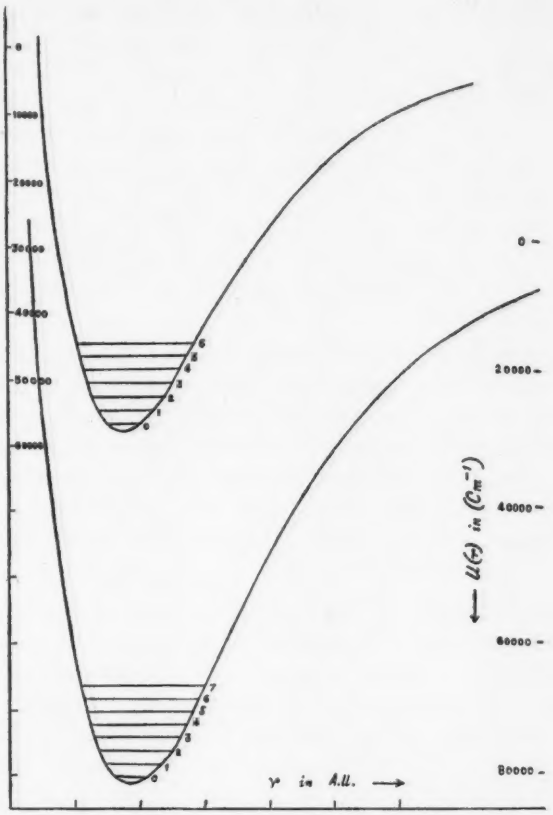

FIG. 3. Rydberg $U(r)$ Curves for Red CN System.

in the case of v'-$v''=-1$ it equals $-1\cdot38\times10^{-4}$ on a relative scale. For v'-$v''=+1$ and -2 sequences the value of a is not very well defined, but it is near about $-1\cdot317\times10^{-4}$ in the case of the latter. In general, it appears that $a>0$ in sequences v'-$v''=0$ and $+1$ and $a<0$ in sequences v'-$v''=-1$ and -2 as indicated by Ornstein and Brinkman.[1]

Conclusions.

In deriving the effective temperature of the radiating source, a linear relation was found between the 'weights' of the various initial levels and the vibrational energy. This shows that there is thermal equilibrium of molecules at the temperature of the source and a vibration temperature does exist in this case, but its value is rather too high for the source used. However, according to Ornstein and Brinkman,[1] temperatures between

5,000°K. and 7,000°K. exist in the carbon arc depending on the current and length of the arc as determined by spectroscopic methods. They have found in the case of CN bands a vibration temperature 5,870° K. for a current of 1.7 amp. in the carbon arc. Considering this, the temperature 7,210°K. ±500 in our case (for current strength 3 amps.) is not improbable, especially in view of the probable sources of error due to unknown causes in this type of work. If in different zones of the arc different temperatures exist, it is quite likely that two band systems arising in the same arc source but giving two different effective temperatures for that source, are excited in different zones. This aspect of the problem requires elucidation and work in this direction is in progress.

There is not much to differentiate between the results of maximum transition probabilities as derived from Morse and Rydberg potential energy functions. Both the curves agree well within the observed limits of the vibrational levels of the system. The Condon parabola derived from both is practically the same and there is satisfactory agreement of the experimental curve with this parabola as can be seen from Fig. 1 and Table II. The narrowness of the parabola is to be expected for a molecule of this type where $r'_e < r''_e$.

The theoretical aspect of the subject of spectral intensities in band systems has been treated by Hutchisson[5] on the basis of quantum mechanics. Hutchisson considers that his formula for calculating the intensity of vibrational levels is applicable to symmetric molecules only, but Dunham[7] shows that it is of general applicability. Hence in CN which is a non-symmetric molecule, it should be possible by Hutchisson's formula to calculate theoretical intensities and to see their agreement with experiment. It is intended to investigate this in a later paper.

The experimental part in connection with this problem was carried out at the University of London King's College and all the later work was done at the Royal Institute of Science, Bombay. The author is much indebted to Dr. R. C. Johnson for his interest in the work and to Prof. A. Fowler of the Royal College of Science, London, for allowing the use of his microphotometer.

Summary.

Quantitative estimation of vibrational intensities in $^2\Sigma \rightarrow {}^2\Sigma$ system of CN has been made by the method of heterochromatic spectral photometry.

The results have been utilized to examine some aspects of Condon's theory and effective temperature derived on the assumption of the thermal distribution of molecules in vibrational levels.

Some features of intensities in sequences are discussed.

REFERENCES.

1. Ornstein and Brinkman, *K. Akad. Amsterdam, Proc.*, 1931. **34**, 33-41.
2. Johnson and Tawde. *Proc. Roy. Soc.*, 1932, **137A**, 575.
3. Johnson and Dunston, *Phil. Mag.*, 1933, **16**, 472.
4. Tawde, *Proc. Phys. Soc.*, 1934, **46**, 324.
5. Hutchisson, *Phys. Rev.*, 1930, **36**, 410.
6. Tawde, *Proc. Ind. Acad. Sci.*, 1935, **2A**, 67.
7. Dunham, *Phys. Rev.*, 1930, **36**, 1553.

THE ABSORPTION SPECTRA OF SOME AROMATIC COMPOUNDS.

Part I.—Hydrocarbons.

By P. K. Seshan.

(From the Indian Association for the Cultivation of Science, Calcutta.)

Received December 29, 1935.
(Communicated by Prof. K. S. Krishnan, D.SC.)

1. Introduction.

The absorption spectra of benzene and some of its simple derivatives have been studied in great detail by Henri[1] and his collaborators, and they yield much useful information regarding the optical and other constants of the molecules. For molecules containing more than one benzene ring, the analysis of the spectrum is naturally more difficult. Some of the molecular constants, however, are easily obtained, as for example, the electronic frequencies of the molecule, and its vibration frequencies in the normal and in the excited states. It would be of interest to follow the progressive variation of these constants and of the general characteristics of the absorption bands, with the addition of extra benzene rings, both of the condensed and uncondensed types, in different positions, and to interpret these variations in relation to the structure of these molecules. The present paper concerns itself with such a study. Several aromatic hydrocarbons are studied for their absorption spectra in the vapour state, and among them are (1) naphthalene, anthracene, and naphthacene, with linear condensed benzene rings; (2) phenanthrene, chrysene, and dibenzanthracene, with side condensed rings; (3) pyrene and perylene, with close-packed rings; (4) acenaphthene, fluorene and fluoranthene, with incomplete rings; (5) diphenyl, terphenyl, diphenylmethane, dibenzyl, triphenylmethane and triphenylbenzene, with uncondensed benzene rings; and (6) durene and hexamethylbenzene. The results are discussed in relation to the structure of the molecules and their characteristic electronic and vibrational frequencies.

Since the absorption spectra of the molecules are known to be considerably influenced by the state of aggregation of the molecules, we have also studied the absorption spectra of these substances in the state of solution in different

[1] Henri, *Jour. Physique*, 1922, **3**, 181; Orndorff, Gibbs, McNulty and Shapiro, *Jour. Am. Chem. Soc.*, 1928, **50**, 831.

solvents, and, occasionally in the molten and in the solid states as well. The positions of the absorption bands of a substance in the different physical states are compared.

2. *Experimental.*

The absorption measurements for the vapours extended in general, from 7000 Å to 2300 Å, and were made with a Hilger quartz E_2 spectrograph. Where the absorption bands were very sharp, Hilger E_1 spectrograph, with a much higher dispersion, was used. Iron arc was used as the standard for the wave-length measurements.

The source of continuous spectrum used for the absorption measurements in the ultra-violet was a specially designed water-cooled hydrogen discharge tube described in an earlier publication by the author,[2] giving an intense spectrum upto about 2100 Å. For the visible and the near ultra-violet regions a Zeiss tungsten linear filament lamp, fitted with a quartz window, was found to be a more suitable source.

The substances were in general obtained from standard firms,[3] and were further purified by crystallisation or sublimation.

The absorption spectra of the solutions were studied in the usual manner with a graduated Baly absorption tube fitted with quartz windows.

For the study of the absorption in the vapour state, the substance was introduced in an absorption tube of pyrex glass, 75 cms. long and 2 cms. in diameter, fitted with quartz windows at the ends. It was placed in a suitably devised air oven with a double jacket, where it could be heated and maintained at any desired temperature up to 300° C. (All the substances studied here melt below 250° C.) The temperature of the absorption tube was raised in stages of 10° C., and the absorption spectrum was photographed at each stage. From these absorption spectra, corresponding to gradually increasing vapour pressures, photographed in succession the intensity wave-length curves can be easily traced on an arbitrary scale, just as in the absorption photographs for the solution by the Baly method in which the thickness of the column of solution is gradually increased. The positions of the maxima and the minima of absorption are located in this manner more precisely than from single photographs of the absorption.

The absorption and fluorescence spectra of single crystals of many of these hydrocarbons have been studied by us in detail, particularly in relation to the influence of the direction of vibration of the incident light with reference to the crystal axes on the positions and the intensities of the bands. A

[2] *Jour. Sci. Instruments*, 1935, 12, 230.

[3] The author's thanks are due to Prof. L. F. Fieser of the Harvard University and to Prof. A. Dadieu of the Vienna University for the supply of naphthacene and perylene.

report of this work is being published separately, to which the reader may be referred for a description of the experimental arrangement used for these absorption measurements, and for the details of the results. We may mention here that though the intensities of the various absorption bands show a remarkable dependence on the direction of the light-vector in the crystal, the *positions* of the bands are practically independent of the direction of the vector. The data for the positions of the absorption bands in the solid state quoted in the next section are all taken from this paper.

3. Results.

The experimental results are collected together in this section. The different substances are considered separately, and the special characteristics of the bands are described under each. In the tables are entered the wave-lengths of the absorption maxima, and the corresponding wave numbers in cm.$^{-1}$ The difference between the wave-numbers of successive bands are entered in the next column. The intensities of the bands are indicated by arbitrary numbers.

The absorption data for the substance in solution in alcohol, and for the substance in the solid state, are also given for comparison with the vapour data. On comparing the absorption spectra for the solid, liquid and the solution with that of vapour, we find that the positions of the bands are widely different; even for the solutions they are different for different solvents. A closer comparison of the spectra in the different physical states, however, shows that except for a bodily shift of the absorption spectra towards the longer-wave-length side as we go from the vapour to the solution, and further in the same direction as we go from solution to molten liquid and still further when we pass to the solid, and a progressive change in the diffuseness of the bands, the relative positions of different components of the bands system are more or less the same for the different physical states. There is thus an approximate one to one correspondence between the prominent absorption bands in the different states; the corresponding bands in the different states are also easy to identify. In the following tables the data for the corresponding bands in the different physical states are entered in the same *row*, so as to facilitate comparison.

The actual absorption spectrograms are also reproduced, from which the general nature of the absorption bands and their other characteristics will be clear.

Among the substances studied here naphthalene vapour has been already studied in great detail by Henri and Laszlo.[4] Some preliminary

[4] Henri and Laszlo, *Proc. Roy. Soc.*, A, 1926, **105**, 355; Laszlo, *Zeits. Phys. Chem.*, 1925, **118**, 369.

absorption measurements are available for the anthracene vapour,[5] and for solid anthracene and phenanthrene at low temperatures.[6] In the state of solution most of these substances have previously been studied, by Baly,[7] Clar,[8] Dadieu[9] and others. The solution data given in the tables are those obtained by us, and they agree well with those given by these earlier investigators. Alcohol was the usual solvent in our measurements.

In general the absorption spectrum consists of a large number of prominent bands more or less equally spaced; the spacing interval is about 1300 to 1400 cm.$^{-1}$ These bands are accompanied by feeble satellites usually one each, on the shorter-wave-length side, separated from the main band by about 400 cm.$^{-1}$ They do not generally exhibit any rotational fine structure; naphthalene and acenaphthene are striking exceptions.

Accompanying this banded absorption there is also a strong background of continuous absorption, which consists of two distinct regions separated by a region of transmission. The first absorption region, usually in the near ultra-violet, begins more or less abruptly, and reaches a feeble maximum. Beyond it is a region of relative transparency, and further beyond begins the second region of absorption, which is much stronger than the first. For some of the substances there is also a second region of feeble transmission in the ultra-violet. The bands in the first region stand out from the continuous background much more prominently than those in the second region; indeed in the second region two or three bands only can be observed, near the long-wave-length end of the region.

We now proceed to the detailed report of the results.

1. *Naphthalene.*

See Figs. 1 (*a*) and (*b*), Plate V. Many of the bands in the long-wave-length region exhibit fine-structure and they are indicated by an asterisk; a double asterisk indicates that the fine-structure is very prominent. There is a region of transmission from 2600 Å to 2250 Å, beyond which there is again absorption; the bands in the latter region are broad and diffuse. The bands in the solution and solid state do not show any fine-structure.

---

[5] Capper and Marsh, *Jour. Chem. Soc.*, 1926, 724.

[6] Obreimow and Prichotjko, *Phys. Zeits. Sow. Union*, 1932, **1**, 203.

[7] *Jour. Chem. Soc.*, 1908, **93**, 1902.

[8] Several papers in *Berichte*, 1931–1933.

[9] *Zeits. Phys. Chem.*, 1933, **135**, 347.

TABLE 1. *Absorption spectrum of naphthalene.*

	Vapour			Solution			Solid		
	λ	ν	$\Delta\nu$	λ	ν	$\Delta\nu$	λ	ν	$\Delta\nu$
**	3190	31320					3270	30580	
			460						450
*	3145	31780		3190	31320		3220	31030	
			240			460			410
**	3120	32020		3145	31780		3180	31440	
			370			470			500
**	3085	32390		3100	32250		3130	31940	
			340			↑			400
**	3055	32730				420	3090	32340	
			200 ↑			↓			470
*	3035	32930	420	3060	32670		3045	32810	
			220 ↓			320			
**	3015	33150		3030	32990				
			290 ↑			220			
*	2990	33440	490	3010	33210				
			200 ↓			340			
**	2975	33640							
			420						
*	2935	34060		2980	33550				
			290			450			
*	2910	34350		2940	34000				
			400			590			
*	2875	34750		2890	34590				
			350			360			
	2850	35100		2860	34950				
			310			370			
	2820	35410		2830	35320				
			420			460			
**	2790	35830		2795	35780				
			450			310			
*	2755	36280		2770	36090				
			470			460			
*	2720	36750		2735	36550				
			410						
*	2690	37160							
			490						
*	2655	37650		2670	37440				
			450						
*	2625	38100							
			570						
	2585	38670							
			450						
	2555	39120		2590	38590				
			480						
	2525	39600							
			470						
	2495	40070							

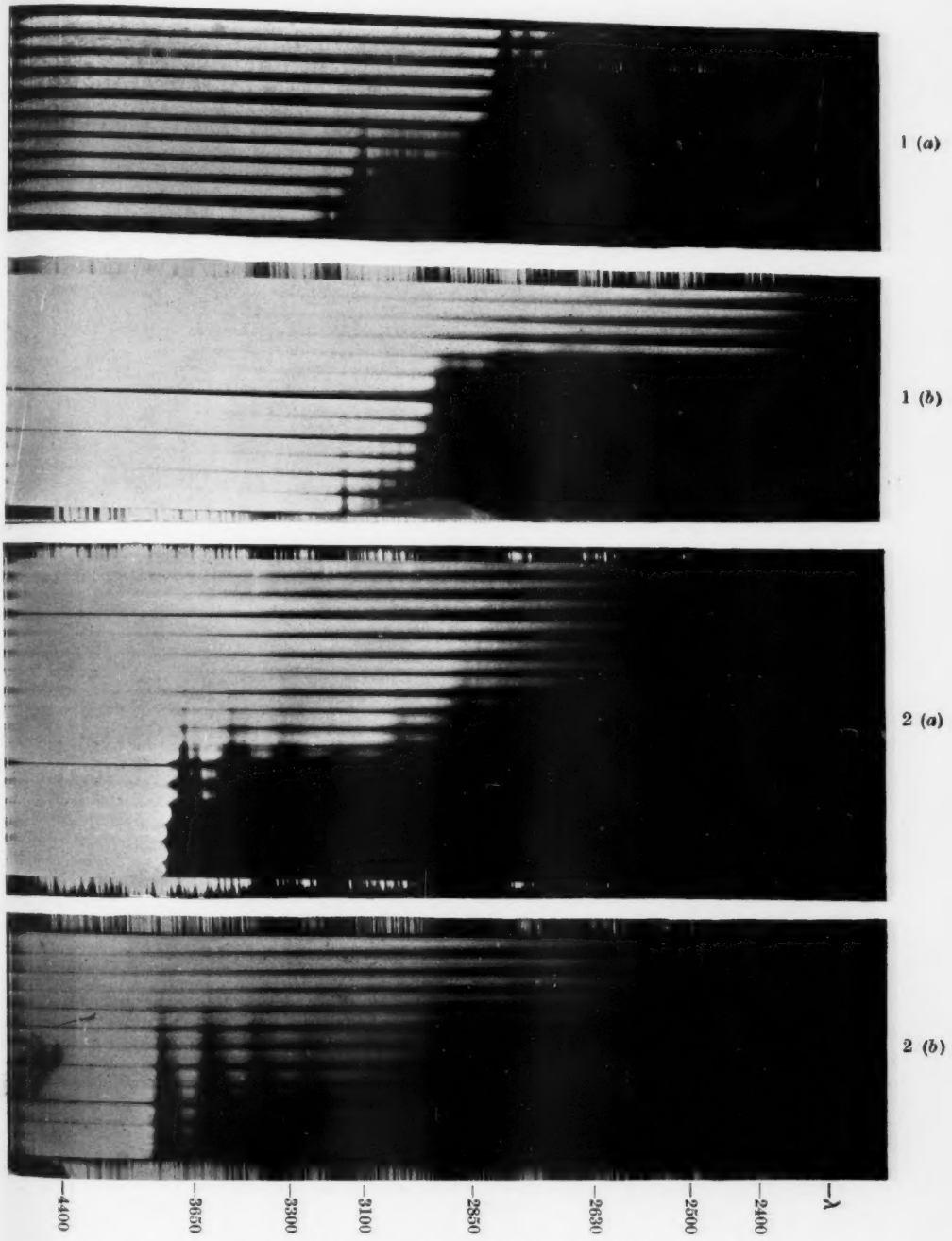

FIG. 1. Naphthalene: (*a*) Vapour, (*b*) Solution.
FIG. 2. Anthracene: (*a*) Vapour, (*b*) Solution.

2. *Anthracene.*

Figs. 2 (*a*) and (*b*), Plate V. In the first region of absorption, which extends from about 3700 Å to 3100 Å, the absorption bands appear prominently, the continuous background being very feeble. The bands are spaced at intervals of 1400 to 1350 cm.$^{-1}$, and many of them are accompanied by satellites at intervals of 350 to 400 cm.$^{-1}$

In solution and in the solid state, most of these satellites disappear, the bands retaining only one satellite each, on the short-wave-length side at 400 cm.$^{-1}$

Near about 3100 Å is the region of feeble transmission, and as will be seen from the photographs, there is an indication of another such region much less transparent, at about 2600 Å.

TABLE 2. *Absorption spectrum of anthracene.*

Int.	Vapour			Solution			Solid		
	λ	ν	Δν	λ	ν	Δν	λ	ν	Δν
1	3680	27170					4000	24990	
			370						550
5	3730	27540		3750	26660		3915	25540	
			390			430			460
3	3580	27930		3690	27090		3845	26000	
			430						
2	3525	28360	1480			1460			1480
			240						
1	3495	28600							
			420						
5	3445	29020		3555	28120		3700	27020	
			380			400			440
3	3400	29400		3505	28520		3640	27460	
			400	1460		1460			1460
2	3355	29800							
4	3280	30480		3380	29580		3510	28480	
			370			400			370
2	3240	30850	1410	3335	29980	1420	3465	28850	1450
3	3135	31890		3225	31000		3340	29930	
			410			440			
1	3095	32300	1440	3180	31440	1460			1410
5	3000	33330		3080	32460		3190	31340	

TABLE 2—(*Contd.*)

Int.	Vapour			Solution			Solid		
	λ	ν	Δν	λ	ν	Δν	λ	ν	Δν
1	2960	33770	440 / 1500			1490			
7	2870	34830		2945	33950				
			370						
4	2840	35200							
2	2790	35830	1390			1440			
			390						
7	2760	36220		2825	35390				
			400						
4	2730	36620							
			410						
2	2700	37030	1500			1430			
			270						
2	2680	37300							
			420						
7	2650	37720		2715	36820				
			440						
4	2620	38160	1410			1410			
8	2555	39130		2615	38230				
			1510			1440			
10	2460	40640		2520	39670				
			1440						
10	2380	42080							
			1380						
10	2300	43460							

3. *Naphthacene.*

The absorption spectrum of this substance bears a striking resemblance to that of anthracene, the main bands being spaced at intervals of 1350 to 1400 cm.$^{-1}$, with satellites at intervals of 400 cm.$^{-1}$ The continuous spectrum in region I is even less feeble than in anthracene, and the bands appear therefore more prominently than in anthracene. See Figs. 3 (*a*), (*b*), (*c*) and (*d*), Plate VI.

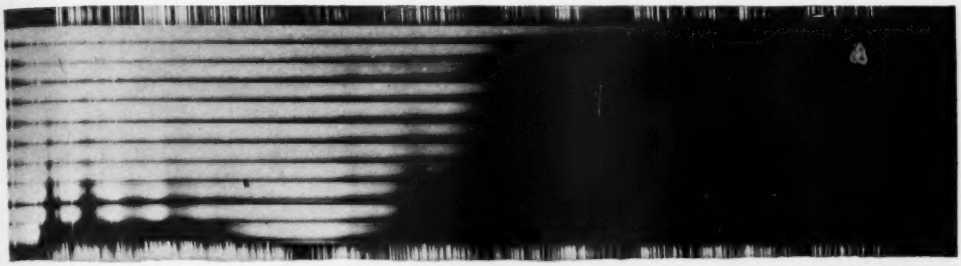

3 (*a*)

3 (*b*)

3 (*c*)

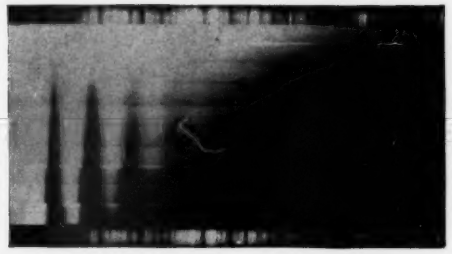

3 (*d*)

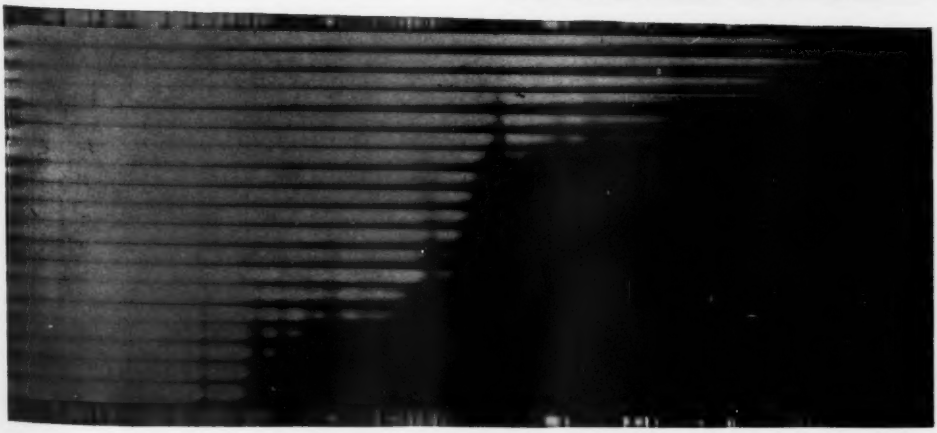

4 (*a*)

FIG. 3. Naphthacene: (*a*) Vapour. (*b*) Solution.
(visible region): (*c*) Vapour, (*d*) Solution.

FIG. 4. Phenanthrene: (*a*) Vapour.

TABLE 3. *Absorption spectrum of naphthacene.*

Int.	Vapour			Solution			Solid		
	λ	ν	Δν	λ	ν	Δν	λ	ν	Δν
6	4500	22220		4680	21360		4850	20610	
			420			390			
4	4415	22640		4595	21750				1460
			420			1410			
2	4335	23060	1410						
6	4230	23630		4390	22770		4530	22070	
			400			420			
4	4160	24030		4310	23190				1450
			410			1410			
1	4090	24440	1390						
5	3995	25020		4135	24180		4250	23520	
			420			440			
3	3930	25440		4060	24620				
			1390			1390			
5	3785	26410		3910	25570				
			1440			1410			
4	3590	27850		3705	26980				
			1380			1380			
3	3420	29230		3525	28360				
			1380			1410			
6	3195	31290		3335	29980				
			1330			1280			
8	3060	32670		3185	31390				
			1320			1330			
10	2940	34000		3060	32670				
			1300			1260			
10	2830	35320		2940	34000				
			1320			1290			
10	2730	36620		2835	35260				
			1260			1310			
9	2635	37940		2735	36550				
8	2550	39200		2640	37860				

4. *Phenanthrene.*

Figs. 4 (*a*) and (*b*), Plates VI and VII. The compound contains usually, as was pointed out by Capper and Marsh, anthracene as an impurity, and has to be specially freed from the latter.

The general nature of both the continuous and the banded absorptions is very different from that of anthracene or naphthacene. The progression of the intensities of the absorption bands does not show the correspondence with that of the continuous absorption accompanying the bands, that is observed in anthracene or naphthacene.

TABLE 4. *Absorption spectrum of phenanthrene.*

Int.	Vapour			Solution			Solid		
	λ	ν	Δν	λ	ν	Δν	λ	ν	Δν
3	3630	27540		3750	26660		3830	26100	
			350 ↑			390 ↑			450 ↑
2	3585	27890	1440	3695	27050	1460	2765	26550	|
			↓			↓			400
3	3450	28980		3555	28120		3710	26950	1440
			730 ↑			730 ↑			590 ↓
3	3365	29710	1500	3465	28850	1460	3630	27540	
			770 ↓			730 ↓			780 ↑
3	3280	30480		3380	29580		3530	28320	1480
			660 ↑			710 ↑			700 ↓
3	3210	31140	1410	3300	30290	1420	3445	29020	
			750 ↓			710 ↓			730 ↑
3	3135	31890		3225	31000		3360	29750	1410
			730 ↑			790 ↑			680 ↓
3	3065	32620	1440	3145	31790	1460	3285	30430	
			710 ↓			670 ↓			760 ↑
3	3000	33330		3080	32460		3205	31190	1460
			730 ↑			750			700 ↓
7	2935	34060	1440	3010	33210		3135	31890	
			710 ↓			910			780
4	2875	34770		2930	34120		3060	32670	
			490			470 ↑			
10	2835	35260		2890	34590	|		
			320 ↑			430			
8	2810	35580	|	2855	35020				
			380						
8	2780	35960	1430			1460			
			330 |			|		
8	2755	36290							
			400 ↓			↓			
9	2725	36690		2810	35580				
			750 ↑			↑			
9	2670	37440	1470			1450			
			720 ↓			↓			
7	2620	38160		2700	37030				
			1430			1420			
8	2525	39590		2600	38450				
			1450			1460			
10	2435	41040		2505	39910				
			1410			1480			
10	2355	42450		2415	41390				

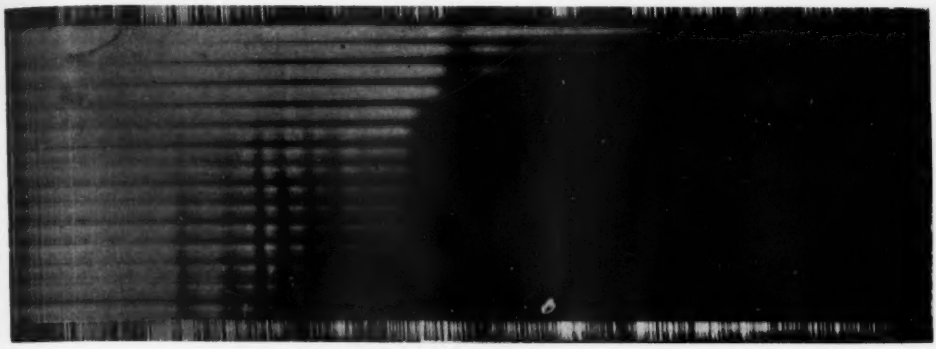

4 (b)

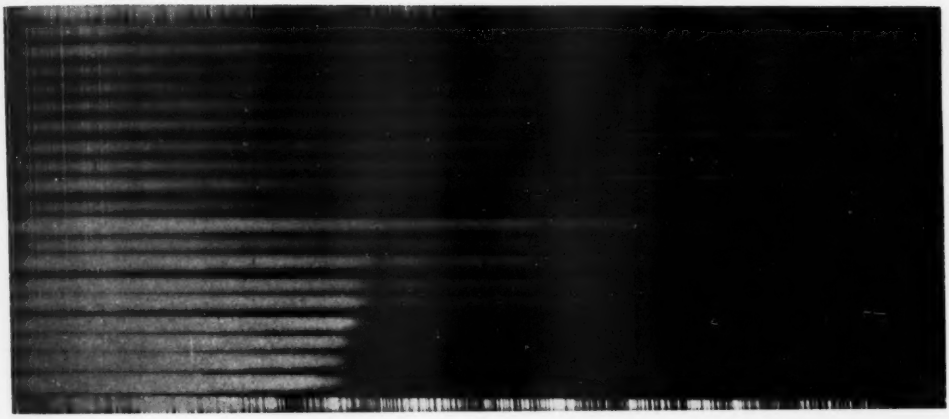

5 (a)

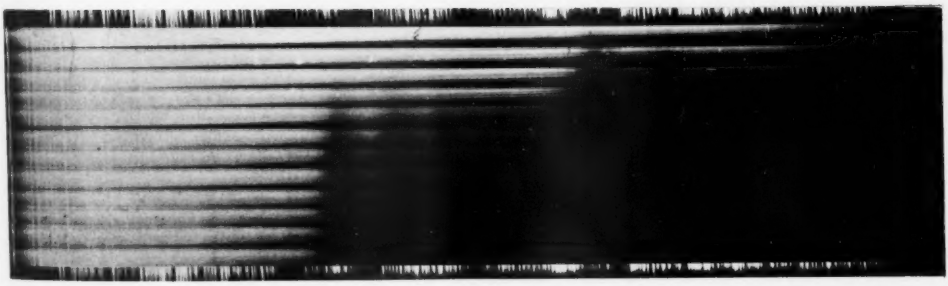

5 (b)

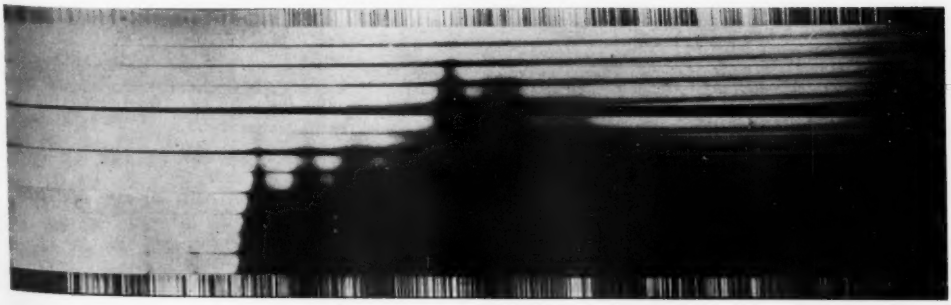

6

FIG. 4.—Phenanthrene : (*b*) Solution.
FIG. 5.—Chrysene : (*a*) Vapour, (*b*) Solution.
FIG. 6.—Dibenzanthracene Solution.

5. *Chrysene* (1·2 *Benzophenanthrene*).

The spectrum resembles that of phenanthrene. Figs. 5 (*a*) and (*b*), Plate VII.

TABLE 5. *Absorption spectrum of chrysene.*

Int.	Vapour			Solution			Solid		
	λ	ν	Δν	λ	ν	Δν	λ	ν	Δν
5	3605	27730		3745	26690		3920	25510	
			750 ↑			770 ↑			450
4	3510	28480	1420	3640	27460	1510	3850	25960	
			670 ↓			740 ↓			460
2	3430	29150		3545	28200		3785	26420	
			780 ↑			730 ↑			460
3	3340	29930	1520	3455	28930	1500	3720	26880	
			740 ↓			770 ↓			440
1	3260	30670		3365	29700		3660	27320	
			770 ↑			↑			440
1	3180	31440	1580			1540	3600	27760	
			810 ↓			↓			410
3	3100	32250		3200	31240		3550	28170	
			370 ↑			↑			480
1	3065	32620	1300			1320	3490	28650	
			↓			↓			500
3	2980	33550		3070	32560		3430	29150	
			340 ↑			↑			390
1	2950	33890	1300			1270	3385	29540	
			↓			↓			
3	2870	34850		2955	33830				
			350 ↑			↑			
0	2840	35200	1300			1310			
			↓			↓			
6	2765	36150		2845	35140				
			1430			1080			
10	2660	37580		2760	36220				
			720 ↑			↑			
5	2610	38300	|			|		
			370 |			1530		
4	2585	38670	1470			|			
			380 ↓			↓			
9	2560	39050		2580	38750				
			1420			1400			
8	2470	40470		2490	40150				
			1450						
7	2385	41920							

6. 1. 2. 5. 6. *Dibenzanthracene.*

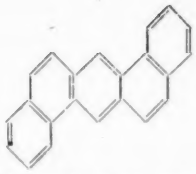

The vapour spectrum was not studied. The substance was, however, studied in solution and in the solid state. See Fig. 6, Plate VII.

TABLE 6. *Absorption spectrum of dibenzanthracene.*

Int.	Solution			Solid		
	λ	ν	$\Delta\nu$	λ	ν	$\Delta\nu$
				4685	21340	
						1380
				4400	22720	
				4040	24740	
						790 ↑
2	3970	25190		3915	25530	1460
			700			670 ↓
1	3860	25890		3815	26200	
			700			460
2	3760	26590		3750	26660	
			680			730
4	3665	27270		3650	27390	
			1460			1010
2	3480	28730		3520	28400	
			760 ↑			
5	3390	29490	1380			1480
			620 ↓			
2	3320	30110		3450	28980	
			940 ↑			
6	3220	31050	1380			
			440 ↓			
6	3175	31490				
			810			
8	3095	32300				
			1360			
9	2970	33660				
			1420			
9	2850	35080				
			880 ↑			
10	2780	35960	1540			
			↓			
10	2730	36620				

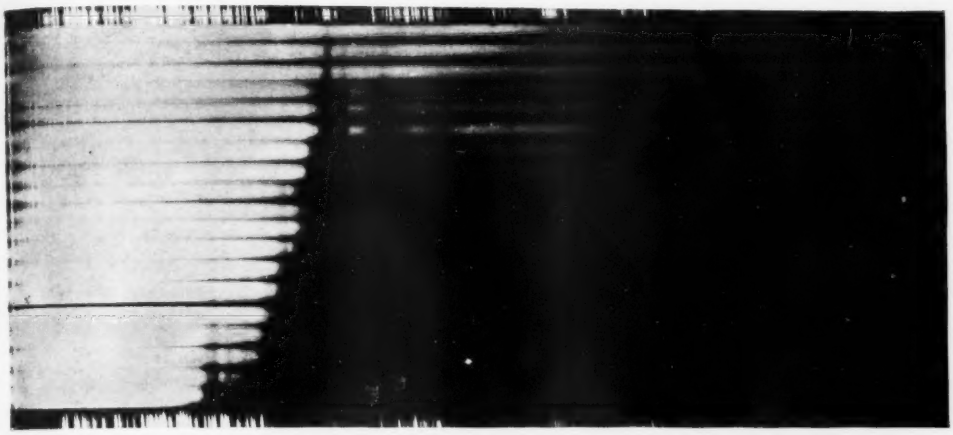

7 (*a*)

7 (*b*)

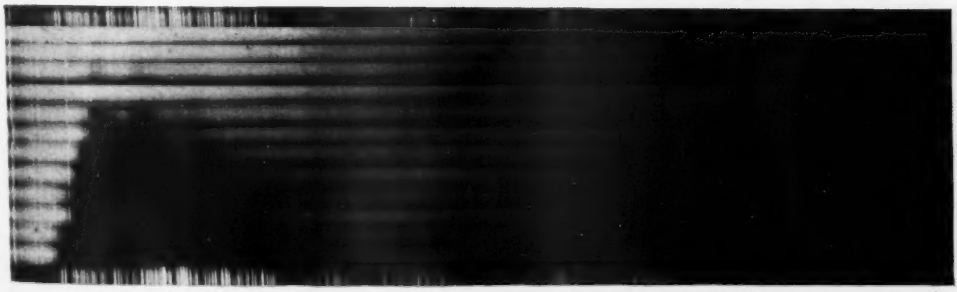

8 (*a*)

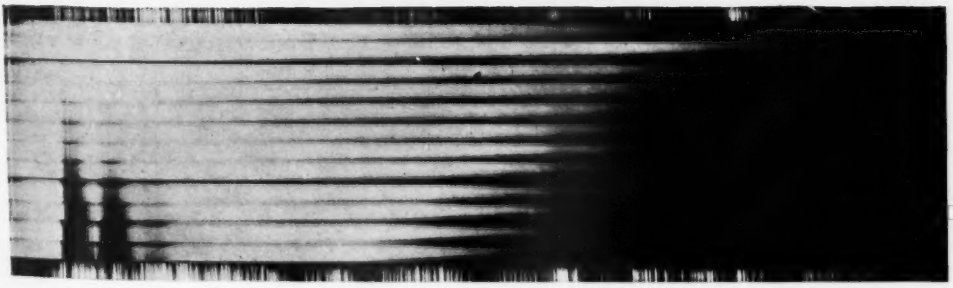

8 (*b*)

FIG. 7. Pyrene: (*a*) Vapour. (*b*) Solution.
FIG. 8. Perylene: (*a*) Vapour. (*b*) Solution.

7. *Pyrene.*

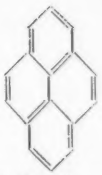

The spectrum resembles more that of the linear ringed compounds like naphthacene and anthracene, than that of phenanthrene or chrysene. It shows however, less details than either anthracene or naphthacene. See Figs. 7 (*a*) and (*b*), Plate VIII.

TABLE 7. *Absorption spectrum of pyrene.*

Int.	Vapour			Solution			Solid		
	λ	ν	Δν	λ	ν	Δν	λ	ν	Δν
3	3630	27540		3795	26340		3770	26520	
			540			530			460
2	3560	28080		3720	26870		3705	26980	
			520						450
2	3495	28600					3645	27430	
			590						460
3	3425	29190					3585	27890	
			560						430
2	3360	29750		3500	28560		3530	28320	
			540			500			
2	3300	30290		3440	29060				
			380						
4	3260	30670							
			380						
10	3220	31050		3350	29840				
			390			450			
6	3180	31440		3300	30290				
			400						
4	3140	31840	1460			1430			
			310						
3	3110	32150							
			360						
9	3075	32510		3195	31270				
			370			460			
6	3040	32880		3150	31730				
			330						
4	3010	33210	1440			1450			
			390						
3	2975	33600							
			350						
8	2945	33950		3055	32720				

TABLE 7—(*Contd.*)

Int.	Vapour			Solution			Solid
	λ	ν	Δν	λ	ν	Δν	
5	2920	34240	290				
3	2890	34590	350			1400	
7	2825	35390	1440	2930	34120		
6	2715	36820	430				
2	2680	37300	480			1390	
10	2650	37720	1330	2815	35510		
7	2625	38080	420				
4	2600	38450	360			1240	
7	2550	39200	1500	2720	36750		
4	2530	39510	370			1480	
5	2460	40640	1440	2615	38230		
3	2375	42090	310			1440	
6	2295	43550	1450	2520	39670		
			1460	2430	41140	1470	

8. *Perylene.*

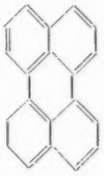

The region of transmission is conspicuous. The spectrum shows very few details, even less than that of pyrene. In addition to the general strong absorption in region II, there seems to be a feeble continuous spectrum, *which starts abruptly* at about 2800 Å, which shows also a feeble banded structure. See Figs. 8 (*a*), (*b*), (*c*) and (*d*), Plates VIII and IX.

8 (*c*)

8 (*d*)

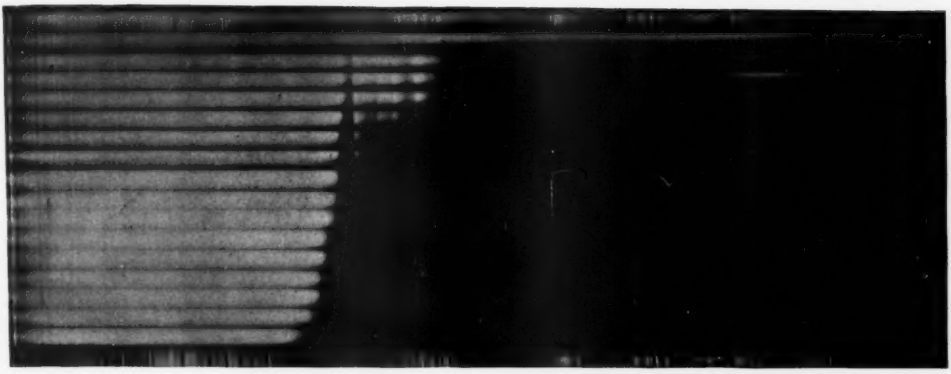

9 (*a*)

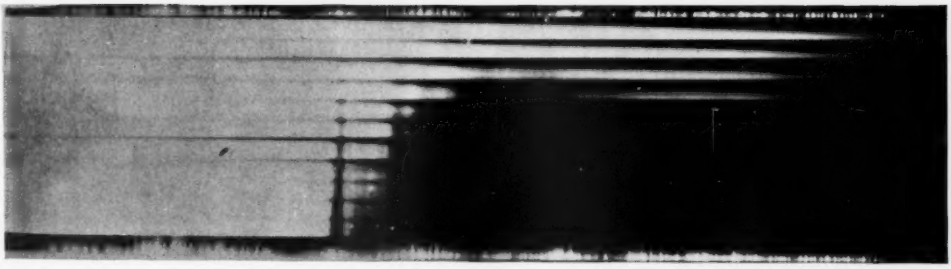

9 (*b*)

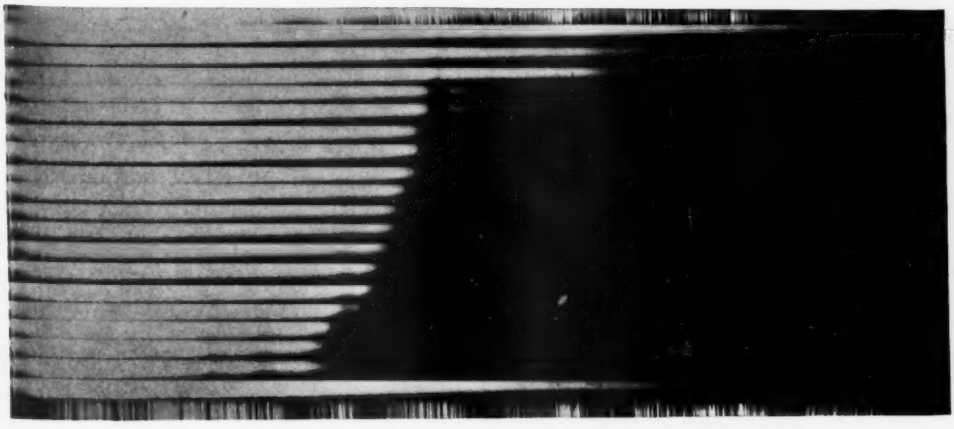

10 (*a*)

FIG. 8. Perylene (visible region): (*a*) Vapour, (*b*) Solution.
FIG. 9. Acenaphthene: (*a*) Vapour, (*b*) Solution.
FIG. 10. Fluorene: (*a*) Vapour.

TABLE 8.

Absorption spectrum of perylene.

Int.	Vapour			Solution			
	λ	ν	Δν	λ	ν	Δν	
2	4245	23550					
		480					
6	4160	24030		4250	23520		
		500	↑		480	↑	
4	4075	24530	|	4165	24000	|	
		490	1470			1440	
3	3995	25020	↓			↓	
		480					
5	3920	25500		4005	24960		
		460	↑		510	↑	
4	3850	25960	|	3925	25470	|	
		490	1410			1450	
3	3780	26450	↓			↓	
		460					
5	3715	26910		3785	26410		
		480	↑		500	↑	
4	3650	27390	|	3715	26910	|	
		510	1490			1440	
3	3585	27900	↓			↓	
		500					
4	3520	28400		3590	27850		
			1440			1470	
3	3350	29840		3410	29320		
			1450			1440	
1	3195	31290		3250	30760		
			1490				
1	3050	32780					
			1400				
0	2925	34180					
			1460				
0	2805	35640					
			1450				
2	2695	37090		2850	35080		
			1430			1470	
3	2595	38520		2735	36550		
			1470			1460	
4	2500	39990		2630	38010		
			1400			1430	
3	2415	41390		2535	39440		
			1510				
3	2330	42900					

9. *Acenaphthene.*

The most striking feature of the spectrum of this substance is the sharp edge of the bands on the short-wave-length side.

There is a very feeble transmission at about 2450 Å. The spectrum closely resembles that of naphthalene. See Figs. 9 (*a*) and (*b*), Plate IX.

TABLE 9.

Absorption spectrum of acenaphthene.

	Vapour			Solution		
	λ	ν	Δν	λ	ν	Δν
**	3190	31340		3220	31040	
			500			500
**	3140	31840		3170	31540	
			620			450
	3080	32460		3125	31990	
			420			470
	3040	32880		3080	32460	
			550			420
	2990	33430		3040	32880	
			460			440
	2950	33890		3000	33320	
			460			450
	2910	34350		2960	33770	
			480			470
	2870	34830		2920	34240	
			490			410
	2830	35320		2885	34650	
			510			490
	2790	35830		2845	35140	
			460			440
	2755	36290		2810	35580	
			400			
	2725	36690				
			470			
	2690	37160				
			560			
	2650	37720				
			430			

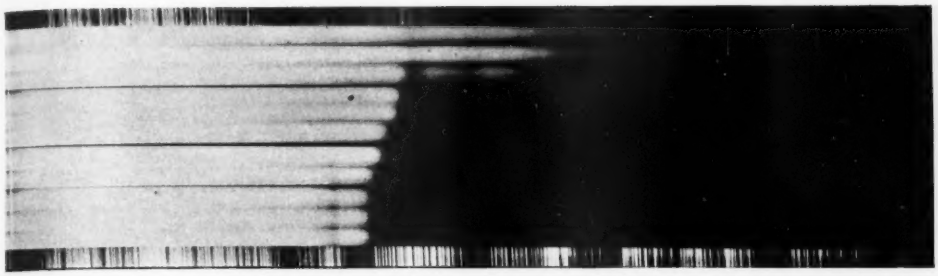

10 (*b*)

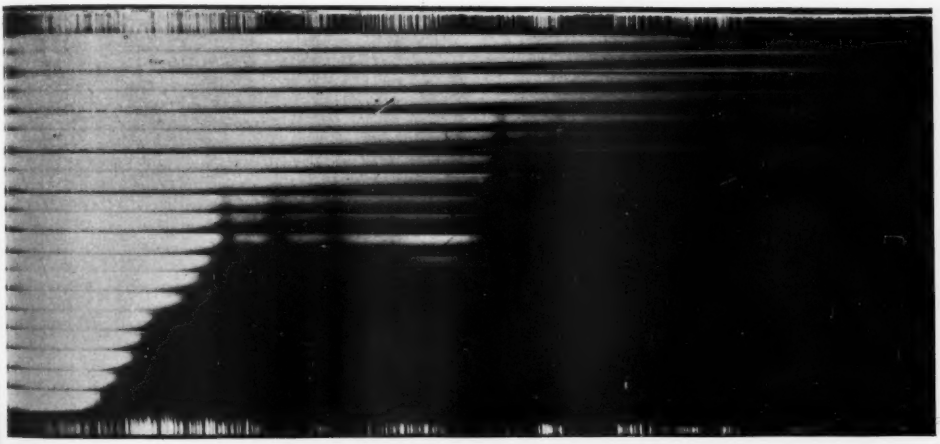

11 (*a*)

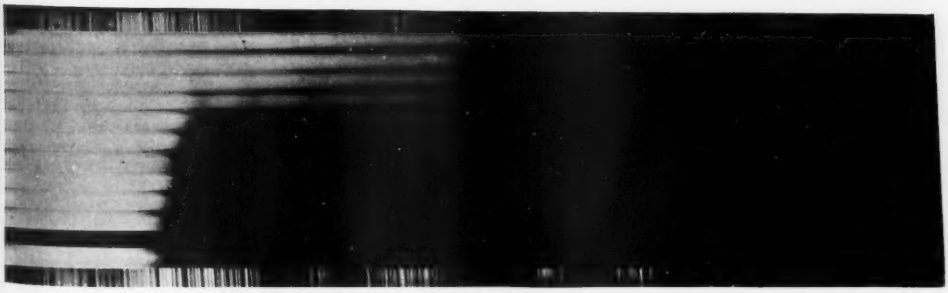

11 (*b*)

FIG. 10. Fluorene: (*b*) Solution.
FIG. 11. Fluoranthene: (*a*) Vapour, (*b*) Solution.

TABLE 9—(*Contd.*)

	Vapour			Solution		
	λ	ν	$\Delta\nu$	λ	ν	$\Delta\nu$
	2620	38150				
			440			
	2590	38590				
			460			
	2560	39050				
			620			
	2520	39670				
			480			
	2490	40150				
			490			
	2460	40640				
			500			
	2430	41140				
			510			
	2400	41650				
			350			
	2380	42000				
			360			
	2360	42360				
			540			
	2330	42900				
			560			
	2300	42460				

10. *Fluorene.* 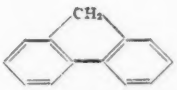

This substance also shows bands sharp on the ultra-violet side. There are also four or five well-defined equally spaced bands, clearly separated from the region of continuous absorption. See Figs. 10 (*a*) and (*b*), Plates IX and X.

TABLE 10.

Int.	Vapour			Solution			Solid		
	λ	ν	$\Delta\nu$	λ	ν	$\Delta\nu$	λ	ν	$\Delta\nu$
3	3675	27200		3735	26770		3845	26000	
			410 ↑			400 ↑			410 ↑
1	3620	27610	1440 ↓	3680	27170	1390 ↓	3785	26410	1420 ↓
3	3490	28640		3550	28160		3645	27420	
			420 ↑			360 ↑			390 ↑
1	3440	29060	1470 ↓	3505	28520	1460 ↓	3595	27810	1510 ↓
3	3320	30110		3375	29620		3455	28930	
			410 ↑			400 ↑			390 ↑
1	3275	30520	1420 ↓	3330	30020	1570 ↓	3410	29320	1550 ↓
3	3170	31530		3205	31190		3280	30480	
			410 ↑			300 ↑			330 ↑
1	3130	31940	1470 ↓	3175	31490	1370 ↓	3245	30810	1360 ↓
3	3030	33000		3070	32560		3140	31840	
			720 ↑			760 ↑			
9	2965	33720		3000	33320				
			170						
6	2950	33890							
			350 1470			1500			
3	2920	34240							
			230 ↓			↓			
8	2900	34470		2935	34060				
			480 ↑			470 ↑			
6	2860	34950		2895	34530				
			500 1550			1390			
6	2820	25450							
			570 ↓			↓			
5	2775	36020		2820	35450				
			460						
5	2740	36480							
			410						
4	2710	36890		2770	36090				
			340			590			
3	2685	37230		2725	36680				
			420						
3	2655	37650							
			720						
3	2605	38370							
			830						
3	2550	39200		2640	37870				
			790			360			
3	2500	39990		2615	38230				
			650			820			
3	2460	40640		2560	39050				

11. *Fluoranthene.*

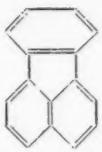

The spectrum resembles that of fluorene, but is much richer in bands. See Figs. 11 (*a*) and (*b*), Plate X.

TABLE 11. *Absorption spectrum of fluoranthene (Benzo-acenaphthene).*

Int.	Vapour			Solution		
	λ	ν	Δν	λ	ν	Δν
6	3510	28480		3585	27890	
			750 ↑			↑
3	3420	29230	1450			1470
			700 ↓			↓
6	3340	29930		3405	29360	
			740 ↑			↑
3	3260	30670	1460			1490
			720 ↓			↓
6	3185	31390		3240	30850	
			1440			1500
3	3045	32830		3090	32350	
			1410			1480
4	2920	34240		2955	33830	
			710 ↑			↑
2	2860	34950	1270			1000
			560 ↓			↓
9	2815	35510		2870	34830	
			510 ↑			
7	2775	36020				
			600 |		680	
6	2730	36620	1450			
			↓			
8	2705	36960		2815	35510	
			450 ↑			
5	2665	37410	|		710	
			460 |			
5	2640	37870	1420			
			510 ↓			
5	2605	38380		2760	36220	
			370		600	
5	2580	38750		2715	36820	
			380			
5	2555	39130				1480
			380			

TABLE 11—(*Contd.*)

Int.	Vapour			Solution		
	λ	ν	Δν	λ	ν	Δν
5	2530	39510		2610	38300	
			480			
3	2500	39990				1240
			650			
3	2460	40640		2525	39540	
			750			1260
2	2415	41390		2450	40800	

12. *Diphenyl.*

The spectrum shows no banded structure, and is in striking contrast to that of benzene or naphthalene.

13. *Terphenyl.*

The spectrum is similar to that of diphenyl with no indication of a band system.

14. *Diphenylmethane.* 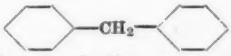

The continuous absorption spectrum is similar to that of diphenyl; there appear, however, five or six bands spaced at intervals of 450 cm.$^{-1}$, which are absent from the spectrum of diphenyl. See Figs. 12 (*a*) and (*b*) Plate XI.

TABLE 12. *Absorption spectrum of diphenylmethane.*

Vapour			Solution		
λ	ν	Δν	λ	ν	Δν
2670	37440		2695	37080	
		430			400
2640	37870		2665	37480	
		430			460
2610	38300		2635	37940	
		450			510
2580	38750		2600	38450	
		470			440
2550	39220		2570	38890	
		450			460
2520	39670		2540	39350	
		400			400
2495	40070		2515	39750	

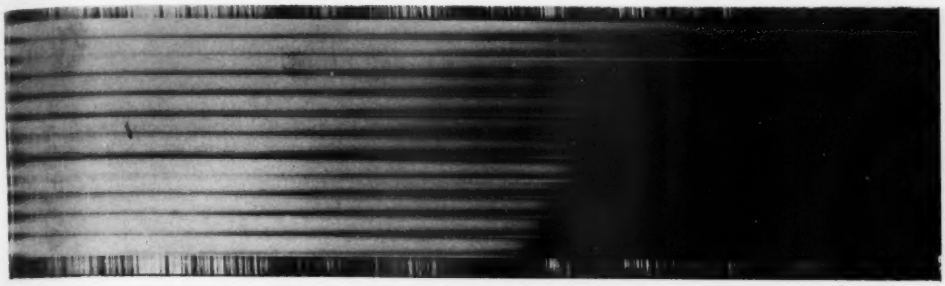

12(*a*)

12(*b*)

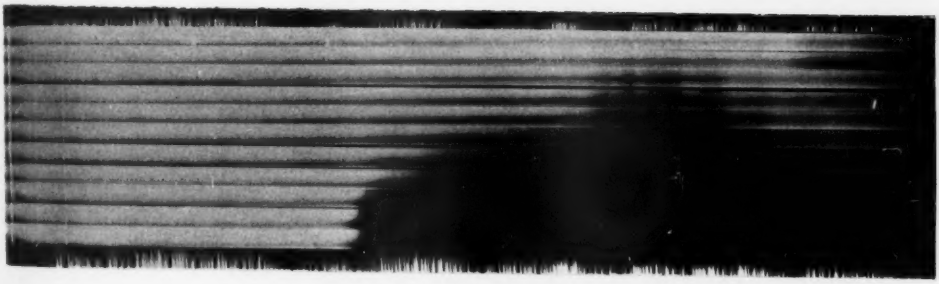

13(*a*)

13(*b*)

FIG. 12.—Diphenylmethane: (*a*) Vapour, (*b*) Solution.
FIG. 13.—Dibenzyl: (*a*) Vapour, (*b*) Solution.

15. *Diphenylethane* (*dibenzyl*). 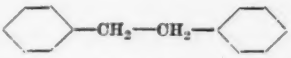

The absorption spectrum resembles that of diphenylmethane. See Figs. 13 (*a*) and (*b*), Plate XI.

TABLE 13.

Absorption spectrum of dibenzyl.

Vapour			Solution		
λ	ν	Δν	λ	ν	Δν
2690	37160		2715	36820	
		420			480
2660	37580		2680	37300	
		430			420
2630	38010		2650	37720	
		440			440
2600	38450		2620	38160	
		450			440
2570	38900		2590	38600	
		460			450
2540	39360		2560	39050	
		390			460
2515	39750		2530	39510	
		480			470
2485	40230		2500	39980	
		410			410
2460	40640		2475	40390	

16. *Triphenylmethane.*

17. *s-Triphenylbenzene.*

These substances again show no banded absorption in the region investigated.

18. *Durene* (*s-tetramethylbenzene*). 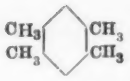

TABLE 14.

Absorption spectrum of durene.

Vapour		
λ	ν	$\Delta\nu$
2780	35970	
		660
2730	36630	
		680
2680	37310	
		710
2630	38020	

19. *Hexamethylbenzene.* 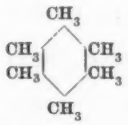

Here again there is no banded absorption.

4. Analysis of the Absorption Bands.

A complete analysis of the absorption spectrum of such complicated molecules is naturally difficult, but as was mentioned in the introduction, some of the molecular constants, as for example, the vibrational frequencies in the initial and excited states, and the electronic frequencies, can be readily obtained. To a first approximation if we neglect the rotational fine-structure and also the anharmonicity of the vibrations, we can represent the frequencies of the various absorption bands by the simple formula

$$\nu = \nu_e + m\alpha + n\beta + \ldots\ldots\ldots p\alpha_0 - q\beta_0 - \ldots\ldots\ldots \quad (1)$$

where ν_e is the frequency corresponding to the transition from the zero vibrational level of the normal molecule to a similar level of the excited molecule, α, β,.. are the vibrational frequencies of the excited molecule, and α_0, β_0,.... are the vibrational frequencies of the normal molecule, m, n,.., p, q,.. are simple integers. There is one striking difference between the values of the vibrational quantum numbers m, n,.. characteristic of the excited molecule, and those of p, q,.. characteristic of the normal molecule, occurring in (1). Whereas m, n,.. can assume any value from zero up to large numbers, the quantum numbers p and q can assume small values only, usually 0, 1, and 2. This is conditioned by the fact that the intensity of any absorption

band corresponding to a given value of p will be proportional to the population of the molecules which are normally in the pth vibrational state, and the number of molecules in the different vibrational states $p = 0$, $p = 1, \ldots$ should, according to the Boltzmann distribution, be in the ratio

$$1 : e^{-\epsilon/kT} : e^{-2\epsilon/kT} : \ldots\ldots\ldots,$$

where $\epsilon = hca_0$. Taking T as 300° k (the temperature of the room), and a_0 to be of the order of 400 cm.$^{-1}$ (which, as we shall see presently, is of the order of magnitude of the vibrational frequencies of these molecules in the normal state), the above ratios would be equal to 1 : 1/7 : 1/50 ; so that the number of molecules present even in the second vibrational state would be quite small, namely, 1/50, while those present in the higher vibrational levels would be negligible.

This circumstance enables us to distinguish the vibrational frequencies characteristic of the normal molecule, namely, α_0, β_0,..from the frequencies $\alpha, \beta, \ldots$.characteristic of the molecule in the higher electronic level. Whereas the former frequencies are repeated only once or twice, the latter appear in regular succession.

Taking for example anthracene, it is easy to see, using this criterion, that there is only one prominent frequency for the excited molecule, equal to 1450 cm.$^{-1}$ (See Table 2) and one for the normal molecule, equal to 400 cm.$^{-1}$ and the various absorption frequencies are therefore expressed by the simple equation

$$\nu = 27540 + n \times 1450 - p \times 400. \quad .. \quad .. \quad .. \quad (2)$$

For the other molecules also the vibrational and the electronic frequencies can be obtained in the same manner, and their values are collected together in Table 15.

5. Absorption Spectra in Relation to Molecular Structure.

The absorption spectrum, as is well known, is very sensitive to changes in molecular structure. For example, when we pass from benzene to durene (*s*-tetramethylbenzene), practically all the wealth of details that we observe in the spectrum of benzene vapour disappears, and in hexamethylbenzene there is not even an indication of a banded structure. The same effect is strikingly brought out in the spectra of diphenyl, *p*-diphenyl benzene, triphenyl benzene and triphenyl methane, none of which shows any banded absorption, in spite of the fact that the benzene rings in these compounds have the same structure as in the benzene molecule. On the other hand, diphenylmethane and diphenylethane show a diffuse band structure.

When the benzene rings, instead of being discreate as in diphenyl or terphenyl, fuse together so as to form naphthalene or anthracene or

TABLE 15. *Molecular Frequencies.*

No.	Molecule	ν	Vibrational Frequency			
			Excited Molecule		Normal Molecule	
			α	β	α_0	β_0
1	Naphthalene ..	31320	420		230	
2	Anthracene ..	27540	1450		400	
3	Naphthacene ..	22220	1400		400	
4	Phenanthrene ..	27540	1450		720	350
5	Chrysene ..	27730	1300	1400	600	400
6	Dibenzanthracene .		1300		700	400
7	Pyrene ..	27540	1450		300	500
8	Perylene ..	24030	1450		480	
9	Acenaphthene ..	31340	400		280	
10	Fluorene ..	27200	1450		400	
11	Fluoranthene ..	28480	1450		700	350
12	Diphenylmethane ..	37160	450			
13	Dibenzyl ..	37440	450			

phenanthrene, the absorption spectrum is very rich in bands. On the basis of the general character of the absorption spectrum, the condensed-nuclear compounds may be divided into the following groups :—(1) compounds like naphthalene, anthracene and naphthacene in which the benzene rings are arranged linearly ; they all have sharp absorption bands whose intensities follow in a general manner the intensities of the continuous spectrum of absorption accompanying them ; the two regions of absorption are clearly marked ; (2) pyrene and perylene, with close-packed condensed nuclei ; they have more or less the same characteristics as compounds (1) ; (4) compounds like phenanthrene, chrysene and dibenzanthracene ; the two regions of absorption are not so well defined as in (1) and (2), and the progression of intensities of the bands is also different ; (4) molecules with incomplete rings, as acenaphthene, fluorene and fluoranthene; the bands are quite sharp and are crowded in

a small region of the spectrum ; most of these bands have sharp edges on the short-wave-length side, while they shade gradually on the long-wave-length side ; some of the absorption bands of naphthalene also have this characteristic.

Considering the different molecules in the same group, the band spectrum becomes more and more diffuse as we go to the higher members, and moreover shifts continually towards the red end of the spectrum. For example, naphthalene spectrum shows a number of fine-structure details, which are absent from that of either anthracene or naphthacene ; as we pass from naphthalene to anthracene, the absorption bands shift towards the red by about 4970 $cm.^{-1}$, and again by 5320 $cm.^{-1}$ when we pass from anthracene to naphthacene ; (See Table 15).

In connection with the Table 15, we should also remark that the vibrational frequencies, both of the excited and of the normal molecules, are practically of the same magnitude for all the compounds. This is not surprising since the vibrational frequencies of a molecule are not so sensitive to changes in its structure as its electronic frequencies are, as we know from Raman and infra-red investigations on organic substances.

We mentioned in an earlier section that the influence of the physical state on the absorption spectrum is a general broadening of the bands, and consequent loss of fine details, as the medium gets dense, and a lateral shift of the band system towards the red, *relative positions of the components of the band system remaining practically unaffected.* These results are clearly seen from the tables of the absorption spectra for the different physical states, and form the spectrograms reproduced ; they suggest that the *vibrational* frequencies α, β,...., α_0, β_0,.... of the molecules are practically the same in the different physical states, but their *electronic* frequencies ν_e show a progressive diminution as we pass from the vapour to the solution and thence to the solid state.

Summary.

Several aromatic hydrocarbons have been studied for their absorption spectra in the vapour state over the spectral range 7000 Å to 2200 Å. A general analysis is made of the band systems, and the values of vibrational frequencies of the molecules in the normal and in the excited states, and of the electronic frequencies of the molecules, are calculated therefrom. These frequencies are discussed in relation to the structure of the molecules, and in relation to their physical states of aggregation.

The author desires to express his thanks to Prof. K. S. Krishnan for his guidance and keen interest in the progress of this work.

THE ABSORPTION SPECTRA OF SOME AROMATIC COMPOUNDS.

Part II. Quinones and Hydroquinones.

By P. K. Seshan.
(From the Indian Association for the Cultivation of Science, Calcutta.)

Received December 29, 1935.
(Communicated by Prof. K. S. Krishnan, D.Sc.)

1. *Introduction.*

The absorption spectra of quinones and hydroquinones are of great interest from the point of view of their molecular structure. Among these compounds only benzoquinone has been studied in detail, by Purvis,[1] Lifschitz and Rosenbohm,[2] and more recently by Louis Light,[3] and the spectrum shows a number of interesting features. Some preliminary work has been done on naphthoquinone and anthraquinone. Hydroquinone has been studied in solution only, in which state it shows some broad regions of absorption. We have therefore studied the absorption spectra of vapours of quinhydrone, hydroquinone, phloroglucinol, 1,4-naphthoquinone, 9,10-anthraquinone, 9,10-phenanthraquinone, β-hydroxyanthraquinone and naphthazarin (5,8-dihydroxy-1,4-naphthoquinone), in some detail, from 7000 to 2200 Å, with a spectrograph of high dispersion: we have also extended the studies on *p*-benzoquinone further into the ultra-violet than has been done previously. The present paper gives an account of these investigations.

These substances have been studied by us in other physical states also, *e.g.*, in a state of solution in suitable solvents, and sometimes also in the solid state. The influence of the physical state on the absorption is discussed.

2. *Experimental.*

A water-cooled hydrogen discharge tube, specially designed to give large intensity,[4] served as the source of continuous radiation in the ultra-violet for the various absorption experiments. In the near ultra-violet and in the visible regions, however, this source was not quite so convenient,

[1] *Jour. Chem. Soc.*, 1923, **123**, 1841.

[2] *Zeits. f. Phys.*, 1926, **38**, 61.

[3] *Zeits. f. Phys. Chem.*, 1926, **122**, 414.

[4] *Jour. Sci. Instruments*, 1935, **12**, 260.

since it gave some intense *lines* as well. For these regions a tungsten linear filament lamp, fitted with a quartz window, was found to be very suitable.

The absorption spectra were in general photographed with a Hilger E_1 quartz spectrograph giving a large dispersion. For very diffuse bands, however, a smaller dispersion was desirable, and the Hilger E_2 was used.

The absorption tube was 75 cms. long, closed at both ends by quartz plates. It was placed in a convenient air oven, in which the whole tube could be heated and maintained at any desired temperature up to 300° C. by regulating the supply of the heating gas. The light from the source was collimated with the help of a quartz lens, and after passage through the absorption tube was condensed by another quartz lens on the slit of the spectrograph.

All the substances studied were solids at room temperature. They were either Merck's or Kahlbaum's pure products, which were further purified by sublimation or recrystallisation. They were placed inside the absorption tube, and the temperature was raised in stages of 10° C., and the absorption spectra were photographed. The absorptions would correspond to the *saturation* vapour pressures of the substances at the respective temperatures. An iron arc, photographed in juxtaposition with the absorption spectra, served for the measurements of wave-lengths.

3. *Description of the Absorption Spectra.*

Benzoquinone.—With the lowest vapour pressure, *viz.*, the saturation vapour pressure at laboratory temperature, the absorption of benzoquinone is almost negligible up to 2450 Å, beyond which there appears a set of nine or ten broad equally-spaced bands extending up to 2250 Å (see Fig. 1 *a*, Plate XII). The constant interval between the bands is about 450 cm.$^{-1}$ Beyond 2250 Å, the absorption *diminishes* slightly, though this is not brought out in the spectrograms reproduced in the figure, owing to the rapid enfeebling of the incident light from the hydrogen tube at about this region, but the diminution of absorption beyond 2250 Å is clear in photographs taken with long exposures. We shall refer, for simplicity, to this region of absorption, from 2250 to 2450 Å, as region I.

As the temperature of the absorption tube is increased to about 60–70° C., and consequently the vapour pressure also, a second region of absorption, extending from 2600 to 3150 Å, appears. The bands in this region, which we shall refer to as Region II, are less diffuse than those in region I. They consist of two sets of equally-spaced bands having the same spacing as in I, *viz.*, 450 cm.$^{-1}$, the two sets being displaced relatively to each other by 230 cm.$^{-1}$

TABLE 1. p-*Benzoquinone.*

Regions I and II. $\nu = 31780 + 450\,n - 230\,p$.

n	p	ν calculated	λ calculated	λ observed	Intensity $p=0$	Intensity $p=1$
			Region II.			
0	0	31780	3146	3145	0	
1	1	32000	3124	3125		0
1	0	32230	3102	3103	1	
2	1	32450	3080	3081		0
2	0	32680	3059	3059	2	
3	1	32900	3038	3038		1
3	0	33130	3017	3018	3	
4	1	33350	2997	2998		3
4	0	33580	2977	2978	4	
5	1	33800	2957	2957		5
5	0	34030	2937	2937	5	
6	1	34250	2919	2917		6
6	0	34480	2899	2899	6	
7	1	34700	2881	2880		7
7	0	34930	2862	2861	7	
8	1	35150	2844	2844		8
8	0	35380	2825	2826	8	
9	1	35600	2808	2807		8
9	0	35830	2790	2790	8	
10	1	36050	2773	2774		7
10	0	36280	2755	2756	7	

TABLE 1 (*contd.*)

n	p	ν calculated	λ calculated	λ observed	Intensity $p=0$	Intensity $p=1$
11	1	36500	2738	2740		5
11	0	36730	2722	2723	5	
12	1	36950	2705	2705		3
12	0	37180	2689	2690	3	
13	1	37400	2673	2672		2
13	0	37630	2656	2655	3	
14	1	37850	2641	2640		1
14	0	38080	2625	2628	2	
15	0	38530	2594	2595	1	
16	0	38980	2564	2560	0	
17	0	39430	2535	2530	0	
			Region I.			
18	0	39880	2507	2505	3′	
19	0	40330	2479	2480	3′	
20	0	40780	2451	2450	3′	
21	0	41230	2425	2425	4′	
22	0	41680	2398	2395	5′	
23	0	42130	2373	2390	6′	
24	0	42580	2348	2350	6′	
25	0	43030	2323	2320	4′	
26	0	43480	2299	2295	4′	
27	0	43930	2276	2280	3′	
28	0	44380	2253	2255	2′	

With further increase of temperature, *viz.*, to 85–95° C., a third region of absorption appears, which extends from 4100 to 4750 Å. The absorption bands in this region, III, are very sharp, unlike those in regions I and II, and are accompanied by a number of fine structure components, which are more or less equally spaced ($\Delta \nu \sim 35$ cm.$^{-1}$).

The positions of the ultra-violet bands of benzoquinone and their intensities in arbitrary units are given in Table 1. The significance of the different columns in the table will be clear from the next section. The intensities for the two series $p = 0$, and $p = 1$ are tabulated in different columns, so as to enable the progression of intensities of the two series to be followed separately. Since the bands in region I were photographed at much lower vapour pressures than those corresponding to region II, a different standard of intensity, indicated by dashed numbers, has been adopted for I. The wave-numbers in this and in the following tables are all expressed in cm.$^{-1}$ (For the absorption bands of benzoquinone in the *visible region* see Table 3.)

Hydroquinone.—There are two prominent regions of absorption, both of which are in the ultra-violet (see Fig. 2*a*, Plate XII) :

(1) From 2300 to 2500 Å, consisting of diffuse bands spaced at intervals of 420 cm.$^{-1}$, which are very similar to those of *p*-benzoquinone in region I; this region appears at about 100° C.

(2) The second region appears at about 130° C. and extends from 2500 to 3050 Å ; it consists of about 15 bands having the same spacing as in region I, *viz.*, 420 cm.$^{-1}$; they are, however, much sharper than those in region I, and are accompanied by two or three fine structure components on either side at intervals of 30 cm.$^{-1}$ The benzoquinone bands in this region do not show this fine structure (see Figs. 9*a* and 9*b*, Plate XIV). Besides this main set of bands, there are two other sets of bands in this region having the same spacing of 420 cm.$^{-1}$ as the main set, and displaced with reference to the latter by about 295 and 170 cm.$^{-1}$ respectively towards the larger wavelength side. These bands are very faint compared with the main set, and, even with high vapour pressures, only the early members could be observed ; the bands shifted by 170 cm.$^{-1}$ are feebler than those shifted by 295 cm.$^{-1}$ The positions of these bands are given in Table 2.

As we have already mentioned, hydroquinone does not show any absorption bands in the visible region.

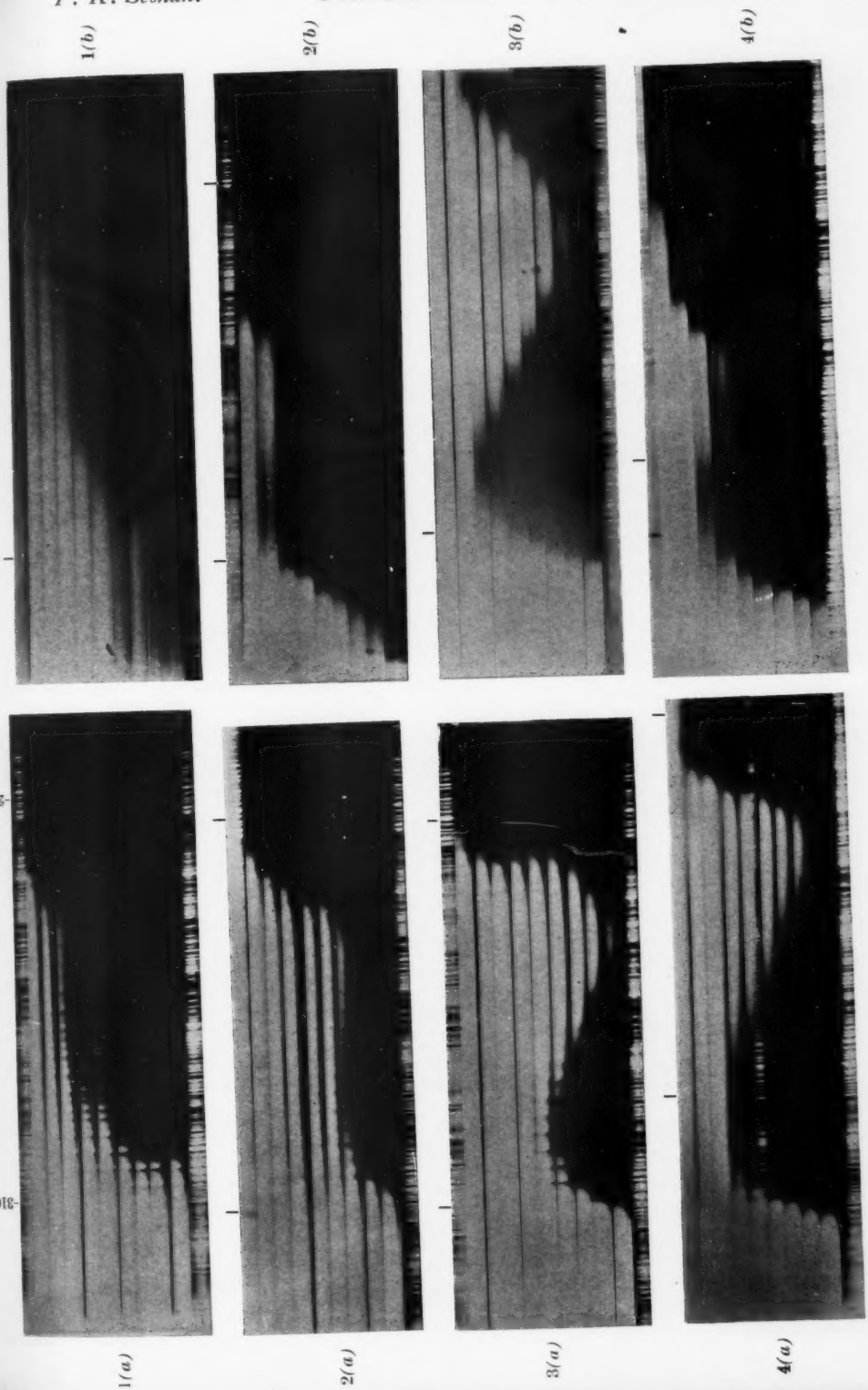
1(b)
2(b)
3(b)
4(b)
2414
3100
1(a)
2(a)
3(a)
4(a)

5 (b)

7 (b)

6 (a)

6 (b)

5 (a)

7 (a)

TABLE 2. *Hydroquinone.*

$\nu = 33070 + 420\,n - 295\,p - 170\,q.$

n	p	q	ν calculated	λ calculated	λ observed	Intensity $p=0$ $q=0$	1 0	0 1
				Region II.				
0	1	0	32775	3050	3050		2	
0	0	1	32900	3039	3040			1
0	0	0	33070	3023	3023	6		
1	1	0	33195	3012	3012		2	
1	0	1	33320	3000	3002			1
1	0	0	33490	2985	2984	7		
2	1	0	33615	2974	2972		2	
2	0	1	33740	2963	2962			1
2	0	0	33910	2948	2948	8		
3	1	0	34035	2937	2936		2	
3	0	1	34160	2926	2927			1
3	0	0	34330	2912	2912	9		
4	1	0	34455	2902	2902		2	
4	0	1	34580	2891	2891			1
4	0	0	34750	2877	2877	10		
5	1	0	34875	2866	2865		2	
5	0	1	35000	2856	2855			1
5	0	0	35170	2843	2843	10		
6	1	0	35295	2832	2830		2	
6	0	1	35420	2822	2820			1
6	0	0	35590	2809	2809	9		

TABLE 2—(*contd.*)

n	p	q	ν calculated	λ calculated	λ observed	Intensity $p=0$ $q=0$	1 0	0 1
7	1	0	35715	2799	2799		2	
7	0	1	35840	2789	2789			1
7	0	0	36010	2776	2776	8		
8	1	0	36135	2767	2765		2	
8	0	0	36430	2744	2744	7		
9	0	0	36850	2713	2712	7		
10	0	0	37270	2682	2680	6		
11	0	0	37690	2652	2650	6		
12	0	0	38110	2623	2625	5		
13	0	0	38530	2594	2595	4		
14	0	0	38950	2566	2565	3		
15	0	0	39370	2539	2540	2		
				Region I.				
16	0	0	39790	2512	2512	1′		
17	0	0	40210	2486	2490	1′		
18	0	0	40630	2461	2460	2′		
19	0	0	41050	2435	2930	3′		
20	0	0	41470	2411	2410	4′		
21	0	0	41890	2386	2390	5′		
22	0	0	42310	2363	2360	5′		
23	0	0	42730	2339	2340	5′		
24	0	0	43150	2317	2320	4′		

8 (*a*) (*b*) (*c*)

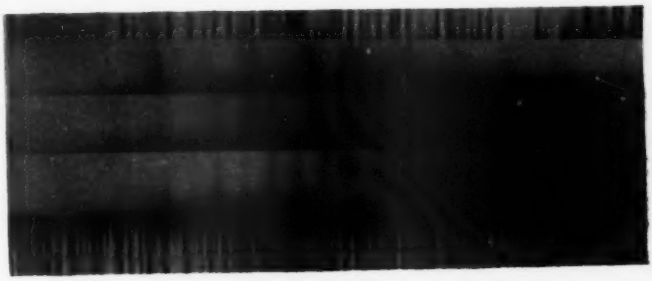

9 (*a*) (*b*) (*c*)

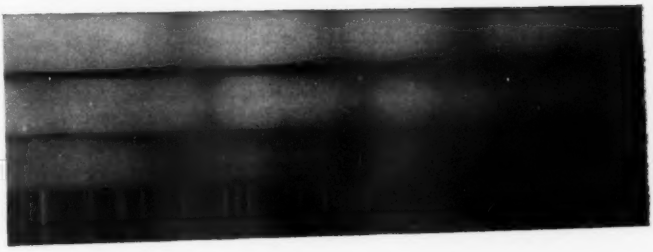

10 (*a*) (*b*)

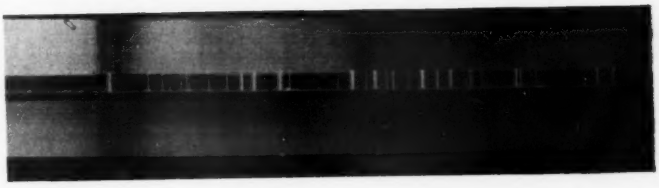

11

Quinhydrone.—The absorption bands in the visible region, given in Table 3, are identical with those of benzoquinone even as regards the finer details. This is brought out clearly in Fig. 10, Plate XIV, where the absorption spectra of these two substances for a small region are exhibited side by side.

The absorption bands of quinhydrone in the ultra-violet are given in Table 4. All the bands that are observed are explicable as being due to either benzoquinone or hydroquinone. (This will be clear from Fig. 8, Plate XIV, which gives the bands in the ultra-violet in juxtaposition with those of *p*-benzoquinone on one side, and those of hydroquinone on the other. Fig. 9 is a similar picture taken under a higher dispersion referring to a small region in the ultra-violet.) The last column in the table indicates the origin of the various bands ; the letter B signifies that the bands are due to benzoquinone, the subscripts 0 and 1 indicating whether they belong to the series $p = 0$ or $p = 1$. The letter H similarly indicates that the band is due to hydroquinone. Only the bands belonging to the series $p = 0$, $q = 0$, could be observed, the other two series, defined by $p = 0$, $q = 1$, and $p = 1$, $q = 0$, being too weak to appear.

It is clear from these Tables and also from Figs. 8, 9, 10, Plate XIV, where the bands of all the three compounds are exhibited side by side, *that the absorption spectrum of quinhydrone can be treated as the superposition of the spectra of benzoquinone and hydroquinone.*

4. *Analysis of the Bands.*

Neglecting, for convenience in discussion, the rotational fine structure, and also the small anharmonic corrections for the vibrations, we may, following Henri[5] and others, represent the frequencies of the various components of a band-system by a formula of the type

$$\nu = \nu_e + m\alpha + n\beta + \cdots\cdots - p\,\alpha_0 - q\,\beta_0 - \cdots\cdots \qquad \ldots\ (1)$$

where ν_e is the electronic frequency corresponding to the transition from the zero vibrational state of the normal molecule to a similar state of the excited molecule. $\alpha, \beta \ldots$ are the vibrational frequencies characteristic of the excited molecule, and similarly $\alpha_0, \beta_0, \ldots$ of the normal molecule. The quantum numbers p and q which refer to the vibrations in the initial state, can have only small values, *viz.*, 0, 1, since the population of the molecules normally occupying the higher vibrational states will be negligible. On the other hand, the quantum numbers m, n, etc., defining the vibrations in the final state, *i.e.*, of the excited molecule, can naturally assume large values.

[5] *Jour. de Chim. Phys.*, 1935, **32**, 353; and previous papers. See also *Tables Annuelles de Constantes*, Paris, 1930.

TABLE 3.

Absorption bands of quinhydrone in the visible (identical with those of p-*benzoquinone).*

λ	Int
4766·2	25
4758·4	17
4750·3	17
4742·0	12
4734·0	10
4557·5	3
4548·1	5
4537·4	25
4529·6	17
4521·9	15
4448·2	5
4440·5	7
4433·6	5
4378·2	5
4370·7	5
4362·7	6
4318·9	20
4312·2	17
4305·2	15
4297·5	12
4291·0	7
4237·6	5
4230·1	5
4224·0	5
4217·8	4
4173·4	3
4166·4	2
4159·8	2

TABLE 4.

Absorption bands of quinhydrone in the ultra-violet.

λ	Int	Origin
3100	1	B_0
3060	2	B_0
3038	3	B_1
3023	3	H
3017	3	B_0
2997	4	B_1
2985	4	H
2979	5	B_0
2968	5	H
2957	5	B_1
2948	5	H
2937	6	B_0
2918	6	B_1
2912	6	H
2900	7	B_0
2880	7	B_1, H
2860	8	B_0
2845	8	B_1, H
2825	7	B_0
2810	7	B_1, H
2790	6	B_0
2775	6	B_1, H
2755	5	B_0
2740	5	B_1, H
2720	4	B_0
2710	4	B_1, H
2690	3	B_0
2655	3	B_0, H
2510	2′	B
2480	3′	B
2450	3′	B
2430	5′	B, H
2400	6′	B, H
2375	6′	B, H
2355	5′	B, H
2330	4′	B, H
2305	3′	B, H

Benzoquinone.—Let us first consider the ultra-violet bands of benzoquinone. From the occurrence of numerous bands at regular intervals of

absorption
λ

450 cm.$^{-1}$, over the entire regions I and II, it is plain that this should be a vibrational frequency of the excited molecule; moreover, there is no other such frequency. It is further clear from Table 1 that for the normal molecule also there is only one vibrational frequency, which should be equal to the relative displacements of the two sets of equally-spaced bands. This displacement, in cm.$^{-1}$, is either 230, or 230 + 450 or again 230 + 2 × 450, none of which is *a priori* improbable. A unique choice between the three alternatives can be made if we can fix definitely the origins (long wave-length limits) of the two sets of bands. As can be seen, however, from the microphotograph* exhibited in Fig. 12, Plate XV, and also from the intensity values given in Table 1, the intensities of both the sets fall off rapidly near the long wave-length end, so that it is very difficult to fix definitely the first band of either series. We shall provisionally adopt 230 cm.$^{-1}$ as the vibrational frequency of the normal molecule and write the general formula in the form

$$\nu = 31780 + n \times 450 - p \times 230 \quad .. \quad .. \quad (2)$$

$n = 0, 1, 2, \ldots . 28$; $p = 0, 1$; though, as we have mentioned, the alternative expressions

$$\nu = 32230 + n \times 450 - p \times 680 \quad .. \quad .. \quad (3)$$

$$\text{and } \nu = 32680 + n \times 450 - p \times 1130 \quad .. \quad .. \quad (4)$$

are not excluded. Data for the infra-red and the Raman spectra for the compound, which at present are not available, may enable us to decide between them.

In region II both the series, corresponding to $p=0$ and $p=1$ respectively, appear, the latter being fainter, as we should expect; beyond 2500 Å, however, *i.e.*, when we pass from region II to region I, the series $p = 1$ fades out, and only that corresponding to $p = 0$, *i.e.*, to transitions from the initial zero vibrational states continues to appear, though more diffusely than in region II.

The bands of benzoquinone in the visible region are more difficult to analyse, because of the fewer repetitions of the vibrational spacing and the appearance of numerous rotational components of more or less the same intensity. The rotational frequency is, however, uniquely determined, and is equal to 35 cm.$^{-1}$ This would correspond to a moment of inertia of 0.8 $\% \times 10^{-40}$ which is of the proper magnitude.

Hydroquinone.—In hydroquinone also there is only one vibrational frequency for the excited molecule, *viz.*, 420 cm.$^{-1}$ For the normal molecule, however, there are two frequencies 170 and 295 cm.$^{-1}$, the former being

* My thanks are due to Dr. I. R. Rao of the Andhra University for the microphotometric records.

feebler than the latter. The general expression for the band frequencies can be written in the form

$$\nu = 33070 + n \times 420 - p \times 295 - q \times 170, \quad .. \quad (5)$$

where n may have any value from 0 up to 25 ; p and q may be both zero or one of them may have a value 1: that is, in the initial state the molecule is either in the zero vibrational state or in the first vibrational state corresponding to either the 295 vibration or the 170 vibration. We should mention immediately that, just as in benzoquinone, owing to the difficulty in fixing the long wave-length limits of the three series, $n=0$, $p=0$, $q=0$; $n=0$, $p=1$, $q = 0$; and $n = 0$, $p = 0$, $q = 1$, the vibrational frequencies of the normal molecule may, instead of being 295 and 170 cm.$^{-1}$, be equal to 290+420 and 170 + 420, or even 295 + 2 × 420 and 170 + 2 × 420. For these latter alternatives the values of ν_e in expression (5) would have to be suitably adjusted.

As in benzoquinone, the series $p = 1$, $q = 0$, and $p = 0$, $q = 1$, appear only in region II. When we pass into region I, only the series $p = 0$, $q = 0$ persists.

The rotational satellites accompanying the earlier members of the series, which are absent in the corresponding bands of benzoquinone in this spectral region, give for hydroquinone nearly the same rotational frequency as for benzoquinone, *viz.*, 30 cm.$^{-1}$

Quinhydrone.—We need not make any special mention here of the analysis of the quinhydrone bands, since some of them are identical with those of benzoquinone and the remaining ones with those of hydroquinone, and thus fit with one or the other of the expressions (2) and (5).

5. *Other Compounds.*

Among the other compounds studied by us, we shall first consider the higher quinones, *viz.*, 1,4-naphthoquinone, 9,10-anthraquinone, and 9,10-phenanthraquinone. They show three or four broad regions of absorption, with their maxima in the positions indicated in Table 7. The absorption spectra taken with an E_2 spectrograph are exhibited in Plate XIII.

These absorption regions, on close examination, show details of a band system, whose positions are as given in Table 5.

Naphthazarin.—There are two regions of absorption, one in the ultra-violet, which is continuous, *i.e.*, without any details of a banded structure, and the other in the visible region, which is much stronger, and shows a set of well-defined bands in the following positions (Table 6). These bands do not have any rotational fine structure (see Fig. 11, Plate XIV).

TABLE 5.

1,4-Naphthoquinone			9,10-Anthraquinone			9,10-Phenanthraquinone		
λ	ν	$\Delta\nu$	λ	ν	$\Delta\nu$	λ	ν	$\Delta\nu$
	I			I			I	
3450	28980	420	3300	30300	460	4095	24420	450
3400	29400	440	3250	30760	480	4020	24870	440
3350	29840	450	3200	31240	390	3950	25310	420
3300	30290	470	3160	31630	410	3885	25730	440
3250	30760	480	3120	32040	420	3820	26170	
3200	31240		3080	32460				
	II			II			II	
						3295	30350	410
2490	40150	490	2660	37580	430	3250	30760	480
2460	40640	500	2630	38010	440	3200	31240	500
2430	41140		2600	38450	370	3150	31740	460
			2575	38820	380	3105	32200	
			2550	39200	400			
			2525	39600				
							III	
						2675	37370	430
						2645	37800	430
						2615	38230	
							IV	
						2465	40550	420
						2440	40970	510
						2410	41480	

TABLE 6.

λ	ν	$\Delta\nu$
5495	18190	
		585
5325	18775	
		655
5145	19430	
		310
5065	19740	
		335
4980	20075	
		325
4900	20400	
		320
4825	20720	
		330
4750	21050	
		335
4675	21385	

The absorptions of β-hydroxyanthraquinone and phloroglucinol do not show any band system at all.

6. Discussion of Results.

Of the various molecules studied, only benzoquinone and hydroquinone, which have the simplest structure, show any rotational fine structure. Indeed as we go to the higher quinones, besides the disappearance of the rotational fine structure, even the vibrational structure of the bands tends to fade away ; for example in naphtho-, anthra-, and phenanthra-, quinones only four or five early members of the vibrational series, corresponding to $n = 0$ to 5, could be detected. In phloroglucinol and the other hydroquinones even the vibrational structure is absent. We further find that, as the complexity of the molecule increases, the band system also shifts towards the visible region of the spectrum, as we should expect.

It is remarkable that the vibration frequency in the excited state is of the same magnitude for all the quinones and hydroquinones, *viz.*, 400–500 cm.$^{-1}$

Quinhydrone requires special mention here. It is generally regarded as a loose molecular compound of benzoquinone and hydroquinone. Its absorption, as we have seen, is found to be a superposition of the absorption spectra of benzo-, and hydro-, quinones. Since the absorption measurements were made at high temperatures, *viz.*, above 100° C., it is difficult to say

whether the superposed absorption spectrum that is observed is actually characteristic of quinhydrone, or of the benzoquinone and hydroquinone into which quinhydrone, may dissociate. The latter alternative seems to be more probable.

7. *Other Physical States.*

In order to find the influence of the physical state of the substance on its absorption spectrum, we have studied also the absorption of these substances in a state of solution in alcohol, and, when the absorption was not too strong, in the solid state as well. The solution absorptions were studied in the usual manner, with a Baly's tube (see Figs. marked (*b*) in Plates XII and XIII). The positions of the maxima of absorption in the different states are given in the following table:—

TABLE 7.

1. Benzoquinone ..	Solid	4960			
	Solution	4700	2950	2440	
	Vapour	4300	2790	2390	
2. Hydroquinone ..	Solid	3010			
	Solution	2930	2420		
	Vapour	2840	2390		
3. 1,4-Naphthoquinone ..	Solution	3230	2620	2450	
	Vapour	3190	2480	2380	
4. 9,10-Anthraquinone ..	Solution	3340	2660	2420	
	Vapour	3130	2570	2370	
5. 9,10-Phenanthraquinone ..	Solution	4270	3260	2640	2560
	Vapour	3770	3050	2580	2440
6. β-Hydroxyanthraquinone	Solution	4740	3720	2730	2420
	Vapour		3120	2500	2300

There are two main results to which we may refer in this place: (1) In solution the vibrational and the rotational structures of the bands are completely quenched, even with the simple molecules, *viz.*, benzoquinone and hydroquinone, which show them conspicuously in the vapour state. (2) The positions of maxima for the solutions are shifted towards the longer wave-lengths with reference to the absorption by the vapour. As we pass from the solution to solid there is a further large shift towards longer wave-lengths. These results show that close proximity of other molecules, whether of the same kind as in the solids, or of a different kind as in the solutions, tends to shift

the absorption maxima towards the red end, and destroy the vibrational and rotational structures.

We have studied in great detail the absorption of naphthacene and a few other hydrocarbons in various physical states, in vapour state, in solution in different solvents, in solid solution and in the solid state ; and the influence of the physical state on absorption will be discussed in a separate publication in connection with these studies.

8. *Summary.*

The absorption spectra of some quinones and hydroquinones in the vapour state have been studied over a wide spectral region, from 7000 to 2200 Å, with a high dispersion spectrograph. Many of them show a vibrational structure, and some of them also a rotational fine structure. The bands for the simplest of the molecules, namely benzoquinone and hydroquinone, have been analysed, and the characteristic vibrational frequencies of the normal and excited molecules have been determined. For the other molecules the vibrational frequencies for the excited state only could be so obtained.

The substances have been studied also in solution. The rotational and vibrational structures observed with the vapours are all quenched, and the maxima of absorption are considerably shifted towards the red end of the spectrum. In the solid state, in which also two of the substances were studied, there is a further shift of the absorption-maxima in the same direction.

The author desires to express his grateful thanks to Prof. K. S. Krishnan, for his guidance and interest in the work.

EXPLANATION OF THE PLATES.

The vapour absorption spectra were taken at intervals of 10°C. between the temperatures indicated. The solutions were all in alcohol. The two iron lines indicated in the reference spectra in Plates XII and XIII are 3100 and 2414 Å.

Plate XII.

1. Benzoquinone.—(*a*) Vapour 30 to 110°C.; (*b*) Solution.
2. Quinhydrone.—(*a*) Vapour 60 to 130° C.; (*b*) Solution.
3. Hydroquinone.—(*a*) Vapour 80 to 150°C.; (*b*) Solution.
4. Naphthoquinone.—(*a*) Vapour 80 to 170°C.; (*b*) Solution.

Plate XIII.

5. Anthraquinone.—(*a*) Vapour 100 to 190°C.; (*b*) Solution.
6. Phenanthraquinone.—(*a*) Vapour 140 to 240°C.; (*b*) Solution.
7. Hydroxyanthraquinone.—(*a*) Vapour 150 to 220°C.; (*b*) Solution.

PLATE XIV.

8. Vapour absorption by (*a*) hydroquinone; (*b*) quinhydrone; (*c*) benzoquinone.
9. Similar to 8 taken under a high dispersion to exhibit the fine structure of the bands: (*a*) hydroquinone; (*b*) benzoquinone; (*c*) quinhydrone.
10. Absorption in the visible region of naphthazarin vapour from 90 to 130°C.

PLATE XV.

11. Microphotometric record of benzoquinone vapour from 3100 to 2700 Å exhibit the progression of intensities of the two sets of bands.

DIAMAGNETIC SUSCEPTIBILITY OF SULPHURIC ACID-WATER MIXTURE.

By B. Nagesha Rao.

(From the Department of Physics, Central College, Bangalore.)

Received February 5, 1936.

(Communicated by Prof. B. Venkatesachar, M.A., F.Inst.P.)

Introduction.

In this paper a study has been made of the diamagnetic susceptibility of sulphuric acid-water mixture. Farquharson[1] has studied the same mixture with Curie-Cheneveau balance. His concentration susceptibility curve abounds in maxima and minima and deviates a good lot from the additive law. Varadachari[2] has also studied the same mixture. He infers the presence of definite hydrates in the solution. Till about 87% of the acid, the values of susceptibilities are less than the additive law and above 87% the values are above the additive law. Points of maximum deviation from the additive law are attributed to the formation of hydrates.

The apparatus in this investigation is the one devised by Sibaiya and Venkataramiah.[3] " The test system of this apparatus consists of a pyrex-glass cylinder from which the opposite quadrants have been ground off. The grinding operation is done so as to obtain exact symmetry in the test-piece since any slight asymmetry would tilt it when immersed in a liquid. A thin glass stem fused to the test-piece along its axis, carries a plane mirror. The free end of the stem is attached to the lower end of a phosphor-bronze suspension, the upper end of which is attached to a brass rod. The test-system and the suspension are encased in a wide glass tube with an opening for cementing a lens, in front of the plane mirror. The torsion head is attached to the top of the glass tube. The liquid is inserted from a side tube. The tap at the bottom of the tube served to empty it after a completion of a set of readings. When the magnetic field is put on, the couple on the test-piece twists the suspension and the deflection of the image on the scale is noted. In order to obtain high sensitiveness the mirror on the test-piece is adjusted parallel to one of its ground faces, which in its zero position is

[1] *Phil. Mag.*, 1931, **12**, 283.

[2] *Proc. Ind. Acad. Sci.*, Aug. 1935, **2**, 161.

[3] *Ind. Jour. Phys.*, 1932, **7**, 393.

also parallel to the lines of force. The relation between the deflections obtained when the magnetic current is switched off and the volume susceptibility of the liquid is linear, thus rendering the calculation of the volume susceptibility very simple. A density determination enables one to calculate the specific susceptibility.

If the volume susceptibility of the material of the test-piece and the surrounding liquid be K_0 and K respectively the couple on the test-piece is $(K_0 - K) \int \frac{1}{2} (\Delta H^2 \times r)\, dv$ where dv_0 is the element of volume, whose position vector is r and H, the field intensity at the point. If C is the couple per unit twist and θ the angular deflection

$$K_0 - K = - \frac{C\theta}{\int \frac{1}{2} (\Delta H^2 \times r) dv} = - \lambda\theta$$

whence $K = K_0 + \lambda\theta$

and it is clear that K and θ are linearly connected and that K_0 is obtainable by interpolation."

Conc. H_2SO_4	X	Conc. H_2SO_4	X	Conc. H_2SO_4	X
0%	·720	41·8	·562	74·9	·452
10·3	·680	43·0	·561	78·9	·442
14·1	·664	44·7	·551	78·9	·442
14·3	·664	48·0	·539	78·9	·441
16·5	·657	49·1	·539	82·7	·429
16·7	·654	53·2	·526	86·5	·420
17·5	·653	56·5	·514	91·2	·410
20·5	·641	57·2	·507	92·8	·410
24·4	·625	58·8	·504	92·8	·411
24·7	·625	59·0	·504	93·5	·407
28·1	·611	60·5	·498	95·0	·407
29·2	·610	61·1	·496	96·0	·404
34·4	·591	62·0	·492	96·0	·405
35·3	·585	65·1	·484	97·3	·402
36·5	·580	67·2	·477	98·0	·401
36·5	·580	70·7	·465	99·8	·400
37·6	·579	71·0	·464		

Care is taken to maintain the level of the liquid in the wide tube always the same. The current is adjusted to the same value every time. The deflections were observed by a mirror and scale arrangement. The solutions were prepared in a clean pyrex-glass flask and every time the solution was prepared, it was cooled to the room temperature, before it was poured into the tube. The tube was thoroughly cleaned with the solution before the reading was taken with the solution. The readings tabulated above were obtained in four sets of different concentration. Constantin Salceanu and Dumitru Gheorghiu[4] and Bhatnagar and Nevgi[5] have used the same form of instrument and find this instrument most suitable for working with liquids.

Results.

The sulphuric acid was analytically pure and was taken from freshly opened bottles. The densities were determined using a specific-gravity bottle. From a knowledge of the density, the concentration was found from *Landolt and Bornstein Tables.*

The graph shows the value of susceptibility plotted against the percentage concentration of sulphuric acid. The susceptibility of water is assumed to be at 25° C. $\cdot 720 \times 10^{-6}$.

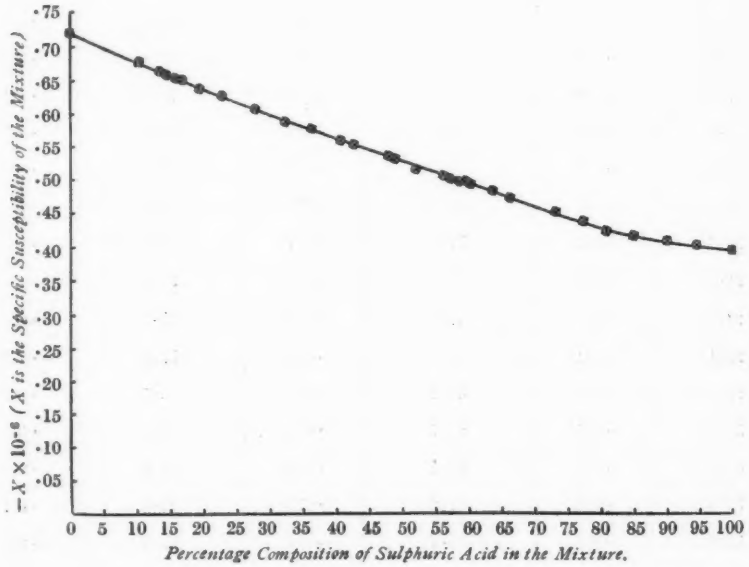

[4] *Comptes Rendus*, Jan. 7, 1935, 120–123.

[5] *Ind. Jour. Phys.*, May, 1935.

Discussion.

The graph shows that there is considerable departure from the additive law. The maximum deviation is about 5%. A smooth curve is drawn passing through a maximum number of points and it is seen that most of the points lie on the curve and the points that lie outside the curve differ from the main curve by distances which are within the limits of experimental error. The values are all higher than the additive value, but I find that even above 86% the values are less than the additive value. If the value is taken as $\cdot 400 \times 10^{-6}$, it will be seen that portion of the curve above 86% also lie below the additive straight line joining ·720 and ·400 and at the same time the maximum deviation from additive law also increases.

The smooth line which has been drawn passing through most of the points shows that there is no definite break anywhere in the concentration susceptibility curve. This shows that the magnetic measurements do not support the theory which assumes the presence of definite hydrates in solution. The deviation from the additive value is plotted against the concentration in the second graph and it is seen that $H_2SO_4.3H_2O$ is absent.

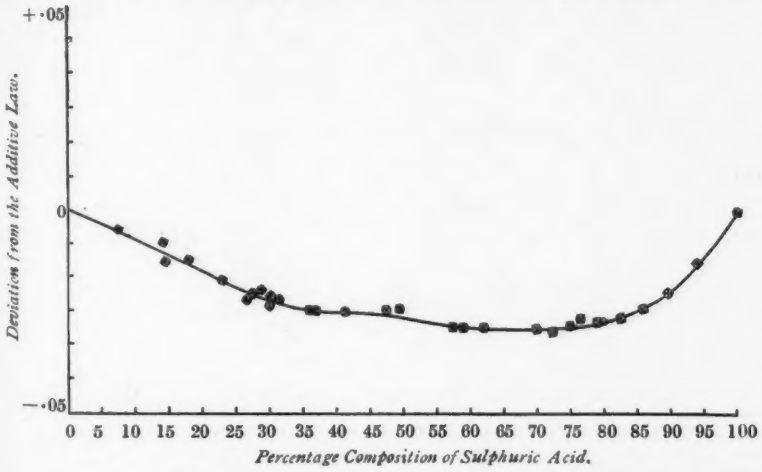
+·05
0
−·05
Deviation from the Additive Law.
0 5 10 15 20 25 30 35 40 45 50 55 60 65 70 75 80 85 90 95 100
Percentage Composition of Sulphuric Acid.

The maximum deviation is, however, at a concentration corresponding to the compound $H_2SO_4.2H_2O$. This has been reported to be the only compound existing from surface tension data.[6] Besides $H_2SO_4.2H_2O$ can be obtained in a crystalline form.[7]

[6] *Zeit. f. Phy. Chem.*, 1935, **173**, 237.

[7] Mellor's *Chemistry*.

In conclusion, I wish to record my grateful indebtedness to Prof. B. Venkatesachar for valuable guidance and suggestions. My thanks are due to Mr. Sibaiya for useful discussion and criticism. I am highly thankful to the University of Mysore for the award of a stipend which made this work possible.

1-36—Printed at The Bangalore Press, Mysore Road Bangalore City, by G. Sreenivasa Rao, Superintendent, and Published by The Indian Academy of Sciences, Indian Institute of Science, Bangalore